

UNIVERSITÀ DEGLI STUDI DI BOLOGNA

---

Facoltà di Ingegneria  
Corso di Laurea in Ingegneria Meccanica

Dipartimento di tecnica delle costruzioni

Tesi di Laurea in Progetti di strutture

A NUMERICAL PROGRAM FOR  
RAILWAY VEHICLE-TRACK-STRUCTURE  
DYNAMIC INTERACTION USING A  
MODAL SUBSTRUCTURING APPROACH

Candidato:  
Gabriel SAVINI

Relatore:  
Chiar.mo Prof. Ing. Marco Savoia

Correlatori:  
Prof. Ing. G. Naldi  
Prof Ing. Roda Buch Alejandro

---

ANNO ACCADEMICO 2009-2010

# Summary

This thesis work proposes a method for the simulation of the dynamic interaction between vehicle and railway track. The model has been designed to take into account the complexity of wheel–rail contact, railpad and ballast, with low computational requirements.

A modal description of the rails and the sleepers is presented, imposing the coupling between these elements and the vehicle by means of the associated interaction forces. This provides a model with a reduced number of coordinates and therefore a low computational cost is achieved.

It is shown that this model also enables to incorporate the associated nonlinear characteristics between the different elements by means of a simple formulation.

In the development of the following work several commercial softwares have been used:

- Mathematica: for a quick analysis of beams vibrational modes.
- Matlab : for the development of the track interaction program.
- c++ : for the .exe final program
- Excel, Latex and others less important ones.

The five working months work have been divided in two parts:

1. development of the track interaction program with the use of Matlab GUI (graphical user interface); This part took half of the total time due to the need of having a program capable of analyzing a wide range of interaction problems, with different kinds of rails, sleepers, ballasts, vehicles etc.
2. once tested the program, lots of simulations have been run and their results have been carefully analyzed.

# Acknowledgments

I would like to thank my friends and all my family, my brother, my mother and my father for helping me in these five years of university.

Moreover I would like to thank prof. ing. *Giovanni Naldi* for giving me the opportunity of going to Wien (Austria) where I have done my three months internship at *Verbund* (Austria's leading electricity company) and *Alejandro Roda Buch* that, as well as being my teacher in the mechanical vibrations field during my Erasmus period, has helped me in the development of this thesis work.

Last but not least I would like to thank prof. ing. *Marco Savoia* for giving me the possibility of going to Valencia to carry out this work.

All the people mentioned above have played an important role in my personal and professional growth.

I hope that in the future I would be able to give them something back especially to my family which gave me the possibility of studying in such a city as Bologna and also abroad like Valencia or Wien with all the costs that this entails.

I got real gratification from this work because it has shown me how I am ready for the work life and, comparing it to my first thesis work done almost two years ago, it emphasizes my professional growth and the technical skills achieved during these five years. Actually if two years ago my abilities were more theoretical, now they have reached a good practical level specially as regards my IT skills.

# Table of contents

|  |            |
|--|------------|
| <b>Summary</b>   | <b>ii</b>  |
| <b>Acknowledgments</b>                                     | <b>iii</b> |
| <b>1 Introduction</b>                                      | <b>1</b>   |
| 1.1 Track interaction theoretical model . . . . .          | 1          |
| 1.1.1 Model Introduction . . . . .                         | 1          |
| <b>2 Mechanical vibrations</b>                             | <b>5</b>   |
| 2.1 Fundamentals of mechanical vibrations . . . . .        | 5          |
| 2.1.1 Types of vibrations . . . . .                        | 5          |
| 2.1.2 Modeling Vibrating Systems . . . . .                 | 6          |
| 2.2 Lumped element model . . . . .                         | 6          |
| 2.2.1 Damped and undamped natural frequencies . . . . .    | 9          |
| 2.2.2 Forced Vibrations . . . . .                          | 10         |
| 2.2.3 Mechanical Resonance . . . . .                       | 13         |
| 2.3 Frequency response or modal model . . . . .            | 14         |
| 2.4 Multiple degrees of freedom models . . . . .           | 17         |
| 2.4.1 FRF in multiple degrees of freedom systems . . . . . | 18         |
| 2.5 Finite Element method FEM . . . . .                    | 18         |
| 2.5.1 Geometry mesh . . . . .                              | 19         |
| 2.6 Spectral Analysis . . . . .                            | 20         |
| <b>3 Mathematical Model definition</b>                     | <b>22</b>  |
| 3.1 Substructuring Techniques . . . . .                    | 22         |
| 3.1.1 Substructuring analysis benefits . . . . .           | 22         |
| 3.1.2 Modal reduction . . . . .                            | 23         |
| 3.1.3 Chosen model . . . . .                               | 24         |
| 3.2 Analysis of the Substructures . . . . .                | 25         |
| 3.3 Elements studied with modal coordinates . . . . .      | 26         |
| 3.3.1 Rails . . . . .                                      | 26         |

|          |  |           |
|----------|--|-----------|
| 3.3.2    | Sleepers . . . . .   | 28        |
| 3.3.3    | Underlying structure . . . . .   | 31        |
| 3.3.4    | Vibration mode shapes . . . . .  | 31        |
| 3.3.5    | Governing differential equations in modal coordinates . . . . .  | 35        |
| 3.4      | Elements modelled with physical coordinates . . . . .  | 36        |
| 3.4.1    | Equation of motion . . . . .   | 38        |
| 3.5      | Constraint equations . . . . .   | 38        |
| 3.5.1    | Wheel-rail contact . . . . .   | 39        |
| 3.5.2    | Fastening elements: Railpads or fasteners . . . . .  | 41        |
| 3.5.3    | The ballast . . . . .  | 42        |
| 3.6      | Time resolution dynamic model . . . . .  | 43        |
| 3.6.1    | Mathematical system . . . . .  | 46        |
| 3.7      | Achievable magnitudes of interest . . . . .  | 47        |
| 3.8      | Frequency response function calculation . . . . .  | 48        |
| 3.8.1    | System coordinates . . . . .   | 49        |
| 3.8.2    | Vehicle model for FRF calculation . . . . .  | 51        |
| 3.8.3    | System equations of motion . . . . .   | 53        |
| 3.8.4    | FRF receptance matrix . . . . .  | 57        |
| <b>4</b> | <b>The Program developed</b>   | <b>59</b> |
| 4.1      | Introduction . . . . .   | 59        |
| 4.2      | Vehicle-Track Dynamic interactions program . . . . .   | 60        |
| 4.3      | User-defined Input Data . . . . .  | 60        |
| 4.3.1    | Program welcome GUI . . . . .  | 60        |
| 4.3.2    | Load data GUI . . . . .  | 60        |
| 4.3.3    | Problem (Model) size . . . . .   | 62        |
| 4.3.4    | Wheels position . . . . .  | 65        |
| 4.3.5    | Rail-Pad properties GUI . . . . .  | 65        |
| 4.3.6    | Sleeper properties GUI window . . . . .  | 66        |
| 4.3.7    | Rails properties GUI window . . . . .  | 69        |
| 4.3.8    | Ballast mathematical model and properties GUI windows . . . . .  | 71        |
| 4.3.9    | Simulated temporal space . . . . .   | 73        |
| 4.3.10   | Other input values . . . . .   | 75        |
| 4.3.11   | Vehicle matrices: DOF matrix ( <i>MAT_DOF</i> ) . . . . .  | 76        |
| 4.3.12   | Vehicle matrices: Inertia rigid body properties Matrix ( <i>IRBP</i> ) . . . . .                         | 78        |
| 4.3.13   | Vehicle matrices: Vehicle external forces( <i>Ext_F</i> ) . . . . .                                      | 79        |
| 4.3.14   | Vehicle matrices: Suspensions matrices ( <i>MAT_LS_K</i> & <i>MAT_LS_C</i> ) . . . . .                   | 80        |
| 4.3.15   | Vehicle matrices: Suspensions connection matrices ( <i>Conn_MAT_K</i><br>& <i>Conn_MAT_C</i> ) . . . . . | 81        |
| 4.3.16   | Wheels irregularities selection . . . . .  | 83        |
| 4.3.17   | Numerical integration method . . . . .   | 84        |

|          |   |            |
|----------|---|------------|
| 4.3.18   | Beams number of modes . . . . .   | 86         |
| 4.3.19   | Saving GUI . . . . .  | 87         |
| 4.4      | Solving part . . . . .  | 87         |
| 4.4.1    | simulation time . . . . .   | 88         |
| 4.4.2    | Output data . . . . .   | 89         |
| 4.5      | Bridge interaction program . . . . .  | 89         |
| 4.6      | Frequency response function FRF program . . . . .   | 90         |
| <b>5</b> | <b>Simulations results</b>  | <b>91</b>  |
| 5.1      | Program Validation . . . . .  | 91         |
| 5.2      | Tests results . . . . .   | 92         |
| 5.3      | Temporal response . . . . .   | 93         |
| 5.3.1    | Vehicle-Track system . . . . .  | 93         |
| 5.3.2    | Vehicle-Track-Structure system . . . . .  | 99         |
| 5.4      | FRF: System Frequency response function . . . . .   | 103        |
| 5.4.1    | Vehicle-Track system . . . . .  | 104        |
| 5.4.2    | Vehicle-Track-Structure system . . . . .  | 106        |
| 5.5      | Rail models: Euler-Bernoulli and Timoshenko . . . . .                                     | 109        |
| 5.6      | conclusions . . . . .   | 109        |
| <b>6</b> | <b>Conclusions</b>  | <b>112</b> |
| 6.1      | Summary . . . . .   | 112        |
| 6.2      | Future developments . . . . .   | 113        |
| 6.3      | Achievements . . . . .  | 114        |
| <b>A</b> | <b>Euler-Bernoulli and Timoshenko Beam theories</b>                                       | <b>115</b> |
| A.1      | Euler-Bernoulli theory . . . . .  | 115        |
| A.1.1    | Equation of motion . . . . .  | 116        |
| A.1.2    | Free Vibration without damping . . . . .  | 118        |
| A.1.3    | characteristic equation and mode shapes of a free- beam and<br>a continuous one . . . . . | 120        |
| A.1.4    | Normalization, main properties and natural frequencies . . . . .                          | 123        |
| A.1.5    | Rigid body modes . . . . .  | 124        |
| A.1.6    | Pinned-pinned constrained beam . . . . .  | 127        |
| A.1.7    | Forced vibrations . . . . .   | 128        |
| A.1.8    | Stresses . . . . .  | 130        |
| A.2      | Timoshenko beam theory . . . . .  | 131        |
| A.2.1    | Equation of motion . . . . .  | 132        |
| A.2.2    | Free vibration . . . . .  | 134        |
| A.2.3    | Modes normalization and natural frequencies . . . . .                                     | 139        |

|          |   |            |
|----------|---|------------|
| <b>B</b> | <b>Winkler Foundation</b>   | <b>143</b> |
| B.1      | Concept of Elastic Foundations . . . . .  | 143        |
| B.2      | Governing Equations For Uniform Straight Beams on Elastic Foundations . . . . . | 144        |
| <b>C</b> | <b>Two step numerical integration method used</b>                               | <b>146</b> |
| C.1      | introduction . . . . .  | 146        |
| C.2      | New Explicit integration method algorithm . . . . .                             | 147        |
| C.3      | Integration scheme . . . . .  | 148        |
| C.4      | Stability . . . . .   | 149        |
| C.5      | Accuracy . . . . .  | 151        |
|          | C.5.1 Numerical dissipation . . . . .   | 151        |
|          | C.5.2 Stability and Accuracy : examples . . . . .                               | 152        |
|          | <b>Bibliography</b>   | <b>155</b> |

# List of tables

|     |  |     |
|-----|--|-----|
| A.1 | Common boundary conditions in beam elements . . . . .        | 120 |
| A.2 | Beam common boundary conditions . . . . .                    | 136 |
| C.1 | Conditions of stability of the new explicit method . . . . . | 150 |



# List of figures

|      |   |    |
|------|---|----|
| 1.1  | Total Track-Way model . . . . .   | 2  |
| 2.1  | mass-spring-damper model . . . . .  | 6  |
| 2.2  | undamped oscillatory motion . . . . .   | 9  |
| 2.3  | damped oscillatory motion with different damping ratios $\zeta$ . . . . .   | 11 |
| 2.4  | Forced Vibration Response . . . . .   | 12 |
| 2.5  | Frequency response model . . . . .  | 15 |
| 2.6  | discretized model and FEM analysis results . . . . .  | 19 |
| 2.7  | 2D geometry mesh: mesh is denser around the object of interest . . . . .  | 20 |
| 3.1  | Substructuring of a conventional track over ballast. Substructures:<br>Rails and sleepers over ballast . . . . .                                    | 23 |
| 3.2  | Dynamic model of the interactive vehicle/track-structure system . . . . .   | 24 |
| 3.3  | global reference system . . . . .   | 25 |
| 3.4  | (a) graphical representation of a two wheelset bogie on a conventional<br>track over ballast;(b) rail free body graphic and acting forces . . . . . | 27 |
| 3.5  | (a) graphical representation of a sleeper on a conventional track over<br>ballast;(b) rail free body graphic and acting forces . . . . .            | 29 |
| 3.6  | Sleeper over ballast model: discrete distribution of punctual forces<br>more eventual elastic Winkler Foundation . . . . .                          | 30 |
| 3.7  | Sleeper over ballast on an underlying structure model . . . . .   | 31 |
| 3.8  | First four mode shapes for a free-free constrained monodimensional<br>beam, 2 rigid body modes (-1 & 0) and 2 flexural ones (1 & 2) . . . . .       | 33 |
| 3.9  | Rail Vehicle representation and lumped element modeling . . . . .   | 37 |
| 3.10 | N lobes polygonal wheel examples . . . . .  | 40 |
| 3.11 | Rails imperfections examples . . . . .  | 40 |
| 3.12 | Track receptance : relation between U point displacement due to an<br>harmonic force in point F . . . . .   | 49 |
| 4.1  | Welcome GUI . . . . .   | 60 |
| 4.2  | Load data GUI . . . . .   | 60 |
| 4.3  | Loading GUI . . . . .   | 61 |
| 4.4  | Message box for data redefinition . . . . .   | 62 |
| 4.5  | Half of the Vehicle-track model . . . . .   | 62 |

|      |   |     |
|------|---|-----|
| 4.6  | Main Model DOF choice . . . . .   | 63  |
| 4.7  | Wheels position . . . . .   | 65  |
| 4.8  | Type of railpad (fastner) . . . . .   | 66  |
| 4.9  | Sleeper properties and mathematical model . . . . .   | 67  |
| 4.10 | Sleeper properties specification . . . . .  | 68  |
| 4.11 | Rails mathematical model . . . . .  | 69  |
| 4.12 | Rails properties . . . . .  | 70  |
| 4.13 | Ballast mathematical model . . . . .  | 71  |
| 4.14 | Ballast GUIs . . . . .  | 73  |
| 4.15 | Simulated time . . . . .  | 74  |
| 4.16 | Some other input velues . . . . .   | 75  |
| 4.17 | DOF matrix . . . . .  | 76  |
| 4.18 | Vehicle components numeration . . . . .   | 78  |
| 4.19 | Inertia rigid body properties Matrix <i>IRPB</i> . . . . .  | 78  |
| 4.20 | External constant forces acting on vehicle DOF . . . . .  | 79  |
| 4.21 | Vehicle suspensions matrix . . . . .  | 80  |
| 4.22 | Vehicle suspensions position . . . . .  | 81  |
| 4.23 | Irregularites selection question dialog box . . . . .   | 83  |
| 4.24 | Irregularites parameters definition . . . . .   | 83  |
| 4.25 | Types of integrators implemented in the program . . . . .   | 84  |
| 4.26 | Number of vibrational modes and spectral damping coefficients used<br>for each beam . . . . .   | 86  |
| 4.27 | Saving GUI . . . . .  | 87  |
| 4.28 | Non linear forces . . . . .   | 88  |
| 4.29 | Main quantities of interest plot . . . . .  | 89  |
| 4.30 | FRF parameters selection . . . . .  | 90  |
| 5.1  | Timoshenko vs Euler-Bernoulli rails natural frequencies . . . . .   | 95  |
| 5.2  | Timoshenko vs Euler-Bernoulli rails natural frequencies . . . . .   | 96  |
| 5.3  | Rail deformation at $t = 0.4355 s$ . . . . .  | 97  |
| 5.4  | Sleepers 17 , 24 , 26 , 30 , 37 , deformation at $t = 0.4355 s$ . . . . .   | 97  |
| 5.5  | Wheels-rail contact forces for some irregular systems . . . . .   | 98  |
| 5.6  | Rails deformation for two irregular cases . . . . .   | 98  |
| 5.7  | Carriage vertical displacement in time for the cases of simple problem<br>(red line), wheels irregularity (blue line) and ballast discontinuity<br>(green line) . . . . . | 99  |
| 5.8  | Timoshenko vs Euler-Bernoulli rails natural frequencies . . . . .   | 101 |
| 5.9  | Rail and bridge deformation at $t = 0.4355 s$ . . . . .   | 101 |
| 5.10 | Sleepers 23 , 27 , 29 , 31 , 33 , deformation at $t = 0.4355 s$ . . . . .   | 102 |
| 5.11 | Wheels-rail contact forces for some irregular systems . . . . .   | 102 |
| 5.12 | Rail and bridge deformation for some irregular cases . . . . .  | 103 |

|      |   |     |
|------|---|-----|
| 5.13 | FRF for a non-damped model with 25 sleeper bays . Comparison between a Timoshenko continuous-continuous rail beam and a Timoshenko free-free one . . . . .  | 104 |
| 5.14 | FRF for a non-damped model with 25 sleeper bays . Comparison between a Timoshenko continuous-continuous rail beam and a Timoshenko free-free one . . . . .  | 105 |
| 5.15 | Vehicle influence on the FRF. Comparison between track-alone system, 1 wheelset-track and 2 wheelsets-track system. . . . .   | 105 |
| 5.16 | Vehicle influence on the FRF. Comparison between FRF calculated for different wheelset positions on the track. . . . .  | 106 |
| 5.17 | FRF for a non-damped model with 25 sleeper bays . Comparison between a Timoshenko continuous-continuous rail beam and a Timoshenko free-free one . . . . .  | 107 |
| 5.18 | FRF for a non-damped model with 25 sleeper bays . Comparison between a Timoshenko continuous-continuous rail beam and a Timoshenko free-free one . . . . .  | 107 |
| 5.19 | Vehicle influence on the FRF. Comparison between track-alone system, 1 wheelset-track and 2 wheelsets-track system. . . . .   | 108 |
| 5.20 | Vehicle influence on the FRF. Comparison between FRF calculated for different single-wheelset positions on the track. . . . .   | 108 |
| 5.21 | (a) Comparison between FRF calculated for different Rail models for the damped system.;(b) Comparison between FRF calculated for different Rail models for the same system but undamped . . . . . | 110 |
| 5.22 | Comparison between contact forces calculated for all the possible rail models combinations . . . . .  | 111 |
| A.1  | Schematic of cross-section of a bent beam showing the neutral axis. . . . .   | 116 |
| A.2  | Free body diagram of a differential element of a beam subject to bending . . . . .  | 116 |
| A.3  | Plot of the Absolute value of the characteristic equation for a free free beam . . . . .  | 122 |
| A.4  | Plot of first 5 vibration modes for a free-free constrained beam (fig (A.4(a))) and for a continuous one (fig(A.4(b))) using the Euler-Bernoulli approach. . . . .                                | 126 |
| A.5  | First 5 modes plot for a pinned-pinned constrained beam . . . . .   | 128 |
| A.6  | Schematic of cross-section of a bent beam showing the neutral axis. . . . .   | 131 |
| A.7  | Free body diagram of a differential element of a Timoshenko beam subject to bending . . . . .   | 132 |
| A.8  | Plot of the characteristic equation for a free-free constrained beam (fig (A.8(a))) and for a continuous-continuous one (fig (A.8(b))) using the Timoshenko approach . . . . .                    | 138 |

|      |   |     |
|------|---|-----|
| A.9  | Plot of first 5 vibration modes for a free-free constrained beam (fig (A.4(a))) and for a continuous-continuous one (fig(A.4(b))) using the Timoshenko approach . . . . . | 140 |
| A.10 | Integral $I_{c_n}$ trend for the first 82 vibration modes for a free-free constrained beam . . . . .  | 141 |
| A.11 | Comparison between Euler-Bernoulli frequencies and Timoshenko ones for the same beam . . . . .  | 142 |
| B.1  | Distributed load $q(x)$ acting on an infinite beam over an elastic foundation of $k$ stiffness . . . . .  | 143 |
| B.2  | Deflections of foundation models under uniform pressure. No beam is present. . . . .  | 144 |
| B.3  | Beam cross section differential element and forces acting on it. . . . .  | 145 |
| C.1  | Minimum time step stability condition for the linear example . . . . .  | 153 |
| C.2  | Minimum time step stability condition for the non-linear example . . . . .  | 153 |
| C.3  | Accuracy of the solution . . . . .  | 154 |

# Chapter 1

## Introduction

### 1.1 Track interaction theoretical model

Railways are experiencing a significant set of problems associated with dynamic interaction of the vehicle-track system. These problems mainly stem from existing wheel and track defects and they affect acoustic emissions, track maintenance and the reliability of the vehicle rolling elements.

In order to study these problems, models have been developed to make possible the simulation of the dynamic response of vehicle-track interaction. Only simple models, which consider the rail as a beam resting on an elastic foundation, have an analytical solution.

This simplicity is lost when the rail is considered as having discrete supports and when nonlinearities are associated with the properties of ballast, railpads and wheel-rail contact.

Several authors have proposed methodologies for studying vehicle-track dynamics.

Perhaps, the most commonly studied problems concern the formation of irregular wear (corrugation) on wheels and rails, and the dynamic response to wheelflat impact (part of the wheel tread is worn off due to unintentional sliding as caused by locked brakes or by low wheel-rail friction). In these two cases the frequency range considered is similar, so the basic dynamic model characteristics are the same for both problems.

#### 1.1.1 Model Introduction

In this paper, a method for calculating the dynamic response of the vehicle-track system is developed to take into account complex models of wheel-rail contact, railpads and ballast at low computational cost.

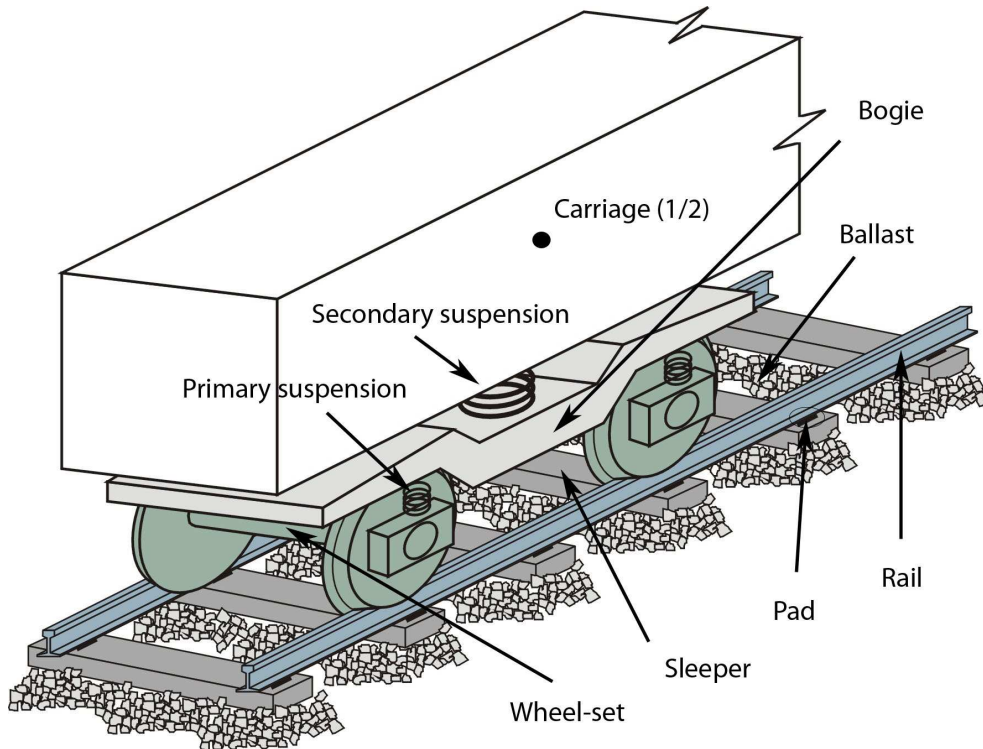


Figure 1.1. Total Track-Way model

The rails and the sleepers are described by their modal coordinates. Wheel-rail, rail-sleeper and sleeper-ballast interactions are modelled using space coordinates and they are coupled to the modal models of rail and sleeper by means of the corresponding interaction forces. The overall model is described by a reduced number of coordinates. In addition, the most significant nonlinearities of the problem can be included easily.

Different types of irregularities can be imposed to the wheels; non-linear forces can be assigned to the springs of to the dumpers that describe the interaction between ballast and sleepers or between sleepers and rails (the last due to the presence of pads between the two elements).

Moreover it is interesting to describe the effects generated by the crossing over different structures like bridges.

The program developed with Matlab wants to give to the operator the possibility of studying all of these different interaction problems but in doing so it want to preserve a low computational cost that permits to normal notebooks to run such simulations.

In doing so it consider different mathematic models for the different parts <sup>1</sup> using

<sup>1</sup>see figure (1.1)

a *substructuring approach*:

- VEHICLE : it consists of three parts:
  1. the Carriage
  2. the Bogies
  3. the Wheel-sets

Every single element is treated with a lumped element model. The simplifying assumptions in this domain are:

- all objects are rigid bodies with all the mass concentrated in the center of gravity ;
- all interactions between rigid bodies take place via kinematic pairs (joints), springs and dampers.

Therefore the *lumped elements* mathematical model, is that in which the inertial, elastic and dumping properties of the physic continuous system are concentrate in different single components; doing so the model consist of rigid masses treatable as point masses and interlinked with springs and dumpers without a mass. Increasing the number of masses the model would better represent the real system, but obviously this would lead to a more complicate model and so a less computationally efficient one.

- RAILS AND SLEEPERS : they are modelled with the continuous Euler beam theory or with the Timoshenko's one , thus described by their modal properties, and they are connected to each other through linear and non linear forces, resulting from the pads, as well as with the Vehicle wheel-sets and with the ballast. They also have two different possibilities for boundary conditions:
  1. free-free B.C.
  2. continuos B.C.
- BALLAST : it is modelled with a discrete series of forces resulting from a discrete series of supports. All the forces consist of two components, a linear one and an optional non-linear (in the program “user choice”):
  - Linear component: it depends on the damping effect, proportional to the displacement velocity and on the elastic one, proportional to the displacement; this last component could be replaced by a uniform Winkler stiffness under each sleeper as it will be shown later.

- Non linear-component: it depends on user choice and takes into account all the possible non linear effects deriving from the ballast properties.
- UNDERLYING STRUCTURE : it is an optional element of the model that could represent a bridge or a viaduct with which the vehicle-track system interacts. In this work it has been studied with a mono-dimensional model, using also in this case, both Euler beam theory and Timoshenko one.

Its boundary conditions are those of pinned-pinned beam.

Finally it is important to note that all this thesis work and specially the program developed has been done respecting a modular approach, that is, giving the possibility of future improvements or in general new developments, taking special care on the usability of it, being the last goal achieved through the use of user friendly GUIs (graphical user interfaces).



# Chapter 2

## Mechanical vibrations

### 2.1 Fundamentals of mechanical vibrations

Vibration refers to mechanical oscillations about an equilibrium point. The oscillations may be periodic such as the motion of a pendulum or random such as the movement of a tire on a gravel road.

Vibration is occasionally “desirable”. For example the motion of a tuning fork, the reed in a woodwind instrument or harmonica, or the cone of a loudspeaker is desirable vibration, necessary for the correct functioning of the various devices.

More often, vibration is undesirable, wasting energy and creating unwanted sound-noise. For example, the vibrational motions of engines, electric motors, or any mechanical device in operation are typically unwanted. Such vibrations can be caused by imbalances in the rotating parts, uneven friction, the meshing of gear teeth, etc. Careful designs usually minimize unwanted vibrations.

The study of sound and vibration are closely related. Sound, or “pressure waves”, are generated by vibrating structures (e.g. vocal cords); these pressure waves can also induce the vibration of structures (e.g. ear drum). Hence, when trying to reduce noise it is often a problem in trying to reduce vibration.

#### 2.1.1 Types of vibrations

Mainly vibrations can be divided in two types:

- FREE VIBRATIONS
- FORCED VIBRATIONS

Free vibration occurs when a mechanical system is set off with an initial input and then allowed to vibrate freely. Examples of this type of vibration are pulling a

child back on a swing and then letting go or hitting a tuning fork and letting it ring. The mechanical system will then vibrate at one or more of its “natural frequency” and damp down to zero.

Forced vibration is when an alternating force or motion is applied to a mechanical system. Examples of this type of vibration include a shaking washing machine due to an imbalance, transportation vibration (caused by truck engine, springs, road, etc.), or the vibration of a building during an earthquake. In forced vibration the frequency of the vibration is the frequency of the force or motion applied, with order of magnitude being dependent on the actual mechanical system characteristics.

### 2.1.2 Modeling Vibrating Systems

It is known that Continuous Elastic bodies possess infinite DOFs (i.e, number of independent coordinates to completely describe motion). Considering that an analytical solution for these physical systems exists only for a few ones, specially those very simple, it is necessary to find a way to model those complicate systems with a simpler mathematical model, that brings to a low cost computational problem but at the same time resemble enough the real one.

In doing so lots of methods have been developed like the *lumped elements*, the *FEM (finite element method)*, *spectral model* and the *Frequency response or modal model* one. Obviously the use of one of these models doesn't preclude the use of the others in fact these methods are often used together to obtain more accurate results. In general, they model a finite number of DOFs (within the boundary wavelengths of interest) and accept a certain degradation in accuracy. Giving an accurate description of each one would be too long but in this section a small presentation of each one will be given.

## 2.2 Lumped element model

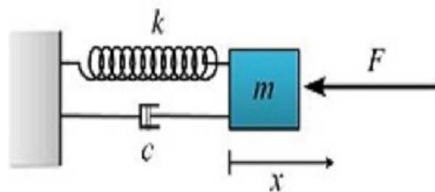


Figure 2.1. mass-spring-damper model

The lumped element model (also called lumped parameter model, or lumped component model) simplifies the description of the behaviour of spatially distributed

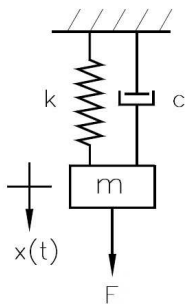
physical systems into a topology consisting of discrete entities that approximate the behaviour of the distributed system under certain assumptions. It is useful in electrical systems (including electronics), mechanical multibody systems, heat transfer, acoustics, etc.

Mathematically speaking, the simplification reduces the state space of the system to a finite number, and the partial differential equations (PDEs) of the continuous (infinite-dimensional) time and space model of the physical system into ordinary differential equations (ODEs) with a finite number of parameters.

The simplifying assumptions in this domain are:

- all objects are rigid bodies;
- all interactions between rigid bodies take place via kinematic pairs (joints), springs and dampers.

In figure 2.1 it is shown a *single degree of freedom* system (SDOF) of a lumped elements model and obviously the following considerations can be extended to a *multi degree of freedom one* (MDOF). The various elements are so treated like perfect ones and the deriving mathematical model is the following (fig 2.1):



Let:

$k$  = spring stiffness constant  $[N/m]$

$c$  = damping coefficient (of a viscous damper)  $[Ns/m]$

$m$  = mass of the element (or equivalent one)  $[kg]$

$F$  = External force  $[N]$

Then, the equilibrium of all forces brings to:

$$m\ddot{x} + c\dot{x} + kx = F \quad (2.1)$$

Assuming the external force equal to zero we obtain a free-vibration case otherwise the problem refers to a forced one. The solution of this equation gives the law of motion of the body.

If we know the mass and stiffness of the system we can determine *the undamped natural frequency* that is the frequency at which the system will vibrate once it is set in motion by an initial disturbance, using the following formula.

$$f_n = \frac{1}{2\pi} \sqrt{\frac{k}{m}} \quad [Hz] \quad (2.2)$$

Note that the angular frequency  $\omega_n$  ( $\omega_n = 2\pi f_n$ ) with the units of radians per second is often used in equations because it simplifies the equations, but is normally converted to “standard” frequency (units of Hz or equivalently cycles per second) when stating the frequency of a system.

Every vibrating system has one or more natural frequencies that it will vibrate at once if it is disturbed. This simple relation can be used to understand in general what will happen to a more complex system once we add mass or stiffness. For example, the above formula explains why when a car or truck is fully loaded the suspension will feel “softer” than unloaded because the mass has increased and therefore reduced the natural frequency of the system.

Others important definitions in vibrations field are:

- Critical damping  $c_c = 2\sqrt{km}$  : it is the value of the damping where the system no longer oscillates (if the damping is increased past critical damping the system is called overdamped).
- Damping ratio (damping factor or % critical damping)  $\zeta = \frac{c}{2\sqrt{km}}$ : it is the ratio of the actual damping over the amount of damping required to reach critical damping.
- Phase shift  $\phi$  : it is the shift between the phase of the exciting force and the system response.
- $\omega$  : it is the applied force angular frequency (as for the system,  $f$  is used for the “standard” one ) : the frequencies of the external force acting on the system .

With this new assumption the *equilibrium equation* (2.1) becomes:

$$\ddot{x} + 2\zeta\omega\dot{x} + \omega^2x = F \tag{2.3}$$

It is also important to notice that usually these systems are linearized and doing so it is possible to use the superposition principle<sup>1</sup>.

The solution of the homogeneous equation (that means of the unforced system) of this mass-spring-damper model brings to:

$$x(t) = e^{-\zeta\omega t}(C_1e^{i\omega t\sqrt{1-\zeta^2}} + C_2e^{-i\omega t\sqrt{1-\zeta^2}}) \tag{2.4}$$

That can also be written as:

---

<sup>1</sup>In physics and systems theory, the superposition principle, also known as superposition property, states that, for all linear systems, the net response at a given place and time caused by two or more stimuli is the sum of the responses which would have been caused by each stimulus individually

$$x(t) = X e^{-\zeta \omega t} \cos(\sqrt{1 - \zeta^2} \omega_n t - \phi) \quad (2.5)$$

### 2.2.1 Damped and undamped natural frequencies

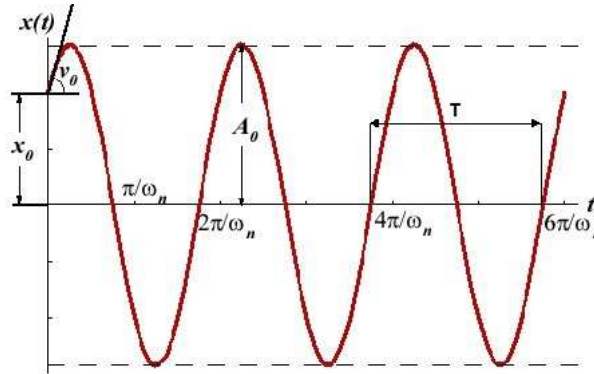


Figure 2.2. undamped oscillatory motion

In figure 2.2 it is represented the plot of a Simple harmonic motion, that means that is neither driven nor damped. Its motion is periodic-repeating itself in a sinusoidal fashion with constant amplitude.

A Simple harmonic motion *SHM* can serve as a mathematical model of a variety of motions, such as a pendulum with small amplitudes and a mass on a spring. It also provides the basis of the characterization of more complicated motions through the techniques of Fourier analysis.

In addition to its amplitude, the motion of a simple harmonic oscillator is characterized by its period  $T$ , the time for a single oscillation, its frequency,  $f$ , the reciprocal of the period  $f = \frac{1}{T}$  (i.e. the number of cycles per unit time), and its phase,  $\phi$ , which determines the starting point on the sine wave. The period and frequency are constants determined by the overall system, while the amplitude and phase are determined by the initial conditions (position and velocity) of the system.

In practice all systems are damped, which means that the energy is dissipated, and the amplitude of the motion gradually gets smaller and smaller until it stops altogether.

Damping can be therefore introduced in the model from various sources but is hard to model accurately.

As aforementioned, one mathematical model is that of viscous damping in which a force, that is proportional to the velocity of the mass and which opposes its motion, is considered.

The major points to note from the solution equation (2.5) are the exponential term and the cosine function:

- The exponential term defines how quickly the system “damps” down (the larger the damping ratio, the quicker it damps to zero).
- The cosine function is the oscillating portion of the solution, but the frequency of the oscillations is different from the undamped case.

As aforementioned the frequency in this case is called the “damped natural frequency”,  $f_d$ , and is related to the undamped natural frequency by the following formula:

$$f_d = \sqrt{1 - \zeta^2} f_n \quad (2.6)$$

Equation (2.6) clearly shows how the damped natural frequency is less than the undamped natural frequency, but it is important to remember that for many practical cases the damping ratio is relatively small and hence the difference is negligible. Therefore the damped and undamped descriptions are often dropped when stating the natural frequency (e.g. with 0.1 damping ratio, the damped natural frequency is only 1 % less than the undamped).

The plots in figure 2.3 present how 0.1 and 0.3 damping ratios effect how the system will “ring” down over time. What is often done in practice is to experimentally measure the free vibration after an impact (for example by a hammer) and then determine the natural frequency of the system by measuring the rate of oscillation as well as the damping ratio by measuring the rate of decay. The natural frequency and damping ratio are not important only in free vibration, but also characterize how a system will behave under forced vibration.

### 2.2.2 Forced Vibrations

In this section it will be described the behavior of the spring mass damper model when an harmonic force is added in the form below. Such a force could be generated, for example, by a rotating imbalance, where, obviously, the angular frequency of the applied force would be the angular velocity of the rotational motion.

The force expression in this last case is:

$$F = F_0 \cos(2\pi ft) \quad (2.7)$$

If we again sum the forces on the mass we get the following ordinary differential equation:

$$m\ddot{x} + c\dot{x} + kx = F_0 \cos(2\pi ft) \quad (2.8)$$

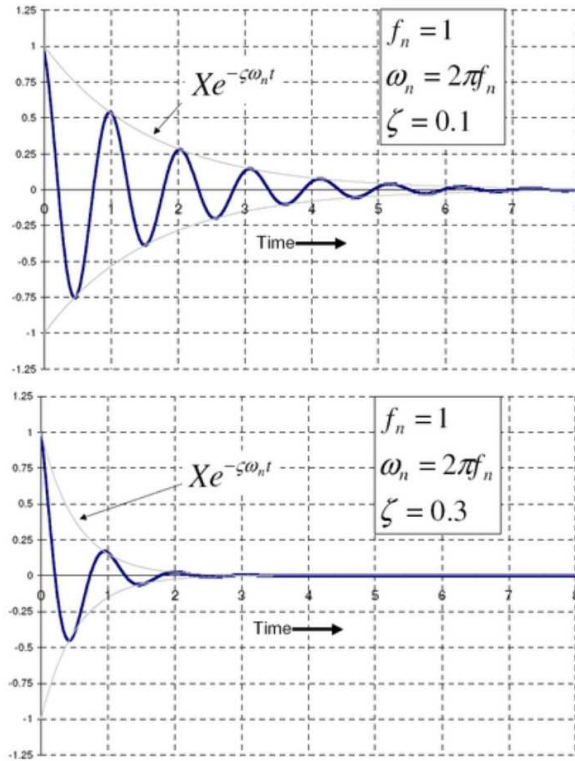


Figure 2.3. damped oscillatory motion with different damping ratios  $\zeta$

where in (2.8)  $2\pi f = \omega$  with  $\omega =$  applied force angular frequency. The steady state solution of this problem can be written as:<sup>2</sup>

$$x(t) = X \cos(2\pi ft - \phi) \quad (2.9)$$

The result states that the mass will oscillate at the same frequency,  $f$ , of the applied force, but with a phase shift  $\phi$ .

The amplitude of the vibration “ $X$ ” is defined by the following formula:

$$X = \frac{F_0}{k} \frac{1}{\sqrt{(1 - r^2)^2 + (2\zeta r)^2}}. \quad (2.10)$$

Where “ $r$ ” is defined as the ratio of the harmonic force frequency over the undamped natural frequency of the mass-spring-damper model :  $r = \frac{f}{f_n}$

<sup>2</sup>A system in a steady state has numerous properties that are unchanging in time. This implies that for any property  $p$  of the system, the partial derivative with respect to time is zero:  $\frac{\partial p}{\partial t} = 0$

Finally the phase shift ,  $\phi$ , is defined by the following formula.

$$\phi = \arctan \left( \frac{2\zeta r}{1 - r^2} \right). \quad (2.11)$$

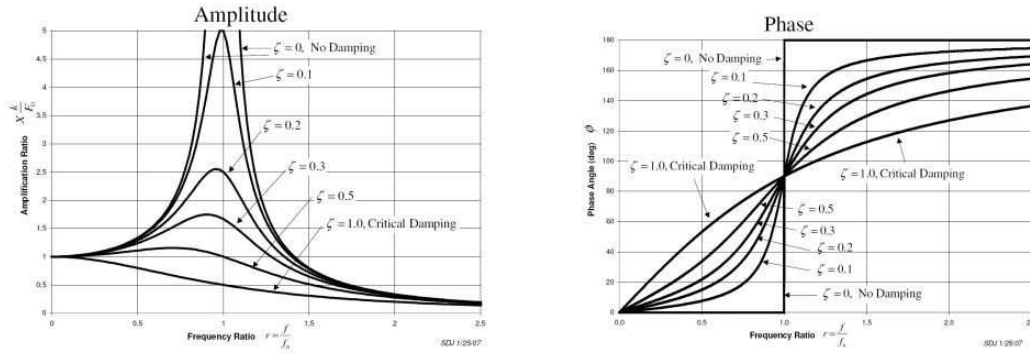


Figure 2.4. Forced Vibration Response

The plot of these functions, called “the frequency response of the system”, presents one of the most important features in forced vibration.

In a lightly damped system when the forcing frequency nears the natural frequency ( $r \approx 1$ ) the amplitude of the vibration can get extremely high.

This phenomenon is called resonance (subsequently the natural frequency of a system is often referred to as the resonant frequency). In rotor bearing systems any rotational speed that excites a resonant frequency is referred to as a critical speed.

If resonance occurs in a mechanical system it can be very harmful-leading to eventual failure of the system. Consequently, one of the major reasons for vibration analysis is to predict when this type of resonance may occur and then to determine what steps to take to prevent it from occurring.

As the amplitude plot shows, adding damping can significantly reduce the magnitude of the vibration.

Also, the magnitude can be reduced if the natural frequency can be shifted away from the forcing frequency by changing the stiffness or mass of the system.

If the system cannot be changed, perhaps the forcing frequency can be shifted (for example, changing the speed of the machine generating the force).

The following statements hold always good in vibration studies:

- At a given frequency ratio, the amplitude of the vibration,  $X$ , is directly proportional to the amplitude of the force  $F_0$  (e.g. if you double the force, the vibration doubles)



- With little or no damping, the vibration is in phase with the forcing frequency when the frequency ratio  $r \leq 1$  and 180 degrees out of phase when the frequency ratio  $r \geq 1$
- When  $r \ll 1$  the amplitude is just the deflection of the spring under the static force  $F_0$ . This deflection is called the static deflection  $\delta_{st}$ . Hence, when  $r \ll 1$  the effects of the damper and the mass are minimal.
- When  $r \gg 1$  the amplitude of the vibration is actually less than the static deflection  $\delta_{st}$ . In this region the force generated by the mass ( $F = ma$ ) is dominating because the acceleration seen by the mass increases with the frequency. Since the deflection seen in the spring,  $X$ , is reduced in this region, the force transmitted by the spring ( $F = kx$ ) to the base is reduced. Therefore the mass-spring-damper system is isolating the harmonic force from the mounting base—referred to as vibration isolation. Interestingly, more damping actually reduces the effects of vibration isolation when  $r \gg 1$  because the damping force ( $F = cv$ ) is also transmitted to the base.

### 2.2.3 Mechanical Resonance

Mechanical resonance is the tendency of a mechanical system to absorb more energy when the frequency of its oscillations matches the system natural frequency of vibration (its resonance frequency or resonant frequency) than it does at other frequencies.

It may cause violent swaying motions and even catastrophic failure in improperly constructed structures including bridges, buildings, and airplanes, a phenomenon known as resonance disaster.

There could be many sources for vibration.

If any source creates a vibration frequency that is equal to or nearly equal to a part resonant frequency, that part will resonate.

For example, the vibrations of even a fairly well-balanced part can be magnified by the structure in which it is assembled. Anyone who has driven an automobile knows that it will vibrate more at a certain speed than at others. According to the formula, centrifugal force varies as the square of rpm.

The vibration amplitude not only increases with rpm, but it suddenly rises at a much higher rate when passing through the responding part resonance or critical speed and then smoothed out as the rpm passes beyond.

This results from vibration at a frequency from any source, such as misalignment, unbalance, gearmesh, electrical hum, etc., that matches the natural frequency or resonant frequency of either a part or total spring system.

To visualize what happens, consider a simple flat spring with a weight mounted at one end (similar to a diving board). When the spring is deflected, by pulling down

on the weight, and then let it go, the spring oscillates and the spring-and-weight system vibrates at its natural frequency.

If only a single impulse is given, the amplitude of the vibration usually progressively decreases with time, due to friction and other energy losses.

If for continuous periodic impulses, the timing or direction of the impulses did not coincide with its natural frequency, the result would be an out-of-tune vibration that does not build up.

If, on the other hand, the timing and direction of the impulses coincided with the spring natural frequency, the result would be a tuned vibration and a progressively larger and larger amplitude with each added cycle.

The amplitude finally reaches a maximum (due to friction or viscous damping forces).

Resonance magnifies the amplitude of vibrations in relatively undamped systems anywhere from 5 to 10 and sometimes 20 times over that of non-resonant vibrations.

Damping often reduces the magnification, but even with this reduction, the amplitude is still large enough to cause excessive wear and sometimes even fracture.

Typically, systems have either more damping or are only partially resonant, with the resulting magnification for example, being only 2 to 5 times what it would have been if completely non-resonant.

Resonance is simple to understand if you view the spring and mass as energy storage elements-with the mass storing kinetic energy and the spring storing potential energy. When the mass and spring have no force acting on them they transfer energy back and forth at a rate equal to the natural frequency. In other words, if energy is to be efficiently pumped into both the mass and spring the energy source needs to feed the energy in at a rate equal to the natural frequency.

The damper, instead of storing energy, dissipates energy. Since the damping force is proportional to the velocity, the more the motion, the more the damper dissipates the energy.

Therefore a point will come when the energy dissipated by the damper will equal the energy being fed in by the force. At this point, the system has reached its maximum amplitude and will continue to vibrate at this level as long as the force applied stays the same.

If no damping exists, there is nothing to dissipate the energy and therefore, theoretically, the motion will continue to grow on into infinity.

## 2.3 Frequency response or modal model

In this section a brief description of the *Frequency response or modal* model will be given, but we will not focus too much on this because only basic knowledge will be necessary to understand obtained results for the system under study.

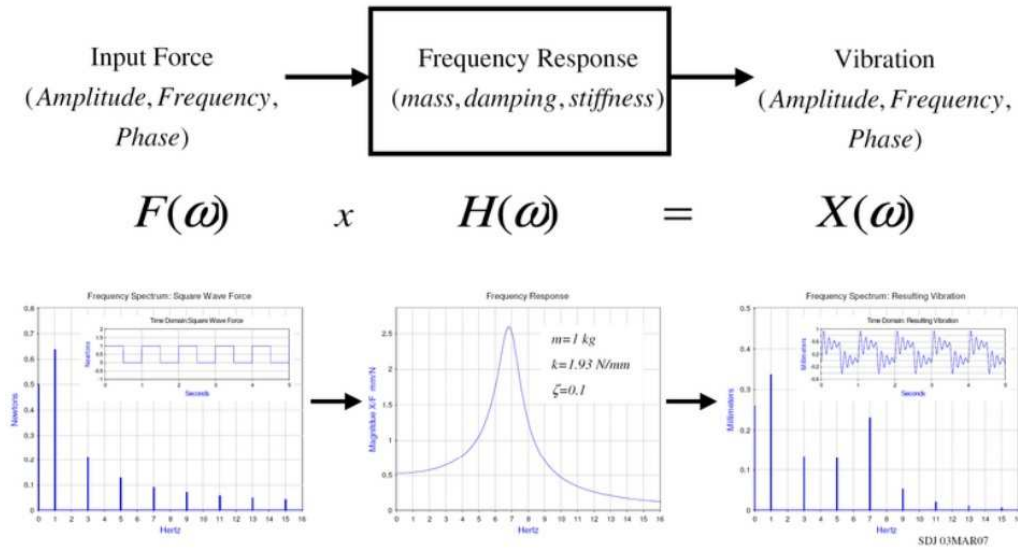


Figure 2.5. Frequency response model

The solution of a vibration problem can be seen as an input/output relation where the force is the input and the output is the vibration.

If we represent the force and vibration in the frequency domain (magnitude and phase) we can write the following relation:

$$X(\omega) = H(\omega) * F(\omega) \tag{2.12}$$

where the following mathematical notation is used:

- $X(\omega)$  : Fourier Transform<sup>3</sup> of the system response (output signal).
- $F(\omega)$  : Fourier Transform of the Applied external forces (input signal).
- $H(\omega)$  : Frequency Response Function (FRF)<sup>4</sup>.

All these variables are represented with complex numbers and so in general composed by two parts, a real component and an imaginary one or they can be

<sup>3</sup>In mathematics, the Fourier transform is the operation that decomposes a signal into its constituent frequencies. Actually it takes a signal, as a function of time (time domain), and breaks it down into its harmonic components as a function of frequency (frequency domain). More precisely, the Fourier transform transforms one complex-valued function of a real variable (time in vibrational studies) into another (frequency in vibrational studies)

<sup>4</sup>Frequency Response Function (FRF) is the measure of any system output spectrum in response to an input signal.

represented by their magnitude and their phase (this last one is more representative in vibrational matters).

For the single DOF system mass-spring-damper the *FRF* is described by the following complex quantity:

$$H(\omega) = \frac{X(\omega)}{F(\omega)} = \frac{\frac{1}{\bar{k}}}{\sqrt{(1-r^2)^2 + i(2\zeta r)^2}} \quad \text{where} \quad r = \frac{f}{f_n} = \frac{\omega}{\omega_n} \quad (2.13)$$

As aforementioned *FRF* can be also represented with its magnitude and phase components:

- The magnitude formula was presented earlier and is:

$$|H(\omega)| = \left| \frac{X(\omega)}{F(\omega)} \right| = \frac{\frac{1}{\bar{k}}}{\sqrt{(1-r^2)^2 + (2\zeta r)^2}} \quad (2.14)$$

- The phase formula is :

$$Ph(H(\omega)) = \arctan \frac{2\zeta r}{1-r^2} \quad (2.15)$$

Figure 2.3 shows the resulting vibrations for a mass-spring-damper system with a mass of 1 kg, spring stiffness of 1.93 Nmm and a damping ratio of 0.1.

It also shows the time domain representation of the resulting vibration. This is done by performing an inverse Fourier Transform that converts frequency domain data to time domain. In practice, this is rarely done because the frequency spectrum provides all the necessary information.

The frequency response function (FRF) does not necessarily have to be calculated from the knowledge of the mass, damping, and stiffness of the system, but can be experimentally measured .

For example, if a known force is applied, the frequency swept and then the resulting vibration measured , the frequency response function can be calculated and the system characterized.

This technique is used in the field of experimental modal analysis to determine the vibration characteristics of a structure and obviously to verify the accuracy of the mathematical model implemented.

## 2.4 Multiple degrees of freedom models

Clearly real life problems can't be studied often with a SDOF model but to reach a certain accuracy of results MDOF *multiple degree of freedom* models have been studied and implemented.

This last matter will not be handled in this paper but a few lectures on this issue are here recommended for a better understanding of the work that is treated in next chapters.

It is only remembered that a general MDOF mathematical model can always be expressed like this:

$$[M] \{\ddot{x}\} + [C] \{\dot{x}\} + [K] \{x\} = \{f\} \quad (2.16)$$

where symmetrical matrices  $[M]$ ,  $[C]$  and  $[K]$  and vectors  $\{x\}$  and  $\{f\}$  represents:

- $[M]$  : Mass matrix
- $[C]$  : Damping matrix
- $[K]$  : Stiffness matrix
- $\{x\}$  : displacements vector
- $\{f\}$  : force vector

Moreover it is important to notice that the *dimension* of the complete mathematical problem is equal to the number  $N$  of DOF considered, that means that the order of all the matrices is  $N \times N$  and for the vectors  $N \times 1$ .

Actually we study an infinite physical space, whose basis has infinite members, with a mathematical subspace whose basis consists of those  $N$  mode shapes taken into consideration.

The mathematical problem is an eigenvalues one, where the natural frequencies of the real system are provided exactly by the eigenvalues of the mathematical one (i.e.  $\omega_1^2, \omega_2^2 \dots \omega_N^2$ ) and eigenvectors represent the mode shapes  $[\phi] = [\{\phi_1\} \{\phi_2\} \dots \{\phi_N\}]$ .

In solving these kinds of problems lots of different mathematical ways have been followed; because of the big size of these problems (as aforementioned a real system has theoretically  $\infty$  DOF ) the focus of the solver is on the reduction of it without big losses in accuracy and this mathematical operation is called *modal truncation*.

We considered only those modes shapes whose natural frequencies are in the range of interest of our problem, and mainly mechanical one is that of low-medium frequencies.

A big mathematical system to solve leads to more expensive computational problems that means long resolution times.

Furthermore lots of numerical problems can be derived from a bad formulated mathematical model but, as aforementioned, this kind of issues will be not discussed in this paper.

### 2.4.1 FRF in multiple degrees of freedom systems

In this short section the definition of the *frequency response function* for a multiple degrees of freedom system is pointed out.

For these models the FRF, as well as the others quantities, is described by a  $N \times N$  matrix  $[H(\omega)]$ , where  $N$  is the number of degree of freedom considered.

The  $H_{ij}(\omega)$  component represents “*the response of the  $i$ -degree of freedom provoked by an unit harmonic force on the  $j$ -degree of freedom*” and in a damped model case is expressed by the following relation:

$$H_{ij}(\omega) = \sum_{r=1}^N \frac{\phi_{ir}\phi_{jr}}{(\omega_{n_r}^2 - \omega^2) + i(2\zeta_r\omega_{n_r}\omega)} \quad (2.17)$$

where

- $\phi_{kl}$  : is the  $k$ -component of the  $l$ -mode shape.
- $\omega_{n_r}$  : is the  $r$  natural frequency.
- $\zeta_r$  : is the  $r$ -damping ratio.

## 2.5 Finite Element method FEM

The finite element method (FEM) is a numerical technique for finding approximate solutions of partial differential equations (PDE) as well as of integral equations.

The solution approach is based either on eliminating the differential equation completely (steady state problems), or rendering the PDE into an approximating system of ordinary differential equations, which are then numerically integrated using standard techniques such as Euler method, Runge-Kutta, etc.

The goal of modal analysis in structural mechanics is to determine the natural mode shapes and frequencies of the studied system during free vibration, that is its modal properties, in order to have the possibility of studying the response to whatever kind of exciting force.

It is common to use the finite element method (FEM) to perform this analysis because, like other calculations using the FEM, the object analyzed can have arbitrary shape and the results of the calculations are often accurate enough.

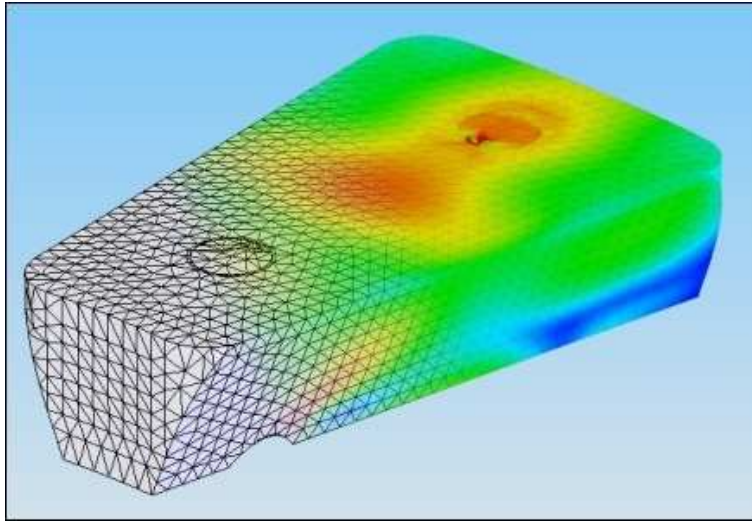


Figure 2.6. discretized model and FEM analysis results

The types of equations which arise from modal analysis are those typical of eigensystems as outlined before.

It is also possible to test a physical object to determine its natural frequencies and mode shapes. This is called an *Experimental Modal Analysis*.

The results of the physical test can be used to calibrate a finite element model, thus establishing if the underlying assumptions made were correct (for example, correct material properties and boundary conditions were used) and using for example an *updating technique* it is possible to improve the Finite element model.

### 2.5.1 Geometry mesh

In finite elements analysis the system geometry is broken into discrete elements interconnected at discrete node points; this operation is called *mesh* that therefore is a discretization of a continuous domain into a set of discrete sub-domains, usually called elements (see fig. 2.6).

The governing equations are solved in these sub-domains and must satisfy the boundary conditions (coherence equations) due to the close elements or to the constraints and the forces acting on the system.

It is also important to notice that using an appropriate mesh yields to less computationally expensive problems, thickening the discretization in those parts that are more complicated or important thus arising the accuracy (increasing the number of DOF) only there (see fig: 2.7).

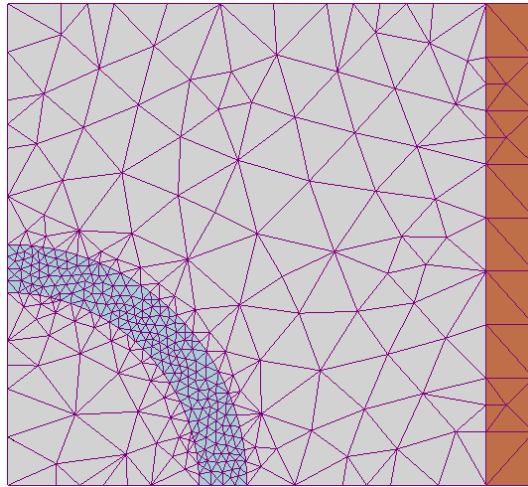


Figure 2.7. 2D geometry mesh: mesh is denser around the object of interest

## 2.6 Spectral Analysis

Spectral methods are a class of techniques used in applied mathematics and scientific computing to numerically solve certain partial differential equations (PDEs), often involving the use of the Fast Fourier Transform. Where applicable, spectral methods have excellent error properties, with the so called “exponential convergence” being the fastest possible.

The spectral method and the finite element method are closely related and built on the same ideas; the main difference between them is that the spectral method approximates the solution as linear combination of continuous functions that are generally nonzero over the domain of solution (usually sinusoids or Chebyshev polynomials), while the finite element method approximates the solution as a linear combination of piecewise functions that are nonzero on small subdomains.

Because of this, the spectral method takes on a global approach while the finite element method consists of a local approach. This is part of why the spectral method works best when the solution is smooth.

Moreover in the spectral method the basis of the mathematical space doesn’t consist of the eigenvectors<sup>5</sup> of a mathematical sub-space resulting from the finite number of DOF used, as in the FEM model, but contains some eigen-functions of the total, infinite mathematical space and doing so it introduces less error in the formulation of the problem.

For these reasons a spectral model can be considered a particular case of a modal model that can be used only for simple cases and simple geometries.

---

<sup>5</sup>in large problems only some eigenvectors of the sub-space are considered, using a *modal truncation* analysis, already discussed in section 2.4, and decreasing the accuracy of the model.



It is also important to notice that in vibration problems this last method has not encountered yet good results, apart from few simple cases.

Notwithstanding the last consideration, this last mathematical method will be used to model rails, sleepers and underlying structure of the trail-way studied, using a mathematical space whose basis is given by the Euler-Bernoulli beam theory or Timoshenko one.

# Chapter 3

## Mathematical Model definition

### 3.1 Substructuring Techniques

#### 3.1.1 Substructuring analysis benefits

In order to have the possibility of studying a vehicle-track system dynamic response it is important to develop a good analytical model as well detailed as simple to solve with a low cost computational problems.

The goals to achieve to obtain a good model are:

- build up a good mathematic model whose governing equations reflect well the real system and are as simple as possible to solve;
- obtain a modular model, that is obtaining a model in which all single components are independent of each other. This will permit model future improvements or developments without the need of building up a new one;
- finally the model must obviously be usefull for the analysis or design of track or vehicle elements.

As anticipated in the introduction chapter 1.1, the vehicle model has been considered like *spatial* (or physical) with a *lumped element model* approach, with the inertial properties centered in the centers of gravity of the wheel-sets, of the bogies and of the carriage. This choice is due to the fact that the elasticity properties of the vehicle elements have a small effect on the vertical dynamics of the medium frequencies.

For this reason it is possible to consider the elements like rigid bodies with point of reference coordinates in their modeling.

Thanks to this modeling choice a sensible reduction of the DOF of the problem was possible without a relevant loss in accuracy regarding vertical dynamics.

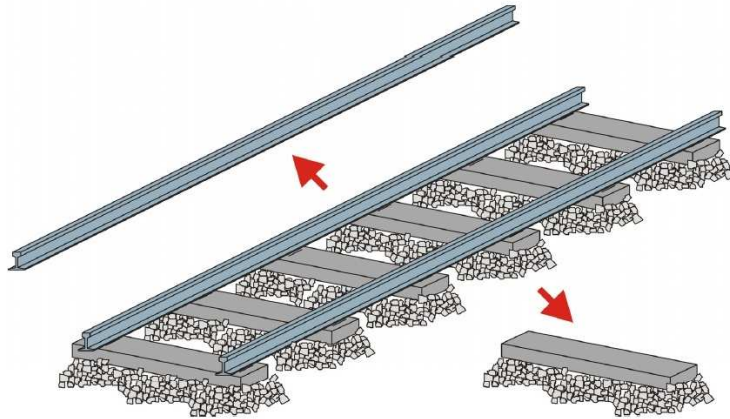


Figure 3.1. Substructuring of a conventional track over ballast. Substructures:  
Rails and sleepers over ballast

The track is a structure whose dimensions are bigger than those of the vehicle. It is a continuous system with a considerable length; for this reason the dimension of its mathematical model could be problematic because it is necessary to correctly represent the deformation of whatever point on it.

To obtain good results FEM programs could be used but this would lead to high cost computationally problems.

A very important simplification of the problem can be obtained when constant properties are considered for the ballast along the track-way or at least if it is modelled through the use of discrete lumped elements.

So, from a longitudinal point of view, the system is composed by two rails supported by equidistant sleepers.

Considering then that rails and sleepers can be modelled as simple beams, a great simplification of the model can be achieved, this because of the simplicity of these elements and also because in this way their dynamic characterization is the same.

A *substructuring approach* leads so to considerable benefits, also in the development of the problem, because it permits to treat independently the different structures, using also more than one of the methods introduced in the previous chapter, and to assembly the total model only in the end, thanks to appropriate constraint equations.

### 3.1.2 Modal reduction

After obtaining the dynamical properties of the different structures another important step is to reduce the dynamic model order, that is to eliminate some degrees

of freedom of the different structures, doing it in spatial or modal coordinates, obviously depending on which mathematical model have been chosen for each one.

To make this reduction first of all it must be considered in which range of frequencies the structure will be mainly excited from applied forces, in order to operate with a *modal truncation* analysis, because this is the range of natural frequencies from which the total response will depend on.

After this, surely others considerations must be kept in mind in operating a DOF reduction and lots of methods have been developed for this, but they will not be treated here for obvious reasons.

### 3.1.3 Chosen model

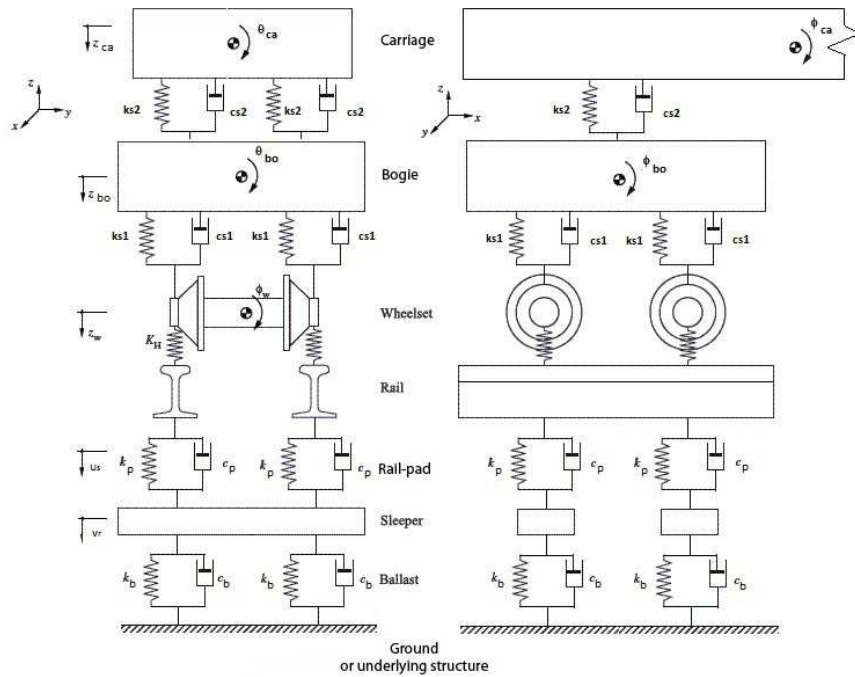


Figure 3.2. Dynamic model of the interactive vehicle/track-structure system

In figure 3.2 it is possible to see the general form of the model used<sup>1</sup> for the vehicle-track-structure system where all the interconnection between different structures and also the reference system are shown.

<sup>1</sup>Actually the vehicle and also other subparts can vary in dimension depending on the level of system complexity required

It should be noticed already that the program has been developed with the possibility of changing the complexity of this model, and for this reason the user is asked to chose the number of degrees of freedom for the various parts of the vehicle/es<sup>2</sup> as well as the number of sleepers and the number of modal shapes with which modeling the various beams etc. etc.

Finally it is reminded that a modular approach was used in this work and so the program offers also the possibility of getting the problem more complicate, giving the possibility of assigning to the vehicle more degrees of freedom of those necessary in this specific work, this made in case future developments would need them.

All of this has been done to permit an increasing in the future of the DOF of rails and sleepers, for instance in order to studying also transversal vibrations.

## 3.2 Analysis of the Substructures

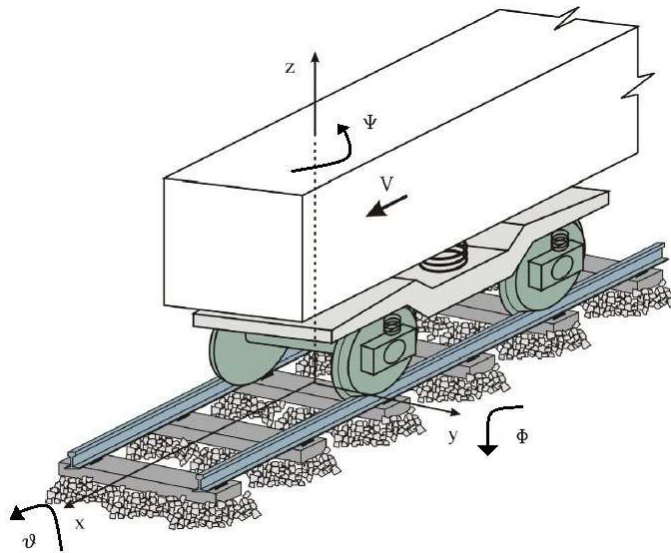


Figure 3.3. global reference system

In next sections the dynamic governing equations of each structure of the total system are developed. First of all are described the substructures studied with a modal approach, more precisely a spectral one, that in this case are the sleepers and the rails; the following describes those ones modelled with physical coordinates, here, vehicle components.

<sup>2</sup>it is also possible to run less computationally expensive simulations with only half of the total vehicle as well as one quarter of the same, removing DOF from the various parts

Finally the constraint equations of the interconnection elements between different parts are developed.

In figure 3.3 the global reference system is shown. During the course of this chapter the meaning of all necessary variables will be defined but it is here anticipated that in general:

- Superscripts of the main variable stands for the element to which the property refers to or that applies it.
- Subscripts stand for the numeration of the various components related to each other.
- Terms in brackets, obviously ,stand for the function independent variables.

For instance,  $F_{r,s}^p(t)$  is the time dependent load that p-rail-pad applies on r-rail from s-sleeper.

### 3.3 Elements studied with modal coordinates

In this thesis work, as aforementioned , a spectral model, that it is a particular case of a modal approach, was used for rails and sleepers.

Their model scheme are shown in figures 3.4 3.5.

#### 3.3.1 Rails

In figure 3.4(a) it is shown a single rail placed on different sleepers with a two wheelsets bogie over it. In figure 3.4(b) it is shown a possible deformation of the rail due to actuating forces.

The displacement of the neutral axis in respect of the unloaded equilibrium position of this element is defined by the variable  $v_r(x,t)$ , where  $x$  is the longitudinal distance of the considered section from one of the rail extremes and  $t$  the time.

The positive direction of the  $x$ -axis in given by the train direction of motion.

The forces that produce the rail deformation arise from the rail-sleepers and rail-vehicle interactions and more exactly from the railpads<sup>3</sup> and wheels.

The following mathematical notation will be used for these contact forces:

- $F_{r,s}^p(t)$  : is the force that  $p$ -railpad applies on rail  $r$  from sleeper  $s$  and it is composed by two components:

---

<sup>3</sup>they are usually called railway fastening setting pads but to be brief they will be here addressed to with “railpads”

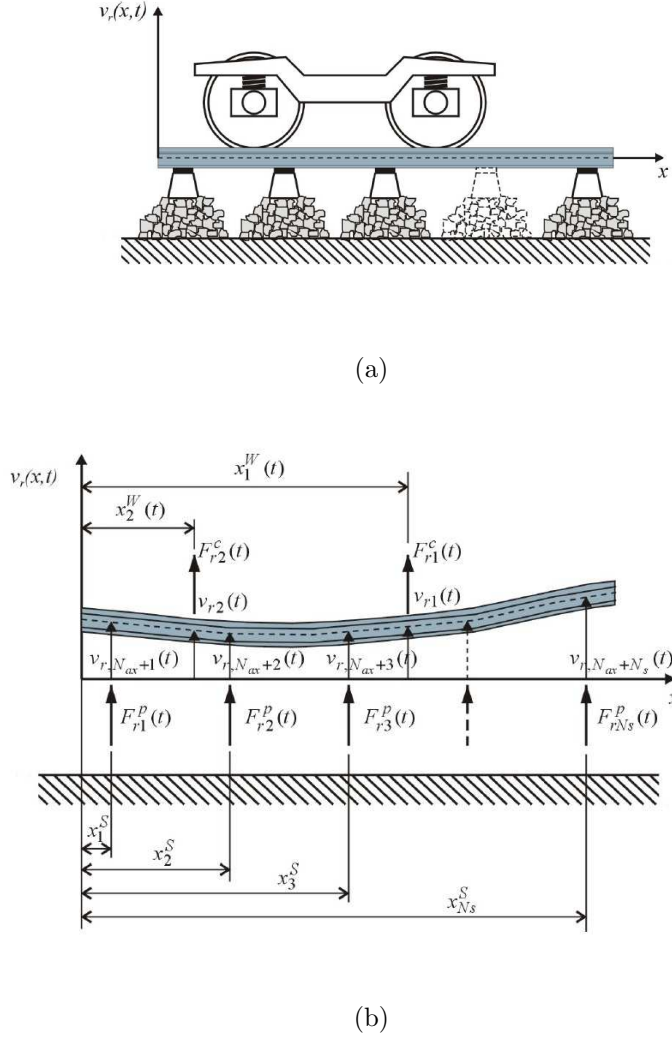


Figure 3.4. (a) graphical representation of a two wheelset bogie on a conventional track over ballast;(b) rail free body graphic and acting forces

- a linear one, given by the stiffness force and a damping one;
  - a non linear that is user-choice.
- $F_{r,a}^c(t)$  : is the contact force on  $r$ -rail arising from the respective wheel of the  $a$ -wheelset that has been modelled with an *hertzian* contact force.

As illustrated in figure 3.4(b) all the forces have been considered positive if upward. The application points of the forces correspond to the connection points

of the rails with the others substructures. The x-coordinate of railpad connection points doesn't depend on time  $t$  and coincides with relative sleeper x-position.

The distance between the application point of this force and the left extreme of the rail is given by  $x_s^S$  variable, where superscript  $S$  suggests that it refers to a *sleeper* connection point and subscript  $s$  points out which one it is considered assuming values from 1 to  $N_s$  that is the total number of sleepers.

On the contrary the contact position between wheel and rail depends on time  $t$  and is function of train velocity  $V$ . The distance from the left rail extreme and the application point of the relative force is:

$$x_a^W(t) = x_{a_0}^W + \int_0^t V(t)dt \quad (3.1)$$

where:

- superscript  $W$  reminds that  $x$  refers to a *wheelset* coordinate ;
- subindex  $a$  refers to which wheelset is considered and assumes values from 1 to  $N_{ax}$ , number of vehicle wheelsets;
- $x_{a_0}^W$  is the initial position ( $t = 0$ ) of the  $a$ -wheelset.

For these reasons the rail deformation is in general a function of  $x$  distance and time  $t$ , while in connection coordinates it is only function of  $t$  and is given by:

- $v_{r,a}(t)$  for  $a$ -wheel and  $r$ -rail contact point;
- $v_{r,N_{ax}+s}(t)$  for  $r$ -rail and  $s$ -sleeper contact point<sup>4</sup>.

### 3.3.2 Sleepers

As for the rail, in figure 3.5(a) it is shown a singular sleeper placed over the ballast that supports two transversal rails, symmetrically placed over it.

The vertical deflection of the  $s$ -sleeper is given by  $u_s(y,t)$  function, where  $y$  transversal coordinate of the system is positive in the leftward sense relative to the Vehicle direction of motion.

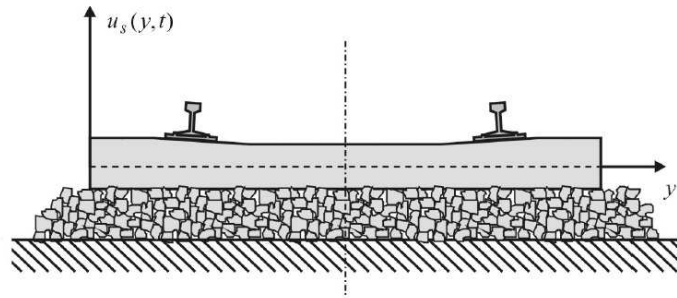
The forces acting on the sleeper isolated from the other substructures are shown in figure 3.5(b) and are:

- $F_{s,r}^p(t)$  ( $r = 1,2$ ) : this is the force caused by the rail  $r$  and transmitted through railpads (superscript  $p$ ) to sleeper  $s$  for each rail  $r$ ;

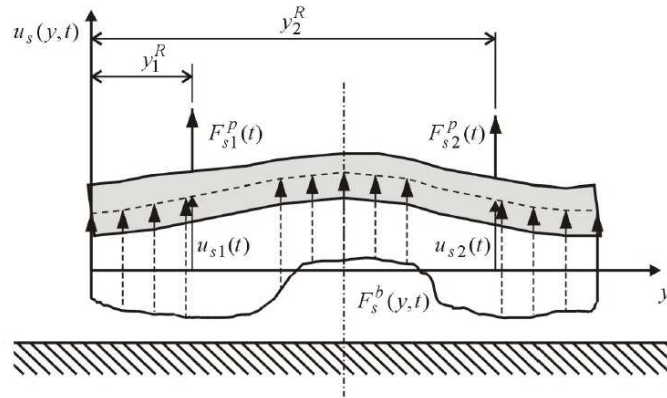
---

<sup>4</sup>in this way there will be  $N_{ax} + N_s$  rail deformation  $v$  values for each time  $t$  and the pads numeration will follow continuously the wheels one.





(a)



(b)

Figure 3.5. (a) graphical representation of a sleeper on a conventional track over ballast;(b) rail free body graphic and acting forces

- $F_s^b(y, t)$  : this represents the pressure distribution due to the presence of the ballast function of the  $y$  transversal position and of the time  $t$ .

The second forces have a difficult behavior to model because the ballast properties are usually non-linear and also not well known. A  $c_b$  viscous damping coefficient more a non-linear user choice function have been used to model the damping and non linear properties added by the ballast.

Whereas for the stiffness properties two different mathematical models have been implemented in the program:

1. the use of Winkler Foundation model<sup>5</sup> (see Annex B) ;
2. a simple distribution of discrete springs with a constant or variable  $k$  coefficient.

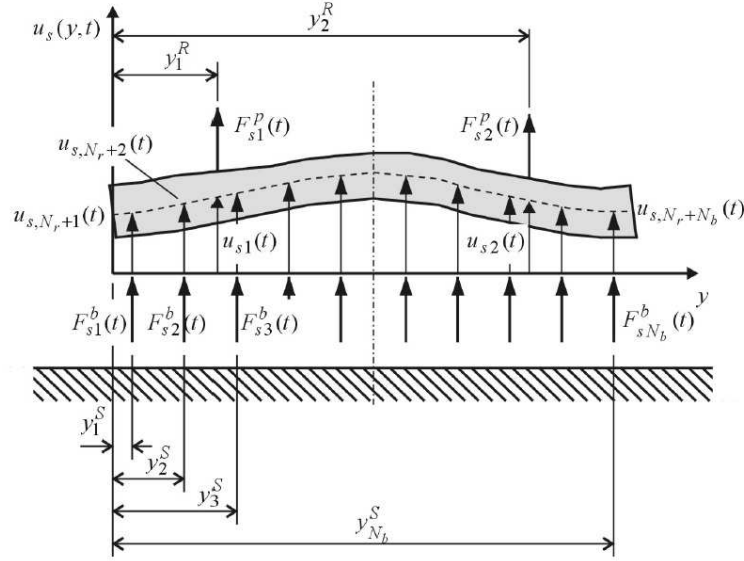


Figure 3.6. Sleeper over ballast model: discrete distribution of punctual forces more eventual elastic Winkler Foundation

The forces due to rails interactions and transmitted through railpads are applied at a constant  $y_r^R$  position from the left sleeper extreme, positions that are so independent from time  $t$ . Moreover these forces have the same module of those applied to the rails through the railpad in figure 3.4, that is  $F_{s,r}^P(t) = -F_{r,s}^P(t)$ .

The complex of forces acting on the sleeper are illustrated in figure 3.6 where al the single  $F_{s,r}^b$  can include the stiffness component or not depending on the model chosen by the user.

The deformation value is a time function and is given by:

- $u_{s,r}(t)$  for connection points between rail  $r$  and sleeper  $s$ ;
- $u_{s, N_r+b}(t)$  for the application point of punctual force  $F_{s,b}^b(t)$  on sleeper  $s$ .

<sup>5</sup>this model can not be used when a case of vehicle-track-structure interaction is studied

### 3.3.3 Underlying structure

When an interaction with an underlying structure is simulated, this last subpart is modelled by its modal coordinates, that is its modal shapes and natural frequencies.

These properties can be obtained with a simple pinned-pinned beam (using an Euler approach) or with a *FEM* simulation of the structure that obviously would led to more accurate results.

Using a mono-dimensional approach with  $N_{Br}$  degrees fo freedom means that the structure would have only the possibility of a vertical displacement  $w^{Br}(x,t)$  and so the distribution of ballast forces represented in figure 3.6 would depend also from this further displacement as illustrated in figure 3.7.

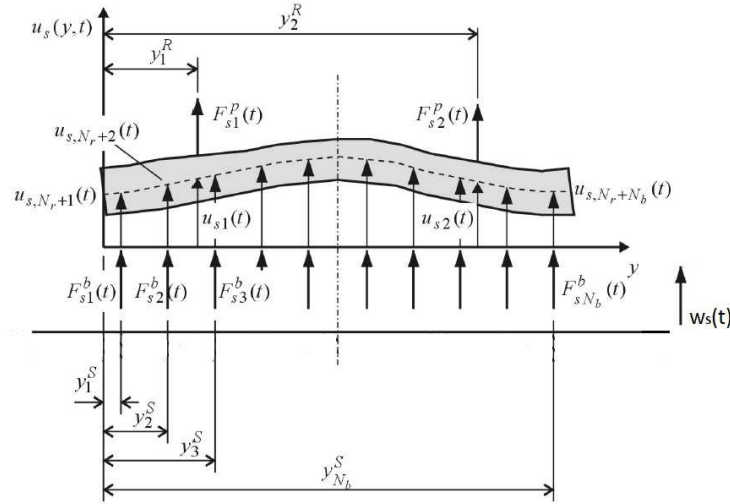


Figure 3.7. Sleeper over ballast on an underlying structure model

Doing so both sides of interconnection elements will move; at the bridge side it moves of a  $y$  independent value  $w_s^{Br}(t)$  while at the sleeper one of a  $y$ -dependent value  $u_s(y,t)$ .

### 3.3.4 Vibration mode shapes

Rails, sleepers and optional underlying structure dynamic behaviour equations, as aforementioned, are introduced in the model through their modal coordinates using a spectral approach. The mathematical relation between the modal coordinates and physical ones is given by the *modal transformation* expressed, in equations (3.2), (3.3) and (3.4) respectively for rails, sleepers and substructure:

$$v_r(x,t) = \sum_{m=-1}^{N_{mr}} \phi_m(x) q_{r,m}^R(t)^6 \quad (3.2)$$

$$u_s(y,t) = \sum_{n=-1}^{N_{ms}} \psi_n(y) q_{s,n}^S(t)^6 \quad (3.3)$$

$$w_b(x,t) = \sum_{l=1}^{N_{mBr}} \varphi_l(x) q_l^{Br}(t)^7 \quad (3.4)$$

where the used variables have the following meaning:

- $\phi_m(x)$  and  $q_{r,m}^R$  represent respectively the  $m$ th-vibration shape for the undamped problem and the relative modal coordinate (amplitude) of the same mode  $m$  of the rail  $r$ ;
- $\psi_n(y)$  and  $q_{s,n}^S$  represent respectively the  $n$ th-vibration shape for the undamped problem and the relative modal coordinate (amplitude) of the same mode  $n$  of the sleeper  $s$ ;
- $\varphi_l(x)$  and  $q_l^S$  represent respectively the  $l$ th-vibration shape for the undamped problem and the relative modal coordinate (amplitude) of the same mode  $l$  of the underlying structure;

It is very important to notice that, in both cases, modes of vibration  $\phi_m(x)$ ,  $\psi_m(y)$  and  $\varphi_l(x)$  are function only of the space variable and, considering an Euler-Bernoulli theory, depend only on the main length of the structure modelled as a beam; for this reason their expression is the same for every rail or sleeper considered and do not depend on beam physical properties.

On the other hand modal coordinates  $q_{r,m}^R$ ,  $q_{s,n}^S$  and  $q_l^S$  depend only on the  $t$  time variable and doing so the problem has been splitted in two independent parts, using the *separation of variables* mathematic method.

Watching carefully equations (3.2), (3.3) and (3.4) it can be seen what aforementioned in section 2.6, that the function space of rails, sleepers or underlying structure possible deformations can be described using a mathematical basis made by the respective mode shapes.

---

<sup>6</sup>m and n numerations start from -1 in free-free beam case whereas in the continuous one they start from 0 as described later in this subsection

<sup>7</sup>in this last case the beam can't have rigid body modes

It will be sufficient to linearly combine the basis members, using appropriate coefficients, to obtain a representation of the total space<sup>8</sup>, and in the studied system these coefficients are the modal coordinates.

It is important to notice that a physical space basis would have an infinite order but using a *modal truncation* analysis only  $N_{mr}$ ,  $N_{ms}$  and  $N_{mBr}$  members (modes) of the total infinite basis are used for rails, sleepers and bridge, respectively.

Notice that this mathematical choice is possible because in reality only a finite number of vibration modes contributes to the system response and generally in mechanical systems these are those at low frequencies.

System range of interest is more or less from 0 to maximum 4000 Hz and so, in the model here considered, only those modes whose natural frequencies fall in this range are taken into consideration.

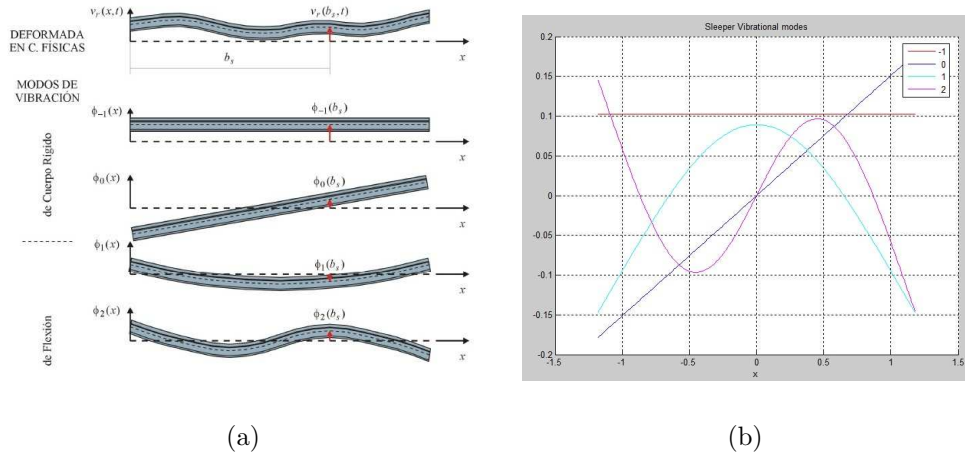


Figure 3.8. First four mode shapes for a free-free constrained monodimensional beam, 2 rigid body modes (-1 & 0) and 2 flexural ones (1 & 2)

To obtain these mode shapes lots of mathematical models have been developed, analytical, numerical and also experimental ones.

Generally, vibration modes are divided in two categories:

- rigid body modes
- flexural modes

<sup>8</sup>In mathematics, a basis function is an element of a particular basis for a function space. Every function, in the function space, can be represented as a linear combination of the basis functions, just as every vector in a vector space can be represented as a linear combination of the basis vectors.

In this thesis work, both an Euler-Bernoulli approach and a Timoshenko one have been used to obtain Rails and sleepers mode shapes, and in addition two different boundary conditions (B.C.) have been implemented for each beam theory :

1. free-free beam boundary conditions
2. continuous beam boundary conditions

Comparisons of the results have been analyzed as described in later chapters and in general it is important to notice that, especially in the rails case, both kinds of B.C. give rise to significant results only away from extremes, this due to obvious reasons.

In figure 3.8(a) the first four modes of a free-free constrained beam are shown, and in figure 3.8(b) are plotted the respective functions calculated with matlab.

This beam theory, with both boundary conditions models are carefully explained in Annex A Here it is only remembered that for a continuous monodimensional beam only one of the two rigid body modes is possible, obviously the rigid translation.

In the system analyzed a free-free model is preferable for sleepers, that in fact do not have constrains at the extremes, while the continuous one is better for rails to prevent oscillating waves from turning back at the righth extreme thus influencing rail dynamics under the vehicle load (with a continuous model the wave would restart from the left extreme and due to the damping effect it would fade away before reaching the first wheelset of the train).

Concerning the mode shapes of the bridge a pinned-pinned beam has been used where no rigid body modes are possible.

The numeration followed for these beam modes is:

- $m = -1, 0, \dots, N_m$  for the free-free beam;
- $m = 0, 1, \dots, N_m$  for the continuous beam;
- $m = 1, \dots, N_m$  for the pinned-pinned beam;

reserving, in doing so, the positive values for the flexure mode shapes.

Using a *Real damping approach* the mode shapes of the beam are obtained considering that they are the same that would have an undamped beam, and after obtaining these modes a certain degree of damping will be introduced in the model considering a constant modal damping coefficient for each vibration mode :  $\zeta_m$  for rails,  $\xi_n$  for sleepers and  $\mu_l$  for the structure.

### 3.3.5 Governing differential equations in modal coordinates

The governing equations of the dynamic behaviour of  $r$ th rail,  $s$ th sleeper and of the bridge, considering natural vibration modes and modal damping, are:

$$\ddot{q}_{r,m}^R(t) + 2\zeta_m \lambda_m \dot{q}_{r,m}^R(t) + \lambda_m^2 q_{r,m}^R(t) = f_{r,m}^R(t) \quad \text{where } m = -1^9, 0, 1, \dots, N_{mr} \quad (3.5)$$

$$\ddot{q}_{s,n}^S(t) + 2\xi_n \omega_n \dot{q}_{s,n}^S(t) + \omega_n^2 q_{s,n}^S(t) = f_{s,n}^S(t) \quad \text{where } n = -1^9, 0, 1, \dots, N_{ms} \quad (3.6)$$

$$\ddot{q}_l^{Br}(t) + 2\mu_l \tau_l \dot{q}_l^{Br}(t) + \tau_l^2 q_l^{Br}(t) = f_l^{Br}(t) \quad \text{where } l = 1, \dots, N_{mBr} \quad (3.7)$$

where the meaning of all used variables is:

- $\lambda_m$ ,  $\omega_n$  and  $\tau_l$  are respectively the  $m$ th rails natural angular frequency, the  $n$ th sleepers and the  $l$ th underlying structure one;
- $\zeta_m$ ,  $\xi_n$  and  $\mu$  are the modal damping coefficients relative to the  $m$ th rail mode shape, to the  $n$ th of the sleepers and to the  $l$ th of the underlying structure;
- $f_{r,m}^R(t)$ ,  $f_{r,m}^R(t)$  and  $f_l^{Br}(t)$  are the modal forces relative to the  $m$ th rail mode shape, to the  $n$ th sleeper mode and to the  $l$ th mode of the underlying structure;

$f_{r,m}^R(t)$ ,  $f_{r,m}^R(t)$  and  $f_l^{Br}(t)$  modal forces can be obtained from those deriving from the wheel contact, the railpads and the ballast using the modal transformations defined by equations (3.8) (3.9) (3.10)

$$f_{r,m}^R(t) = \sum_{a=1}^{N_{ax}} F_{r,a}^c(t) \phi_m(x_a^W(t)) + \sum_{s=1}^{N_s} F_{r,s}^p(t) \phi_m(x_s^S) \quad (3.8)$$

$$f_{s,n}^S(t) = \sum_{r=1}^{N_r} F_{s,r}^p(t) \psi_n(y_r^R) + \sum_{b=1}^{N_b} F_{s,b}^b(t) \psi_n(y_b^S) \quad (3.9)$$

$$f_l^{Br}(t) = \sum_{s=1}^{N_s} F_{s,br}^{b'}(t) \varphi_l(x_s^{Br}) \quad (3.10)$$

where:

- $\phi(x_a^W(t))$ ,  $\phi_m(x_s^S)$  are the values of the  $m$ th rail mode evaluated in the application points of the two forces  $F_{r,a}^c(t)$  and  $F_{r,s}^p(t)$  ;

---

<sup>9</sup>here also m and n numerations start from -1 in free-free beam case whereas in the continuous one they start from 0

- $\psi(y_r^R)$  and  $\psi_m(y_b^S)$  are the values of the  $n$ th sleeper mode evaluated in the application points of the two forces  $F_{s,r}^p(t)$  and  $F_{s,b}^b(t)$  ;
- $\varphi_l(x_s^{Br})$  is the value of the  $l$ -mode of the underlying structure evaluated in application points of  $F_{s,b}^{b'}(t)$  forces, that actually coincide with sleepers x-positions.

In equation (3.10) the  $F_{s,b}^{b'}(t)$  force acting on  $br$ -underlying structure point is the sum of all the forces  $F_{s,b}^b(t)$  exchanged between sleeper interconnection elements and the structure; in fact the force deriving from a set of springs connected in parallel is equal to the sum of the single forces.

With all these assumptions it can be built up a model for a conventional track and for a specific case of  $N_r$  rails,  $N_s$  sleepers and an optional underlying structure, there will be  $N_r$  differential equations systems for the rails represented by the (3.8) equations system,  $N_s$  for the sleepers represented by the (3.9) and an optional last system for the underlying structure (3.10).

### 3.4 Elements modelled with physical coordinates

In this section the vehicle modeling used in this track interaction study is described.

In these kinds of problems lots of vehicles types have been used and usually they consist of a single bogie with two wheelsets that supports the weight of the Carriage but, as it will be discussed in the program chapter, the software developed gives to the user the possibility of choosing which model to use that, as a matter of fact, can choose the number of any element as well as all the main properties of each one and also their degrees of freedom.

Using a Lumped element approach all the elements of the vehicle ( Carriages, bogies and sleepers ) have been treated like rigid bodies with a punctual mass centered on the center of gravity; the suspensions have been modelled with linear springs and viscous dampers placed between wheelsets and bogies (*primary suspensions* ) and between bogie and Carriage ( *secondary suspensions* ).

In figure 3.9 is shown a possible vehicle configuration with :

- 2-degrees of freedom carriage.
- 3-degrees of freedom bogie.
- 2-degrees of freedom wheelsets.

Considering that, studying only vertical dynamics, different carriages would not interact with the others a total model could be considered that of 1 carriage (3 DOF),



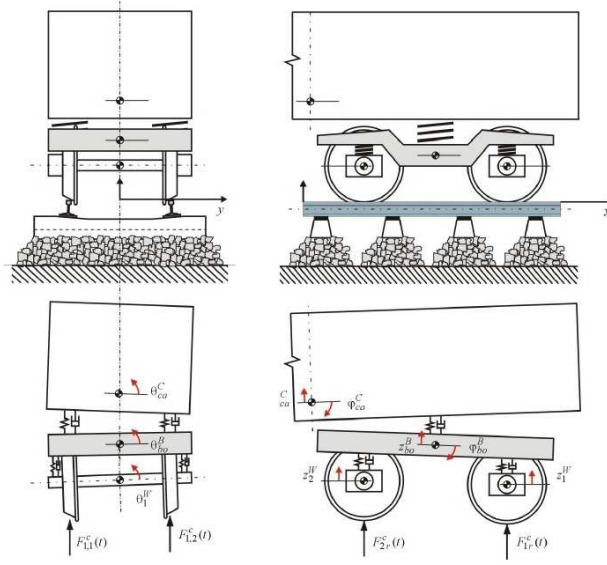


Figure 3.9. Rail Vehicle representation and lumped element modeling

2 bogies (3 DOF) and 4 sleepers (2 DOF) with a total of 12 primary suspensions and 4 secondary ones.

With this consideration, figure 3.9 shows half of the total model and the program gives also the possibility of studying only one quarter in order to reduce problem size.

Notice that, in the future, it would be interesting to continue in developing the program to permit the analysis of transversal dynamics and, for this reason, the vehicle can already assume lots of others configurations that in this particular study are useless but have been implemented anyway because of the modular approach used.

Using the *small displacement theory*, the reference coordinates are punctual ones and for the total vehicle case are illustrated in the following vector :

$$w(t) = [z_1^W \quad \vartheta_1^W \quad z_2^W \quad \vartheta_2^W \quad \dots \quad z_1^B \quad \vartheta_1^B \quad \varphi_1^B \quad \dots \quad z_1^C \quad \vartheta_1^C \quad \varphi_1^C \quad ] \quad (3.11)$$

where:

- $z_a^W$  and  $\vartheta_a^W$  are respectively the vertical displacement and the roll (rotation around x-axis) of *ath* wheelset ( $a = 1, \dots, N_{ax}$  where  $N_{ax}$  is the total number of wheelsets);
- $z_{bo}^B$ ,  $\vartheta_{bo}^B$  and  $\varphi_{bo}^B$  are respectively the vertical displacement, the roll (the rotation around x-axis) and the pitch (rotation around y-axis) of the *bo-th* bogie ( $bo = 1, \dots, N_{bo}$  where  $N_{bo}$  is the total number of bogies used in the model);

- $z_{ca}^C$ ,  $\vartheta_{ca}^C$  and  $\varphi_{ca}^C$  are respectively the vertical displacement, the roll rotation and the pitch one of the  $ca$ -th Carriage ( $ca = 1, \dots, N_{ca}$  where  $N_{ca}$  is the total number of carriages used in the model that in general is one<sup>10</sup>);

The positive sense of displacements and rotations is that of the arrows illustrated in figure 3.3.

### 3.4.1 Equation of motion

The equation of motion of the vehicle in matrix form is:

$$\mathbf{M}\ddot{\mathbf{w}} + \mathbf{D}\dot{\mathbf{w}} + \mathbf{K}\mathbf{w} = \mathbf{F}^{ext} + \mathbf{F}^c \quad (3.12)$$

where  $\mathbf{M}$ ,  $\mathbf{D}$  and  $\mathbf{K}$  are respectively the mass matrix, the viscous damping matrix and the stiffness one;  $\mathbf{F}^{ext}$  is the external forces vector, like the weight and possible suspensions non-linear components could be.

Finally  $\mathbf{F}^c$  includes the forces acting over the DOF of the model due to the forces transmitted in the contact between wheelsets and rails  $F_{a,1}^c(t)$  and  $F_{a,2}^c(t)$  that have the same module and opposite verse of the forces acting on the rail in figure 3.4(b).

## 3.5 Constraint equations

In prior section total system coordinates, for all different substructures, have been defined; at the same time also their governing equations of the dynamic behaviour were established and all of this brings to a system of second order ordinary differential equation *ODE*.

To complete the model, as aforementioned, it is necessary to establish the interaction relationships between the different subparts, that could be defined with specific *constraint equations*.

In the track system, the contact between wheelsets and rails, the rails fixing points and the ballast dynamic characteristics (apart from the linear stiffness if a Winkler's one is used) will establish the relative movement constraints between vehicle, rails, sleepers and bridge or undeformable ground.

It is important also to notice that the ballast mass contribution is considered included in its dynamic properties while the platform is considered with an infinite mass and infinitely rigid differently from the bridge that has its own mode shapes.

---

<sup>10</sup>for the half model case or the 1/4 one the number of carriages is 1 and its mass decreases (1/2 or 1/4) as well as for the bogie which mass halves in the 1/4 model case

### 3.5.1 Wheel-rail contact

The mathematical model chosen for the wheel-rail contact is that called *hertzian contact*. This model is actually well studied and tested for this kind of contact.

The hertzian contact mathematical expression used is :

$$F_{r,a}^c(t) = k_H \delta_{r,a}^{3/2}(t) \quad (3.13)$$

where the following notation was used:

- $F_{r,a}^c(t)$  is the contact force that acts between  $a$ -wheelset and  $r$ -rail;
- $k_H$  is the stiffness of the equivalent contact spring whose S.I. unit is  $[N/m^{3/2}]$ ;
- $\delta_{r,a}(t)$  is the *indentation* or penetration distance between the bodies considered as rigid ones and due to the deformation on the contact zone.

The value of  $k_H$  depends on the elastic and geometrical properties of the contact bodies.

The mathematical *indentation* expression is:

$$\delta_{r,a}(t) = z_{a,r}(t) - v_{r,a}(t) - irr_{r,a}(t) \quad (3.14)$$

where:

- $z_{a,r}(t)$  is the contact point vertical position of the  $a$ -wheelset wheel which rests on  $r$ -rail;
- $v_{a,r}(t) = v_r(x_a^W(t), t)$  is the vertical position of  $r$ -rail contact point with  $a$ -wheelset wheel;
- $irr_{r,a}(t)$  is the irregularities component of  $a$ -wheelset wheel and  $r$ -rail contact surface.

Wheel and rail imperfections are accounted for by an irregularity function, which is defined as the vertical wheel displacement assuming no loss of contact and undeformable wheel and track. A characteristic type of irregularity is associated with the wheelflat.

There are many types of irregularities functions  $irr_{r,a}(t)$  that can be introduced in the system, and it is also important to notice that rails imperfections actuate only in discrete points (i.e. railway joints) or are distributed along the all path (i.e. rail corrugation ) while wheels ones have obviously a periodic effect on the system;

Bearing in mind that a fresh flat is reshaped into a rounded flat shortly after being formed, a cosine function to represent the irregularity function for a rounded flat is

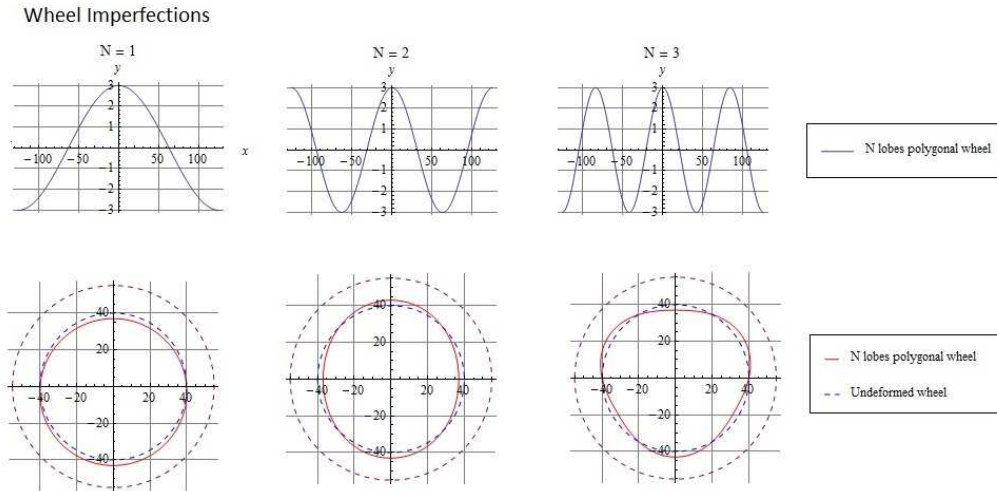


Figure 3.10. N lobes polygonal wheel examples

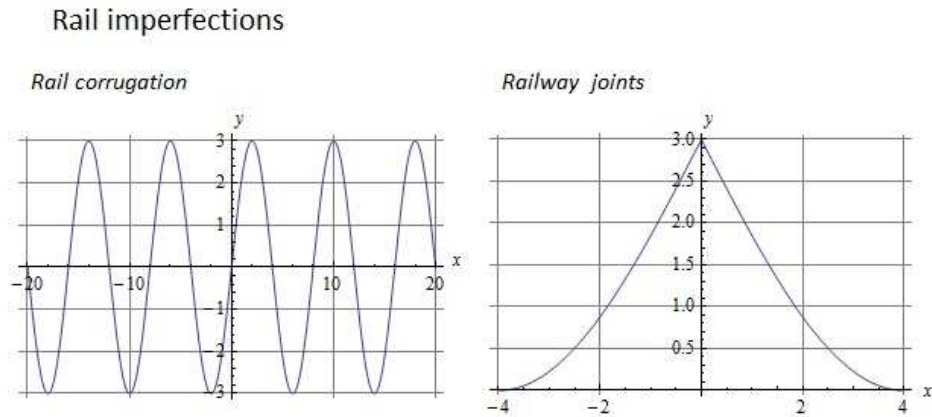


Figure 3.11. Rails imperfections examples

often adopted. In figures 3.10 3.11 some types of irregularities functions commonly used respectively for rails and wheels are shown .

Let:

- $H$  : irregularity amplitude;
- $R$  : Wheel radius;
- $\text{Sign}(x)$  : x-signus (-1, 0 or 1 depending on whether x is negative, zero, or

positive.)

We can then write the mathematical expressions of the irregularities shown in figures 3.10 3.11 as follows:

- **N lobes polygonal wheel function:**

$$irr(x) = H \cos \left( \frac{2\pi x}{2\pi R/N} \right) \quad (3.15)$$

- **Rail corrugation:**

$$irr(x) = H \sin \left( \frac{2\pi x}{L} \right) \quad (3.16)$$

- **Railway joints:**

$$irr(x) = H(1 - \text{Sign}(x)) \sin \left( \frac{\pi x}{L} \right) \quad (3.17)$$

In the track program a N lobes polygonal wheel function has been implemented giving the possibility to the user to analyze the influence of wheel imperfections on the studied system (a wheel with one globe could for instance represents an eccentricity due to the wheel assembly).

### 3.5.2 Fastening elements: Railpads or fasteners

As aforementioned , sleepers and rails are connected together through fastenings or rail pads.

Generally inertial properties of these elements are neglectables compared to those of the other ones, so to model their influence on the system it is sufficient to consider their elastic and damping characteristics sometimes also considering some kinds of non-linear behaviours.

The goal of modelling these interaction forces has been achieved using the following formula for railpads forces:

$$F_{s,r}^p(t) = k_p \chi_{s,r}(t) + c_p \dot{\chi}_{s,r}(t) + h_p(\chi_{s,r}(t), \dot{\chi}_{s,r}(t)) \quad (3.18)$$

where:

- $F_{s,r}^p(t)$  is the interaction force between  $s$ -sleeper and  $r$ -rail;

- $\chi_{s,r}(t), \dot{\chi}_{s,r}(t)$  are the relative displacement and the velocity of  $s$ -sleeper and  $r$ -rail force application points;
- $h_p(\chi_{s,r}(t), \dot{\chi}_{s,r}(t))$  is a non-linear function that could represent possible non linearities of this rail-sleeper interaction.

Relative displacement formula is :

$$\chi_{s,r}(t) = v_{r,N_{ax}+s}(t) - u_{s,r}(t) = v_r(x_s^S(t) - u_s(y_r^R, t)) \quad (3.19)$$

where in equation (3.19)  $v_r(x_s^S(t))$  and  $u_s(y_r^R, t)$  are functions of the modal coordinates through equations (3.2) and (3.3).

### 3.5.3 The ballast

The last component of the system is the ballast<sup>11</sup>. It forms the track-bed upon which railway sleepers are laid.

It is typically made of crushed stone, although ballast has sometimes consisted of other, less suitable materials and for all these reasons it represents a very difficult sub-system to model.

Mainly in the program three different ways of modelling have been followed:

1. A discrete series of lumped elements have been used; the inertial properties are neglectables and so as well as for the railpads the elements consist of a series of springs and viscous dampers modelled with constant  $k$  and  $c$  coefficients.
2. To the same discrete series of elements above it has been given the possibility of varying in the properties having each element a different  $k_i$  stiffness and a  $c_i$  damping coefficient.
3. Finally a continuous constant Winkler stiffness<sup>12</sup> has been implemented with regard to the elastic properties and a discrete series of dampers has been used to model damping effect.

In all three cases the non linear characteristics have been included in a last non linear term, function of the displacements of forces application points.

The formula used for a general case of a track interaction with another structure as a bridge may be, modelled with a discrete series of elements, is given below; it is important to note that in the case of a normal ballast on the ground it would be

---

<sup>11</sup>The term *ballast* comes from a nautical term for the stones used to stabilize a ship.

<sup>12</sup>The Winkler model is obviously not available in bridge interaction program

sufficient to consider it infinitely rigid (zero displacement at springs bootom side ) while using a Winkler approach removes the elastic term<sup>13</sup>.

$$F_{s,b}^b(t) = k_b v_{s,b}(t) + c_b \dot{v}_{s,b}(t) + g_b(v_{s,b}(t), \dot{v}_{s,b}(t)) \quad (3.20)$$

where:

- $F_{s,b}^b(t)$  is the interaction force between the  $s$ -sleeper and the  $b$ -discrete point below the ballast; it could represents the  $b$ -point of the bridge structure or of the infinite rigid ground.
- $k_b$  represents the stiffness of the spring connected to sleeper  $s$ <sup>14</sup>.
- $c_b$  is the viscous damping coefficient used to model ballast damping.
- $g_p(v_{s,b}(t), \dot{v}_{s,b}(t))$  is a non-linear function that represents ballast non linear effects.

Relative displacement formula, in this second case, is :

$$v_{s,b}(t) = u_{s,N_r+b}(t) - w_{s,b}(t) = u_s(y_b^S(t) - w_b(x_b^B, t)) \quad (3.21)$$

where in equation (3.21)  $u_{s,N_r+b}(t)$  and  $w_{s,b}(t)$  and their time derivatives are the displacements and the velocities of forces application points; it is important to notice that using a mono-dimensional model for the bridge means having a constant  $w_{s,b}(t)$  for each  $s$ -sleeper ( $N_r + b$ )-point while is not so for the sleeper displacement  $u_{s,N_r+b}(t)$  that may vary in different points of each  $s$ -sleeper being a function of  $y$ -coordinate.

Finally, as aformentioned, for a common ballast over infinite rigid ground, it is sufficient to require that the  $w_{s,b}(t)$  term is equal to zero.

## 3.6 Time resolution dynamic model

In the following section a dynamic model of time resolution will be described.

The governing equations discussed in the previous section will be assembled and the obtained system will be solved with some kind of numerical integration method. The equations to assembly are:

- Dynamic behaviour governing equations

---

<sup>13</sup>In this case elastic component of the force would be introduced directly in the natural frequencies of the sleepers

<sup>14</sup>in a Winkler model this term would disappear.

1. Vehicle equations (3.12)
2. Rails equations (3.5)
3. Sleepers equations (3.6)
4. Underlying structure equations (3.7)

• Constraint equations of interconnection elements are instead:

1. wheel-rail contact equations (3.13)
2. Rail fasteners equations (3.18)
3. Ballast equations (3.20)

It is important to notice that instead of equations (3.13), (3.18) and (3.20), their modal expressions, given by equations (3.8),(3.9) and (3.10) and obtained through the modal trasformation, will be used in the total modal system.

The set of independent coordinates that describes univocally the movement of whatever point of the total vehicle-track system consists of reference points  $w$  vector of the vehicle and modal coordinates  $q_r^R$ ,  $q_s^S$  and  $q^{Br}$  vectors respectively for rails, sleepers and the underlying structure.

the mathematical expressions of above-mentioned vectors are given by equations (3.22), (3.23), (3.24) and (3.25) shown below:

$$\mathbf{w} = \left\{ \begin{array}{l} z_1^W \\ \vartheta_1^W \\ z_2^W \\ \vartheta_2^W \\ \vdots \\ \text{---} \\ z_1^B \\ \vartheta_1^B \\ \varphi_1^B \\ \vdots \\ \text{---} \\ z_1^C \\ \vartheta_1^C \\ \varphi_1^C \end{array} \right\} \begin{array}{l} \leftarrow \text{ wheelset 1 vertical displacement} \\ \leftarrow \text{ wheelset 1 x-rotation} \\ \leftarrow \text{ wheelset 2 vertical displacement} \\ \leftarrow \text{ wheelset 2 x-rotation} \\ \\ \leftarrow \text{ bogie 1 vertical displacement} \\ \leftarrow \text{ bogie 1 x-rotation} \\ \leftarrow \text{ bogie 1 y-rotation} \\ \\ \leftarrow \text{ carriage 1 vertical displacement} \\ \leftarrow \text{ carriage 1 x-rotation} \\ \leftarrow \text{ carriage 1 y-rotation} \end{array} \quad (3.22)$$



$$\mathbf{q}_r^R = \left\{ \begin{array}{l} q_{r,0}^R \\ q_{r,1}^R \\ q_{r,2}^R \\ q_{r,3}^R \\ \vdots \\ q_{r,N_{mr}}^R \end{array} \right\} \begin{array}{l} \leftarrow \text{rail } r \text{ modal coordinate 0 (vertical displacement)}^{15)} \\ \leftarrow \text{rail } r \text{ modal coordinate 1} \\ \leftarrow \text{rail } r \text{ modal coordinate 2} \\ \leftarrow \text{rail } r \text{ modal coordinate 3} \\ \\ \leftarrow \text{rail } r \text{ modal coordinate } N_{mr} \end{array} \quad (3.23)$$

$$\mathbf{q}_s^S = \left\{ \begin{array}{l} q_{s,-1}^S \\ q_{s,0}^S \\ q_{s,1}^S \\ q_{s,2}^S \\ q_{s,3}^S \\ \vdots \\ q_{s,N_{ms}}^S \end{array} \right\} \begin{array}{l} \leftarrow \text{sleeper } s \text{ modal coordinate -1 (vertical displacement)}^{16)} \\ \leftarrow \text{sleeper } s \text{ modal coordinate 0 (rigid rotation)} \\ \leftarrow \text{sleeper } s \text{ modal coordinate 1} \\ \leftarrow \text{sleeper } s \text{ modal coordinate 2} \\ \leftarrow \text{sleeper } s \text{ modal coordinate 3} \\ \\ \leftarrow \text{sleeper } s \text{ modal coordinate } N_{ms} \end{array} \quad (3.24)$$

$$\mathbf{q}^{Br} = \left\{ \begin{array}{l} q_1^{Br} \\ q_2^{Br} \\ q_3^{Br} \\ \vdots \\ q_{N_{mBr}}^{Br} \end{array} \right\} \begin{array}{l} \leftarrow \text{Underlying structure modal coordinate } 1^{17} \\ \leftarrow \text{Underlying structure coordinate 2} \\ \leftarrow \text{Underlying structure coordinate 3} \\ \\ \leftarrow \text{Underlying structure coordinate } N_{ms} \end{array} \quad (3.25)$$

This set of coordinates is then grouped in one vector  $\mathbf{x}$  that defines univocally all degrees of freedom associated with the dynamic interaction model.

$$\mathbf{x} = \left\{ \mathbf{w}^T | \mathbf{q}_1^{RT} \quad \mathbf{q}_2^{RT} | \mathbf{q}_1^{ST} \dots \mathbf{q}_{N_s}^{ST} | \mathbf{q}^{BrT} \right\} \quad (3.26)$$

In this way the total dimension of the problem can be calculated as follows:

$$DOF = (2 \cdot N_{ax} + 3 \cdot N_{bo} + 3 \cdot N_{ca}) + N_r \cdot N_{mr} + N_s \cdot N_{ms} + N_{mBr} \quad (3.27)$$

---

<sup>15</sup>it is assumed that a continuous beam has been used to model the rail because in this case the first and only rigid body mode is that of vertical displacement

<sup>16</sup>it is assumed that a free-free beam has been used to model the sleeper because in this case the first rigid body mode is that of vertical displacement (-1) and the second is the rigid rotation (0)

<sup>17</sup>the underlying structure does not have rigid body modes because its model is that of pinned-pinned beam

where

- DOF = system total degrees of freedom ;
- $N_{ax}$ ,  $N_{bo}$ ,  $N_{ca}$  are, respectively, the number of wheelsets, the number of bogies and the number of carriages;
- $N_r$  and  $N_s$  are respectively the number of rails (2) and the number of sleepers;
- $N_{mr}$ ,  $N_{ms}$  and  $N_{mBr}$  are the number of modes used to model rails, sleepers and the underlying structure.

Notice finally that when the vehicle is made up with two or only one wheelset, respectively half or a quarter of an entire vehicle, the number of DOF of each part should be reduced to 3 for the bogie and 2 for the carriage in the half-vehicle case and 2 for the bogie and 2 for the carriage in the 1/4 case, this due to obvious considerations as it will be shown later on.

### 3.6.1 Mathematical system

The system of second order ordinary differential equations (second-order ODE) that governs the dynamic behaviour of the total system can be expressed in matricial form as follows:

$$\begin{aligned}
 & \begin{bmatrix} \mathbf{M} & 0 & 0 & 0 & \dots & 0 & 0 \\ 0 & \mathbf{I}^{N_{mr}} & 0 & 0 & \dots & 0 & 0 \\ 0 & 0 & \mathbf{I}^{N_{mr}} & 0 & \dots & 0 & 0 \\ 0 & 0 & 0 & \mathbf{I}^{N_{ms}} & & 0 & 0 \\ \vdots & \vdots & \vdots & & \ddots & & 0 \\ 0 & 0 & 0 & 0 & & \mathbf{I}^{N_{ms}} & 0 \\ 0 & 0 & 0 & 0 & 0 & 0 & \mathbf{I}^{N_{mBr}} \end{bmatrix} \begin{Bmatrix} \ddot{\mathbf{w}}^R \\ \dot{\mathbf{q}}_1^R \\ \dot{\mathbf{q}}_2^R \\ \dot{\mathbf{q}}_1^S \\ \vdots \\ \dot{\mathbf{q}}_{N_{Ns}}^R \\ \dot{\mathbf{q}}^{Br} \end{Bmatrix} + \\
 & \dots + \begin{bmatrix} \mathbf{D} & 0 & 0 & 0 & \dots & 0 & 0 \\ 0 & \text{diag}[2\zeta\lambda] & 0 & 0 & \dots & 0 & 0 \\ 0 & 0 & \text{diag}[2\zeta\lambda] & 0 & \dots & 0 & 0 \\ 0 & 0 & 0 & \text{diag}[2\xi\omega] & & 0 & 0 \\ \vdots & \vdots & \vdots & & \ddots & & 0 \\ 0 & 0 & 0 & 0 & & \text{diag}[2\xi\omega] & 0 \\ 0 & 0 & 0 & 0 & 0 & 0 & \text{diag}[2\mu\tau] \end{bmatrix} \begin{Bmatrix} \dot{\mathbf{w}}^R \\ \dot{\mathbf{q}}_1^R \\ \dot{\mathbf{q}}_2^R \\ \dot{\mathbf{q}}_1^S \\ \vdots \\ \dot{\mathbf{q}}_{N_{Ns}}^R \\ \dot{\mathbf{q}}^{Br} \end{Bmatrix} + \\
 & \dots + \begin{bmatrix} \mathbf{K} & 0 & 0 & 0 & \dots & 0 & 0 \\ 0 & \text{diag}[\lambda^2] & 0 & 0 & \dots & 0 & 0 \\ 0 & 0 & \text{diag}[\lambda^2] & 0 & \dots & 0 & 0 \\ 0 & 0 & 0 & \text{diag}[\omega^2] & & 0 & 0 \\ \vdots & \vdots & \vdots & & \ddots & & 0 \\ 0 & 0 & 0 & 0 & & \text{diag}[\omega^2] & 0 \\ 0 & 0 & 0 & 0 & 0 & 0 & \text{diag}[\tau^2] \end{bmatrix} \begin{Bmatrix} \mathbf{w}^R \\ \mathbf{q}_1^R \\ \mathbf{q}_2^R \\ \mathbf{q}_1^S \\ \vdots \\ \mathbf{q}_{N_{Ns}}^R \\ \mathbf{q}^{Br} \end{Bmatrix} = \begin{Bmatrix} \mathbf{F}^{ext} + \mathbf{F}^{ext} \\ \mathbf{f}_1^R \\ \mathbf{f}_2^R \\ \mathbf{f}_1^S \\ \vdots \\ \mathbf{f}_{N_{Ns}}^R \\ \mathbf{f}^{Br} \end{Bmatrix} \quad (3.28)
 \end{aligned}$$

For short it is possible to refer to equation (3.28) as:

$$\mathbf{M}_{tot}\ddot{\mathbf{x}}(t) + \mathbf{D}_{tot}\dot{\mathbf{x}}(t) + \mathbf{K}_{tot}\mathbf{x}(t) = \mathbf{f}(x,t) \quad (3.29)$$

There are many ways to solve this system and those used in this work will be discussed in later chapters.

Once obtained the  $\mathbf{x}$  vector at each instant of simulation time it is possible to trace the values of all the quantities of interest for the design and the analysis of each system part, as interaction forces and moments as well as main stress components.

Finally it is important to notice that in equations (3.28) and (3.29) the non-linear components of the system affect only the right term  $\mathbf{f}(x,t)$ , that is the force one and this leads to a great simplification in the resolution of the problem.

An usual form for solving such differential equations systems through numerical integration is to consider a new set of equations whose dimension is the double of the ordinary one.

In this way it is possible to rearrange the second order problem in a first order one.

Let:

$$\mathbf{y} = \left\{ \mathbf{w}^T \quad ; \quad \mathbf{q}_1^{RT} \quad \mathbf{q}_2^{RT} \quad ; \quad \mathbf{q}_1^{ST} \quad \dots \quad \mathbf{q}_{N_s}^{ST} \quad | \quad \dot{\mathbf{w}}^T \quad ; \quad \dot{\mathbf{q}}_1^{RT} \quad \dot{\mathbf{q}}_2^{RT} \quad ; \quad \dot{\mathbf{q}}_1^{ST} \quad \dots \quad \dot{\mathbf{q}}_{N_s}^{ST} \right\}^T \quad (3.30)$$

It is so possible to rewrite system (3.29) as:

$$\begin{bmatrix} \mathbf{D}_{tot} & \mathbf{M}_{tot} \\ \mathbf{M}_{tot} & 0 \end{bmatrix} \dot{\mathbf{y}}(t) + \begin{bmatrix} \mathbf{K}_{tot} & 0 \\ 0 & -\mathbf{M}_{tot} \end{bmatrix} \mathbf{y}(t) = \begin{Bmatrix} \mathbf{f}(x,t) \\ 0 \end{Bmatrix} \quad (3.31)$$

Thus the problem is a first order one and to solve it lots of numerical methods have been already implemented in lots of different program languages as *Matlab* is.

Another way to solve the original system (3.29) is to use a second order numerical method and its definition and implementation took a large part of this thesis work.

The chosen second order method is described in annex C.

## 3.7 Achievable magnitudes of interest

In such systems as those here analyzed, interesting magnitudes to obtain are those necessary for the calculation and the design of each single subpart, as deriving loads from interconnection elements and periodical stresses necessary for fatigue studies.

Some magnitudes are for instance:

- Movement and acceleration of each vehicle part and of each track point.

- Interaction forces between different substructures (wheel-rail contact, railpad transmitted ones, pressure over the ballast, forces transmitted through vehicle suspension ect. ect. ).
- Shear forces and bending moments in rails and sleepers.

Each of these values can be derived from total system  $\mathbf{x}$ -vector (equation 3.26) that in fact constitutes system *state of phase*.

To obtain whatever system point movement it is necessary to consider to which substructure the point belongs and so four cases are possible:

- the point belongs to the vehicle: its movement can be so calculated considering the point belonging to a rigid body thus obtainable considering body center of gravity motion whose coordinates are given by the respective components of  $\mathbf{x}$ -vector.
- the point belongs to a rail: its movement can be derived making use of relative modal transformation expressed by equation 3.2;
- the point belongs to a sleeper: its movement can be derived making use of relative modal transformation expressed by equation 3.3;
- the point belongs to the underlying structure: its movement can be derived making use of relative modal transformation expressed by equation 3.4.

Finally, concerning interaction forces, it is sufficient to make use of their expressions aforementioned in this chapter.

## 3.8 Frequency response function calculation

As mentioned in section 2.3 *Frequency response function* is defined as the relation existing between a system point movement and the exciting force that provokes it given by its magnitude and difference of phase.

Making use of a complex notation the harmonic exciting force can be expressed as  $f(t) = \bar{f}e^{i\omega t}$ .

In the particular case where the point movement is defined by its displacement  $u(t)$ , this relation is called *Receptance* and its given by the following relation:

$$\alpha(\omega) = \frac{u(t)}{f(t)} = \frac{\bar{u}e^{i\omega t}}{\bar{f}e^{i\omega t}} = \frac{\bar{u}}{\bar{f}} \quad (3.32)$$

where in equation 3.32  $\bar{u}$  and  $\bar{f}$  are the complex amplitudes of exciting force and point displacement and  $\omega$  is system exciting frequency.

3.32 is thus a complex function whose common representation is given by its complex components: (magnitude and phase).

In this section it is shown the procedure to obtain the FRF of total system.

For sleepers, rails and the underlying structure the necessary modal coordinates are already given by equations (3.5), (3.6) and (3.7) respectively.

Considering the vehicle, a further simplification is here made; as for the temporal model only rigid body modes are considered but from now on the vehicle model will be reduced to wheelsets; primary suspension forces will then take into account bogies and carriage forces.

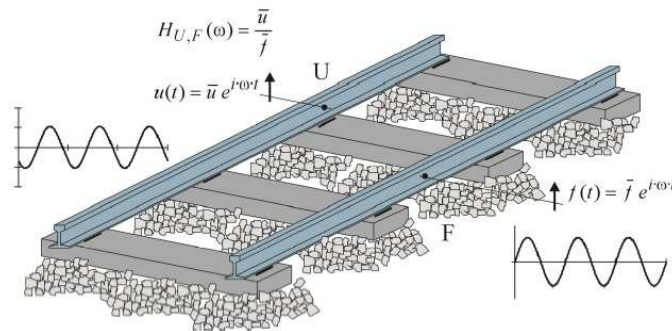


Figure 3.12. Track receptance : relation between U point displacement due to an harmonic force in point F

Each wheelset is so independent from the others from a dynamic point of view, but it is anyway possible to study its influence on the track system dynamic properties.

Obviously a linearization of the model is necessary to study the FRF and so all non linear components will be here streamlined.

### 3.8.1 System coordinates

Frequency response function is usefull in physical coordinates: displacement, velocity and acceleration of total system points. It would be possible to obtain the FRF for whatever system point, but the points of interests are those of connection between different parts, that are the DOF used till now , and so these are the points taken into consideration:

- wheelsets contact points with the rails;
- connections between rails and sleepers;
- connections between sleepers and ballast.

- Ballast contact points

These coordinates are grouped in three vectors:

- $\mathbf{z}_a$ : it includes vertical displacements of wheels connection points with rails;
- $\mathbf{v}_r$ : it includes vertical displacements of rails connection points with both wheelsets and sleepers;
- $\mathbf{u}_s$ : it includes vertical displacements of sleepers connection points with both rails and ground or structure;
- $\mathbf{w}$ : it includes vertical displacements of ballast-sleeper points in the bridge interaction case;

Thus each of these three vectors can be expressed as:

$$\mathbf{z}_a = \begin{Bmatrix} z_{a,1} \\ z_{a,2} \end{Bmatrix} \begin{array}{l} \leftarrow \text{Wheelset } a \text{ contact point with rail 1} \\ \leftarrow \text{Wheelset } a \text{ contact point with rail 2} \end{array} \quad (3.33)$$

$$\mathbf{v}_r = \begin{Bmatrix} v_{r,1} \\ \vdots \\ v_{r,N_{ax}} \\ \dots \\ v_{r,N_{ax}+1} \\ v_{r,N_{ax}+2} \\ \vdots \\ v_{r,N_{ax}+N_s} \end{Bmatrix} \begin{array}{l} \leftarrow \text{Contact point with whellset 1} \\ \leftarrow \text{Contact point with whellset } N_{ax} \\ \leftarrow \text{Contact point with sleeper 1} \\ \leftarrow \text{Contact point with sleeper 2} \\ \leftarrow \text{Contact point with sleeper } N_s \end{array} \quad (3.34)$$

$$\mathbf{u}_s = \begin{Bmatrix} u_{s,1} \\ u_{s,2} \\ \dots \\ u_{s,N_r+1} \\ u_{s,N_r+2} \\ \vdots \\ u_{s,N_r+N_b} \end{Bmatrix} \begin{array}{l} \leftarrow \text{Contact point with rail 1} \\ \leftarrow \text{Contact point with rail 2} \\ \leftarrow \text{Contact point with ballast discretization point 1} \\ \leftarrow \text{Contact point with ballast discretization point 2} \\ \leftarrow \text{Contact point with ballast discretization point } N_b \end{array} \quad (3.35)$$

$$\mathbf{w} = \begin{Bmatrix} w_1 \\ w_2 \\ \dots \\ w_{N_s} \end{Bmatrix} \begin{array}{l} \leftarrow \text{Ballast point 1} \\ \leftarrow \text{Ballast point 2} \\ \leftarrow \text{Ballast point } N_s \end{array} \quad (3.36)$$

Position coordinates are related to phase space physical coordinates through modal transformation as aforementioned in this chapter ((3.2) , (3.3) and (3.4)).

Thus displacements given by equations (3.33), (3.34),(3.35) and (3.36) are related to modal coordinates of wheelsets, rails, sleepers and structure, respectively, through equations (3.37), (3.38), (3.39), (3.40) and (3.41) .

$$v_{r,a}(t) = \sum_{m=0}^{N_{mr}} \phi_{a,m} q_{r,m}^R(t) \quad r = 1, \dots, N_r \quad a = 1, \dots, N_{ax} \quad (3.37)$$

$$v_{r,N_{ax}+s}(t) = \sum_{m=0}^{N_{mr}} \phi_{N_{ax}+s,m} q_{r,m}^R(t) \quad r = 1, \dots, N_r \quad s = 1, \dots, N_s \quad (3.38)$$

$$u_{s,r}(t) = \sum_{n=-1}^{N_{ms}} \Psi_{r,n} q_{s,n}^S(t) \quad s = 1, \dots, N_s \quad r = 1, \dots, N_r \quad (3.39)$$

$$u_{s,N_r+b}(t) = \sum_{n=-1}^{N_{ms}} \Psi_{N_r+b,n} q_{s,n}^S(t) \quad s = 1, \dots, N_s \quad b = 1, \dots, N_b \quad (3.40)$$

$$w_s = \sum_{l=1}^{N_{mBr}} \Gamma_{s,l} q_l^{Br}(t) \quad s = 1, \dots, N_s \quad (3.41)$$

where

$$\phi_{a,m} = \phi_m(x_a^W) \quad m = 0, \dots, N_{mr} \quad a = 1, \dots, N_{ax} \quad (3.42)$$

$$\phi_{N_{ax}+s,m} = \phi_m(x_s^S) \quad m = 0, \dots, N_{mr} \quad s = 1, \dots, N_s \quad (3.43)$$

$$\Psi_{r,n} = \Psi(y_r^R) \quad n = -1, \dots, N_{ms} \quad r = 1, \dots, N_r \quad (3.44)$$

$$\Psi_{N_r+b,n} = \Psi(y_b^S) \quad n = -1, \dots, N_{ms} \quad r = 1, \dots, N_r \quad (3.45)$$

$$\Gamma_{s,l} = \Gamma_l(x_s^S) \quad n = 1, \dots, N_{mBr} \quad s = 1, \dots, N_s \quad (3.46)$$

That are the vibration modes calculated in connection points.

### 3.8.2 Vehicle model for FRF calculation

Generally in this kind of studies the presence of the vehicle is neglected.

Obviously the system modal properties will be affected by the vehicle and so it could be interesting to study its influence on the total system analyzing the differences between FRF in both cases of vehicle presence or not.

The vehicle model used is that of  $N_{ax}$  rigid wheelset.

The bogies and carriages are neglected to simplify the model and because of filtering properties of primary suspension.

Vehicle modal model consider only rigid body modes that could be obtained from a modal trasformation of system (3.12). Natural frequencies of rigid body modes are obviously null and modal damping has here no meaning.

The following considerations would be usefull also when considering wheelset flexural modes, that could be calculated with a FEM program and introduced in the model.

The movement of wheels contact points with rails in analogy with rails, sleepers and the bridge is expressed by the following relation:

$$z_{a,r}(t) = \sum_{h=-1}^0 \Omega_{r,h} q_{a,h}^W(t) \quad r = 1, \dots, N_r \quad a = 1, \dots, N_{ax} \quad (3.47)$$

where :

- $q_{a,-1}^W(t)$  is  $a$ -wheelset vertical movement;
- $q_{a,0}^W(t)$  is  $a$ -wheelset  $x$ -rotation;
- $\Omega_{r,h}$  is  $h$ -vibration mode value in the contact point.

As for rails, sleepers and structure wheelset  $a$  governing differential equation of movement, considering natural modes and relative modal damping, is:

$$\ddot{q}_{a,h}^W(t) + 2\eta_h \sigma_h \dot{q}_{a,h}^W(t) + \sigma_h^2 q_{a,h}^W(t) = f_{a,h}^W(t) \quad h = -1, 0 \quad (3.48)$$

where the used variables have the following meaning:

- $\sigma_h = 0$  is the natural frequency of  $l$ -vibration mode (null because it is a rigid mode);
- $\eta_h$  is  $l$ -relative damping;
- $f_{a,h}^W$  is the  $h$ th-modal force

As for equations (3.8),eq:mod-sleeper-transformation and (3.10), modal forces can be expressed as:

$$f_{a,h}^W(t) = \sum_{r=1}^{N_r} (F_{a,r}^{ext}(t) + F_{a,r}^c(t)) \Omega_{r,h} \quad (3.49)$$

where  $F_{a,r}^c(t)$  is the linearized  $r$ -wheel contact force of wheelset  $a$  and  $F_{a,r}^{ext}$  is the relative external force (weight and primary suspension forces).



### 3.8.3 System equations of motion

Vehicle modal transformations can be expressed in matrix form as:

$$\begin{aligned}
 \mathbf{w}_a &= \mathbf{\Omega} \mathbf{q}_a^W & a = 1, \dots, N_{ax} \\
 \mathbf{v}_r &= \mathbf{\Phi} \mathbf{q}_r^R & r = 1, \dots, N_r \\
 \mathbf{u}_s &= \mathbf{\Psi} \mathbf{q}_s^S & s = 1, \dots, N_s \\
 \mathbf{k} &= \mathbf{\Gamma} \mathbf{q}^{Br}
 \end{aligned} \tag{3.50}$$

where

- $\mathbf{\Omega}$  is wheelsets vibration modes matrix (size:  $2 \times 2$ );
- $\mathbf{\Phi}$  is rails vibration modes matrix (size:  $(N_{ax} + N_s) \times N_{mr}$ );
- $\mathbf{\Psi}$  is sleepers vibration modes matrix (size:  $(N_r + N_s) \times N_{ms}$ );
- $\mathbf{\Gamma}$  is bridge vibration modes matrix (size:  $N_s \times N_{mBr}$ );
- $\mathbf{q}_a^W, \mathbf{q}_r^R, \mathbf{q}_s^S$  and  $\mathbf{q}^{Br}$  are modal coordinates vectors respectively of wheelsets , rails , sleepers and of underlying structure.

Modes Matrices  $\mathbf{\Omega}$ ,  $\mathbf{\Phi}$ ,  $\mathbf{\Psi}$  and  $\mathbf{\Gamma}$  are obviously the same for similar elements if their properties and their number of modes considered is the same.

Considering vectors  $\mathbf{x}$  and  $\mathbf{q}$  that group all system coordinates it is possible to define an extended modal transformation  $\mathbf{T}$  and so to rewrite system (3.50) as:

$$\left\{ \begin{array}{c} \mathbf{z}_1 \\ \vdots \\ \mathbf{z}_{N_{ax}} \\ \dots \\ \mathbf{v}_1 \\ \mathbf{v}_2 \\ \dots \\ \mathbf{u}_1 \\ \vdots \\ \mathbf{u}_{N_s} \\ \dots \\ \mathbf{w} \end{array} \right\} = \left[ \begin{array}{ccc|cc|c} \mathbf{\Omega} & 0 & & & & \\ & \ddots & & & & \\ 0 & \mathbf{\Omega} & & & & \\ \hline & & \mathbf{\Phi} & 0 & & \\ & & 0 & \mathbf{\Phi} & & \\ \hline & & & & \mathbf{\Psi} & 0 & 0 \\ & & & & & \ddots & \\ & & & & 0 & & \mathbf{\Psi} \\ \hline & & & & & & \mathbf{\Gamma} \end{array} \right] \left\{ \begin{array}{c} \mathbf{q}_1^W \\ \vdots \\ \mathbf{q}_{N_{ax}}^W \\ \dots \\ \mathbf{q}_1^R \\ \mathbf{q}_2^R \\ \dots \\ \mathbf{q}_1^S \\ \vdots \\ \mathbf{q}_{N_s}^S \\ \dots \\ \mathbf{q}^{B_r} \end{array} \right\} \quad (3.51)$$

that is

$$\mathbf{x} = \mathbf{T}\mathbf{q} \quad (3.52)$$

Using modal coordinates decouples movement equations of the total system and the following system of second order differential equations results.

$$\ddot{\mathbf{q}} + \mathbf{d}\dot{\mathbf{q}} + \mathbf{k}\mathbf{q} = \mathbf{f} \quad (3.53)$$

where diagonal matrices  $\mathbf{d}$  and  $\mathbf{k}$  are defined as:

$$\mathbf{d} = \text{diag} \left( \left[ \begin{array}{ccc|ccc} 2\sigma\rho \dots 2\sigma\rho & \vdots & 2\lambda\zeta 2\lambda\zeta & \vdots & 2\omega\xi \dots 2\omega\xi & \vdots & 2\mu\tau \end{array} \right] \right) \quad (3.54)$$

$$\mathbf{k} = \text{diag} \left( \left[ \begin{array}{ccc|ccc} \sigma^2 \dots \sigma^2 & \vdots & \lambda^2 \lambda^2 & \vdots & \omega^2 \dots \omega^2 & \vdots & \tau^2 \end{array} \right] \right) \quad (3.55)$$

In equations (3.54) and (3.55) the variables used represent:

- $\sigma$ ,  $\lambda$ ,  $\omega$  and  $\tau$  are diagonal matrices with vehicle, rails, sleepers and bridge angular natural frequencies values, respectively;
- $\tau$ ,  $\zeta$ ,  $\xi$  and  $\mu$  are diagonal matrices with vehicle, rails, sleepers and bridge modal damping coefficients values, respectively;

where the dimensions of the used matrices are:

- $\sigma$  and  $\tau$  :  $2 \times 2$  ;

- $\lambda$  and  $\zeta : N_{mr} \times N_{mr}$ ;
- $\omega$  and  $\xi : N_{ms} \times N_{ms}$ ;
- $\tau$  and  $\mu : N_{mBr} \times NmBr$ .

$\mathbf{f}$  is then the modal forces vector that can be calculated from system forces expressed in physical coordinates using the following transformation:

$$\mathbf{x} = \mathbf{T}\mathbf{q} \quad (3.56)$$

$$\left\{ \begin{array}{c} \mathbf{f}_1^W \\ \vdots \\ \mathbf{f}_{N_{ax}}^W \\ \dots \\ \mathbf{f}_1^R \\ \mathbf{f}_2^R \\ \dots \\ \mathbf{f}_1^S \\ \vdots \\ \mathbf{f}_{N_s}^S \\ \dots \\ \mathbf{f}^{B_r} \end{array} \right\} = \left[ \begin{array}{c|c|c|c|c} \mathbf{\Omega}^T & 0 & & & \\ & \ddots & & & \\ 0 & & \mathbf{\Omega}^T & & \\ \hline & 0 & \mathbf{\Phi}^T & 0 & \\ & & 0 & \mathbf{\Phi}^T & \\ \hline & 0 & & \mathbf{\Psi}^T & 0 & 0 \\ & & 0 & & \ddots & \\ & & & 0 & & \mathbf{\Psi}^T \\ \hline 0 & & & & & \mathbf{\Gamma}^T \end{array} \right] \left\{ \begin{array}{c} \mathbf{F}_1^W \\ \vdots \\ \mathbf{F}_{N_{ax}}^W \\ \dots \\ \mathbf{F}_1^R \\ \mathbf{F}_2^R \\ \dots \\ \mathbf{F}_1^S \\ \vdots \\ \mathbf{F}_{N_s}^S \\ \vdots \\ \mathbf{F}^{B_r} \end{array} \right\} \quad (3.57)$$

Vector  $\mathbf{F}$  includes all external and interconnection forces acting on the system expressed in physical coordinates . It is defined , in agreement with the signs of external forces  $F_a^{ext}$ , contact forces  $F_{r,a}^c$ , railpads forces  $F_{r,s}^p$  and ballast ones  $F_{s,b}^b$ , as:

$$\mathbf{F} = \left( \begin{array}{c} \sum \mathbf{F}_1^{ext} + \sum_{r=1}^{N_r} \mathbf{F}_{1,r}^c \\ \vdots \\ \sum \mathbf{F}_{N_{ax}}^{ext} + \sum_{r=1}^{N_r} \mathbf{F}_{N_{ax},r}^c \\ \dots \\ \sum_{a=1}^{N_{ax}} \mathbf{F}_{1,a}^c + \sum_{s=1}^{N_s} \mathbf{F}_{1,s}^p \\ \sum_{a=1}^{N_{ax}} \mathbf{F}_{2,a}^c + \sum_{s=1}^{N_s} \mathbf{F}_{2,s}^p \\ \dots \\ \sum_{r=1}^{N_r} \mathbf{F}_{1,r}^p + \sum_{b=1}^{N_b} \mathbf{F}_{1,b}^b \\ \vdots \\ \sum_{r=1}^{N_r} \mathbf{F}_{N_s,r}^p + \sum_{b=1}^{N_b} \mathbf{F}_{N_s,b}^b \\ \dots \\ \sum_{s=1}^{N_s} \mathbf{F}_s^{Br} \end{array} \right) = -\mathbf{K}^{inter} \mathbf{x} - \mathbf{D}^{inter} \dot{\mathbf{x}} + \mathbf{F}^{ext} \quad (3.58)$$

where

- $\mathbf{K}^{inter}$  and  $\mathbf{D}^{inter}$  are matrices that contain damping and stiffness interaction terms between different structures;
- $\mathbf{x}$  and  $\dot{\mathbf{x}}$  are displacements and velocities of FRF points of interest.
- $\mathbf{F}^{ext}$  is the external forces vector.

As well known the study of the FRF of a system needs the system to be linear (the superposition principle is valid only for linear systems and FRF is based on this principle).

As aforementioned track system interaction forces are non linear so obviously equations (3.13) , (3.18) and (3.20) non linear terms need to be linearized.

In order to achive this linearization of interaction forces Taylor expansion is used keeping only the linear term.

Thus linear interaction forces expressions are :

$$\begin{aligned}
 F_{r,a}^{cL} &= F_{r,a_0}^{cL}(t) + k_{HL}(z_{a,r}(t) - v_{r,a}(t)) \\
 F_{s,r}^{pL} &= F_{s,r_0}^{pL}(t) + k_{pL}(v_{r,N_{ax+s}}(t) - u_{s,r}(t)) + c_{pL}(\dot{v}_{r,N_{ax+s}}(t) - \dot{u}_{s,r}(t)) \\
 F_{s,b}^{bL} &= F_{s,b_0}^{bL}(t) - k_{bL}(u_{s,N_{r+b}}(t) - w_s(t)) - c_{bL}(\dot{u}_{s,N_{r+b}}(t) - \dot{w}_s(t))
 \end{aligned} \tag{3.59}$$

where

- $F_{r,a}^{cL}$ ,  $F_{s,r}^{pL}$  and  $F_{s,b}^{bL}$  are linear interaction forces of wheel contact, railpads and ballast, respectively;
- $F_{r,a_0}^{cL}$ ,  $F_{s,r_0}^{pL}$  and  $F_{s,b_0}^{bL}$  are static interaction forces;
- $k_{HL} = 1.5\sqrt{k_H^2 \cdot F_{r,a_0}^{cL}}$  is the linearized hertzian stiffness;
- $k_{pL}$ ,  $c_{pL}$ ,  $k_{bL}$  and  $c_{bL}$  are elastic and viscous properties of railpad and ballast and they include non linear terms  $h_p(\chi_{s,r}(t), \dot{\chi}_{s,r}(t))$  and  $g_b(\nu_{s,b}(t), \dot{\nu}_{s,b}(t))$  of equations (3.18) and (3.20).

Considering  $\mathbf{f}$  vector as the sum of the external forces term and an interaction one and taking in mind the relation between  $\mathbf{x}$  vector and  $\mathbf{q}$ , given by equations (3.56) and (3.57), it is possible to write the following modal forces expression:

$$\mathbf{f}^{inter} + \mathbf{f}^{ext} = -(\mathbf{T}^T \mathbf{K}^{inter} \mathbf{T} \mathbf{q} + \mathbf{T}^T \mathbf{D}^{inter} \mathbf{T} \dot{\mathbf{q}}) + \mathbf{T}^T \mathbf{F}^{ext} \tag{3.60}$$

Combining then equations (3.60) and (3.53) and rearranging its terms, it results the following system of decoupled equations:

$$\ddot{\mathbf{q}} + (\mathbf{d} + \mathbf{T}^T \mathbf{D}^{inter} \mathbf{T}) \dot{\mathbf{q}} + (\mathbf{k} + \mathbf{T}^T \mathbf{K}^{inter} \mathbf{T}) \mathbf{q} = \mathbf{f}^{ext} \tag{3.61}$$

### 3.8.4 FRF receptance matrix

The matrix  $\mathbf{H}^q(\omega)$  whose terms  $\mathbf{H}_{i,j}^q(\omega)$  relate  $i$ -modal coordinate (DOF) response to an exciting unit harmonic force acting on  $j$ -coordinate (DOF) with an angular frequency  $\omega$  is called *Receptance Matrix* and it can be expressed as follows:

$$\mathbf{H}^q(\omega) = [-\omega^2 \mathbf{I} + i\omega (\mathbf{d} + \mathbf{T}^T \mathbf{D}^{inter} \mathbf{T}) + (\mathbf{k} + \mathbf{T}^T \mathbf{K}^{inter} \mathbf{T})]^{-1} \tag{3.62}$$

where  $\mathbf{I}$  is the identity matrix.

Each  $\mathbf{H}_{i,j}^q(\omega)$  component is a complex number that relates amplitude and phase displacement between modal coordinates  $\mathbf{q}_i$  and harmonic force  $\mathbf{f}_j^{ext}$  acting on modal coordinate  $\mathbf{q}_j$ , and it is a function of  $\omega$  frequency.

Thus it is possible to write the following relation:

$$\mathbf{H}_{i,j}^q(\omega) = \frac{\mathbf{q}_i}{\mathbf{f}_j^{ext}} \quad (3.63)$$

FRF matrix can be expressed also in physical coordinates ( $\mathbf{H}^x(\omega)$ ) and it can be derived from equations (3.56) and (3.60) as follows:

$$\mathbf{x} = \mathbf{T}\mathbf{q} = \mathbf{T}\mathbf{H}^q(\omega)\mathbf{T}^T\mathbf{F}^{ext} = \mathbf{H}^x(\omega)\mathbf{F}^{ext} \implies \mathbf{H}^x(\omega) = \mathbf{T}\mathbf{H}^q(\omega)\mathbf{T}^T \quad (3.64)$$

Similarly to modal receptance,  $\mathbf{H}_{i,j}^x(\omega)$  components relate  $i$  physical coordinate (DOF) response to an unitary harmonic force, of  $\omega$  frequency, acting on  $j$ -physical coordinate (DOF)

# Chapter 4

## The Program developed

### 4.1 Introduction

A large part of the work was taken up by the definition of the program, built up with the use of *Matlab* software.

In total four versions of the program were developed and they permit to study respectively:

1. Track-vehicle interactions and temporal response of the system when there is no underlying structure;
2. Track-vehicle interactions and temporal response of the system when there is an underlying structure (called *Bridge* in the program but that could represent whatever structure as, for instance, a viaduct);
3. Frequency response function for the system without underlying structure;
4. Frequency response function for the system with underlying structure.

To develop these programs, as aforementioned, a “modular” approach was used and, certainly, this gives the possibility of future improvements.

The main features used were *Matlab* GUIs (*Graphical user interfaces*) which make the program more lightweight and easier to use.

It was decided to use this kind of programming approach to permit to everyone to use the software and making it easier it was reduced the possibility of user inputs errors.

All the quantities are expressed in the international system units a part from those few cases where it is differently specified.

In this chapter an accurate description of developed programs is given, this to permit a better understanding of all the GUI windows used in the program and to remove all possible doubts.

## 4.2 Vehicle-Track Dynamic interactions program

This has been the first program developed and it contains all the main GUIs used.

The other versions have been obtained with simple changes from this first one and for this reason it will be given an accurate description only for this version, while for the others, only the main differences will be then described.

## 4.3 User-defined Input Data

Hereafter all the *GUI* windows used will be shown and their function, in the definition of the model parameters, described.

### 4.3.1 Program welcome GUI

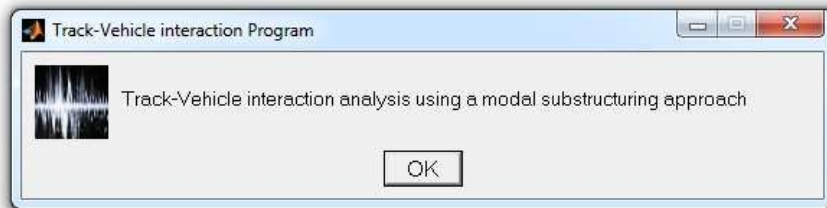


Figure 4.1. Welcome GUI

### 4.3.2 Load data GUI



Figure 4.2. Load data GUI



This is the request window for loading old simulations data. Clicking the button “set up a new set of data” (the default one) will start the input data part of the program, while clicking the “load an old set of data” button will open a loading window with all the input files saved in other simulations (fig:4.3).

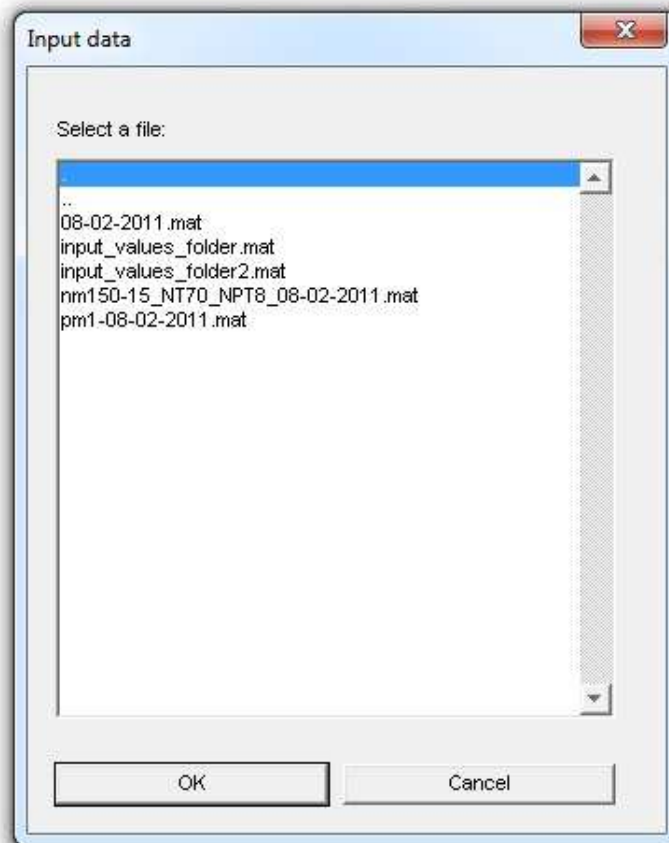


Figure 4.3. Loading GUI

Obviously, here after, the program is split in two parts. The *model set up* part is hereafter described because the only difference in loading an old model is the possibility of redefining those data that the user wants to change.

An apposite GUI will ask the user to redefine those data that he wants to change and then to type return in *Matlab* command window (figure:4.4).

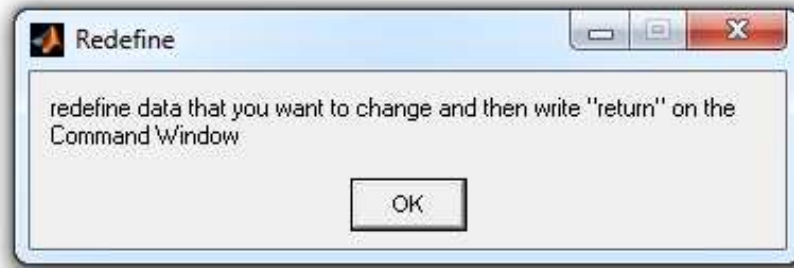


Figure 4.4. Message box for data redefinition

### 4.3.3 Problem (Model) size

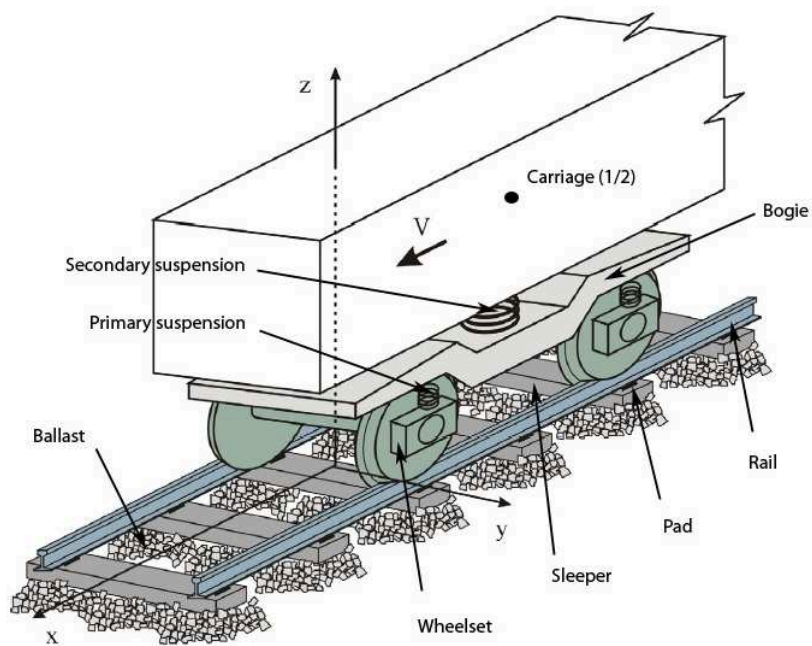


Figure 4.5. Half of the Vehicle-track model

At this step of the program two GUIs appear simultaneously:

1. an input data GUI (figure: 4.6) ;
2. a figure that represents half of the Vehicle-Track model (figure 4.5) .

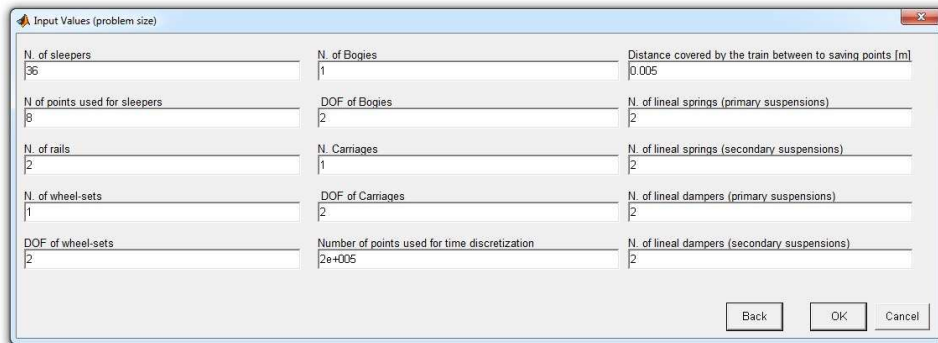


Figure 4.6. Main Model DOF choice

The figure is only explicative while in the input data GUI the operator is asked to choose the main DOF of the model to study:

- N. of sleepers ( $NT$ ): is the number of sleepers in the track way stretch considered.
- N. of points used for sleeper ( $NPT$ ): is the number of sleeper discretization points.
- N. of Rails ( $NR$ ): is the number of rails; by default it is 2 and it should not be changed<sup>1</sup>
- N. of wheel-sets ( $NEJ$ ): is the number of wheel sets of the Vehicle, that in the total vehicle are four, in the half model two and so long.
- DOF of wheel-sets ( $GDLEJ$ ): it is the number of degrees of freedom of each wheelset, and it should be changed according to the chosen model. The actual version of program doesn't permit yet to give more than 2 DOF to wheelsets because only vertical vibration is taken into account (thus a rigid wheelset can only have two DOF, rigid vertical traslation and rigid rotation). In future developments it will be easy to increase the number of DOF of the Vehicle because its connection matrices are already assebled according to its DOF as it will be shown later.
- N. of bogies ( $NB$ ): is the number of Bogies: 2 for the total vehicle, 1 for both half or a quarter of the vehicle (in the last case it is the mass that halves).

<sup>1</sup>it could be an input value only in future developments to study smaller models when the problem is symmetric.

- DOF of Bogies (*GDLB*): Similar to wheelsets this value depends on the vehicle model chosen. When 2 or 1 entire bogie is considered its DOF are in the actual version<sup>2</sup> 3, as aforementioned in chapter 3, because two rigid vibration modes are here possible. Considering a quarter of the vehicle needs instead 2 bogie DOF for the same reason of wheelsets.
- N. of carriages (*NC*): it is the number of carriages (also in this case it is the mass of the carriage that halves or become a quarter in the half-vehicle model or in the one quarter one, respectively).
- DOF of carriages (*GLDC*): it is the number of DOF of each carriage: 3 for the total model or 2 for the half and for the one quarter ones (Here also all the considerations done for wheelsets and bogies hold good).
- time discretization step (*dt*): the integrator implemented, not the matlab one (see annex C), needs a time discretization with a minimum time step<sup>3</sup>. The number of time points will be later calculated in the program following this relation:

$$NPtime = \frac{Tf - Ti}{dt} + 1 \quad (4.1)$$

where  $Tf$  and  $Ti$  are the initial simulation time and the final one, respectively.

- Distance covered by the train between two saving points [m] ( $\Delta s$ ): whichever solver is used the program will save the solution components every  $\Delta t$  seconds, where  $\Delta t$  is a function of train  $V$  velocity and  $\Delta s$  space discretization.

$$\Delta t = \frac{V}{\Delta_s} \quad \text{where } V \text{ is a constant} \quad (4.2)$$

- N. of linear springs (primary suspension) (*NRL1*): it is the total number of primary linear springs connecting wheelsets to bogies. As illustrated in figure 4.5, there are two primary suspensions per wheelsets, so the total number is  $NRL1 = NEJ * NS1$ , where  $NS1$  is the number of primary suspensions per wheelsets.  $NRL1$  is not a variable of the system yet, but also here, considering that in the future it could be possibly interesting to increase the number of suspensions, the program gives the possibility of changing it.
- N. of linear springs (secondary suspension) (*NRL2*): it is the total number of secondary linear springs connecting bogies to carriage. The same considerations above hold good also in this case.

---

<sup>2</sup>also here the relative matrix is assembled considering the number of DOF so future improvements are considered.

<sup>3</sup>it depends time after time by the non-linearity degree of the problem.

- N. of linear dampers (primary suspension)  $NAL1$  and (secondary suspension)  $NAL2$  are the dampers to model damping properties of suspensions and all springs considerations hold true.

#### 4.3.4 Wheels position

Hereafter an *half-vehicle* model is considered and all the figures below refer to this case (GUI windows are always the same but the data inside them change obviously with the model of the vehicle).

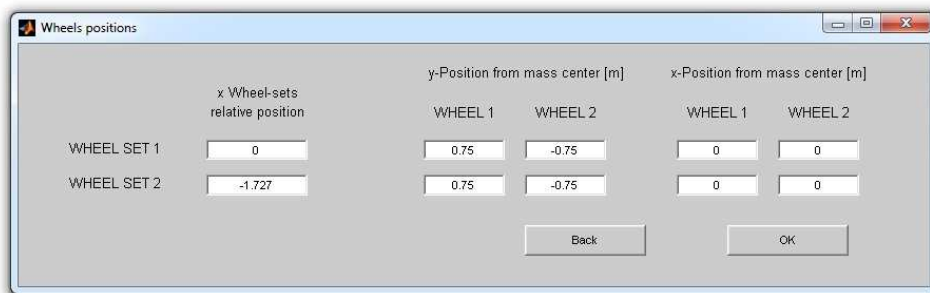


Figure 4.7. Wheels position

Referring to figure 4.5 it is possible to better understand this GUI.

It is also important to take in mind that the all problem is studied simmetrically and that wheel 1 as well as rail 1 are the ones located on y-positive position (on the left watching the vehicle from the rear).

For each wheelset the user is here asked to enter the values of the x negative distance ( $EJE\_POS_i, i = 1 \dots NEJ$ ) from the first wheelset (considering the first at  $x = 0$  position), the y-distance from the middle point between two rails (half of the distance between two rails) and the x-distance from the respective wheelset center of gravity; the last value stands for possible misalignments that would provoke irregularities (actually this value is not so meaningful and normally it is taken equal to zero).

The program will then locate the last wheelset (the nearest to the beginning of the way) at five sleepers from the first sleeper, this because with the boundary conditions chosen to model rails the solution is not very meaningful at the extremes of the track way.

#### 4.3.5 Rail-Pad properties GUI

The user here should simply chose which kind of pad use, left-clicking on the apposite check box. Four kind of different values are possible and these are taken from different

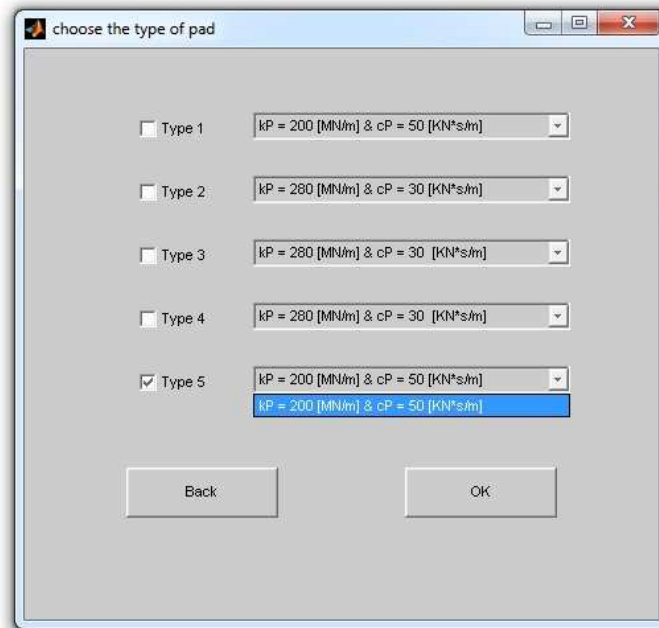


Figure 4.8. Type of railpad (fastner)

references.

### 4.3.6 Sleeper properties GUI window

This is the GUI window for the sleeper model.

Notice that in this version of the program rails and sleepers properties are the same for all the components of the track but it could be interesting in future developments to diversify these properties at least for some components to study the effect on the total system of this kind of irregularities.

In the upper part of the window there are the check boxes that permit to select which mathematical model to use in modelling the sleeper.

Thus there are four possibility as said in chapter 3:

1. Free-free constrained Euler-Bernoulli beam;
2. Continuous Euler-Bernoulli beam;
3. Free-free constrained Timoshenk beam;
4. Continuous Timoshenko beam;

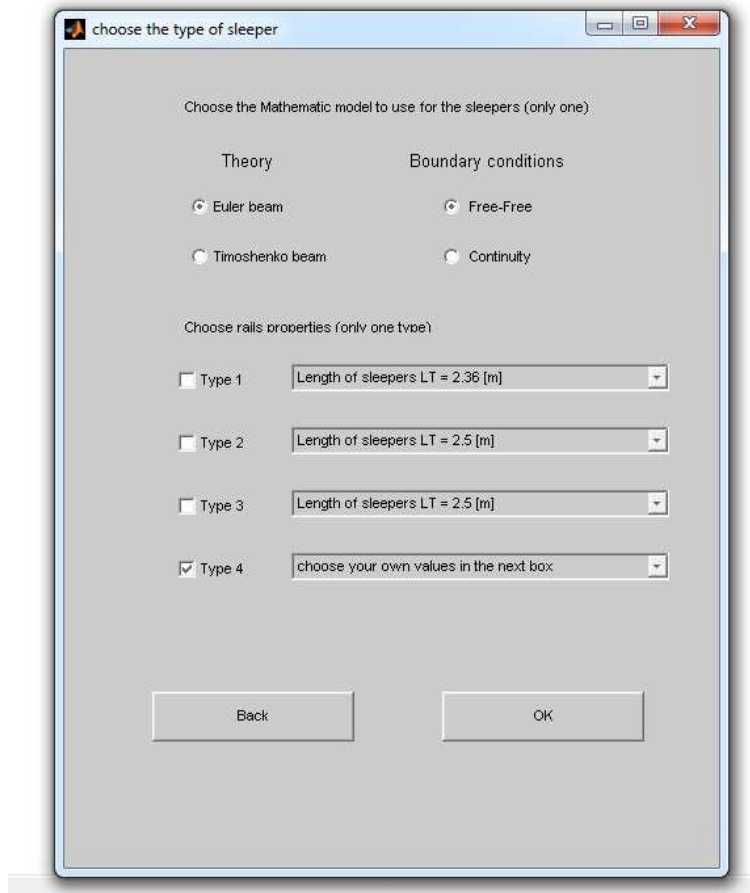
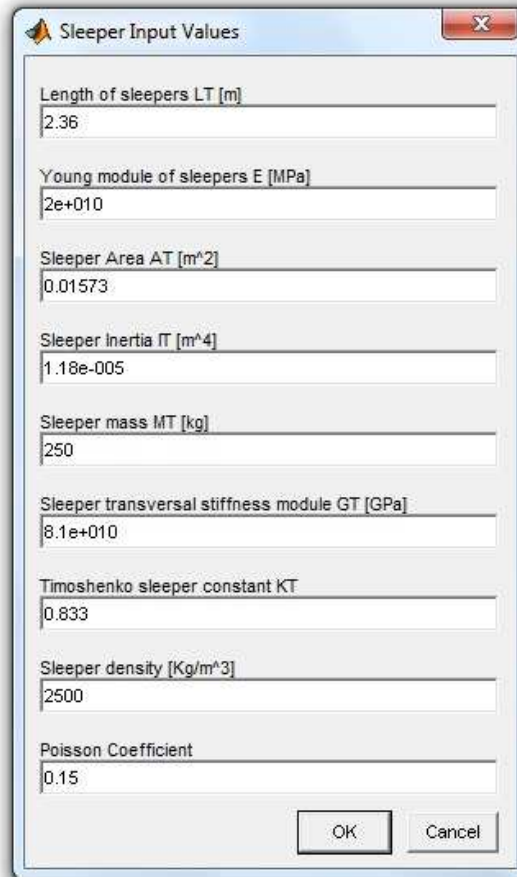


Figure 4.9. Sleeper properties and mathematical model

The user must here only check the respective boxes (one for the method and one for boundary conditions). The default one is the free-free Euler-Bernoulli beam because this is the most appropriate and also the one used in Ref. [1] in the already validated model taken as a started point for this work.

In the low part there are four check boxes beside four list boxes (to view the values of each list box just left click on the small button with a reverse arrow). The user must here check the check box relative to the list of values chosen to model the sleepers or the last one in case that he wants to set new values.

Chosing the last option next GUI will ask for sleeper properties specification as shown in figure 4.10. Otherwise Sleepers properties would be those specified in the selected list .



The image shows a software dialog box titled "Sleepers Input Values". It contains several input fields, each with a label and a value. The fields are: "Length of sleepers LT [m]" with value "2.36"; "Young module of sleepers E [MPa]" with value "2e+010"; "Sleepers Area AT [m^2]" with value "0.01573"; "Sleepers Inertia IT [m^4]" with value "1.18e-005"; "Sleepers mass MT [kg]" with value "250"; "Sleepers transversal stiffness module GT [GPa]" with value "8.1e+010"; "Timoshenko sleepers constant KT" with value "0.833"; "Sleepers density [Kg/m^3]" with value "2500"; and "Poisson Coefficient" with value "0.15". At the bottom right of the dialog box are "OK" and "Cancel" buttons.

| Property                                       | Value     |
|--|-----------|
| Length of sleepers LT [m]                      | 2.36      |
| Young module of sleepers E [MPa]               | 2e+010    |
| Sleepers Area AT [m <sup>2</sup> ]             | 0.01573   |
| Sleepers Inertia IT [m <sup>4</sup> ]          | 1.18e-005 |
| Sleepers mass MT [kg]                          | 250       |
| Sleepers transversal stiffness module GT [GPa] | 8.1e+010  |
| Timoshenko sleepers constant KT                | 0.833     |
| Sleepers density [Kg/m <sup>3</sup> ]          | 2500      |
| Poisson Coefficient                            | 0.15      |

Figure 4.10. Sleepers properties specification



### 4.3.7 Rails properties GUI window

The same done for sleeper is now necessary for Rails and so next two GUIs, 4.11 and 4.12, refer to rails model. The same mathematical models are also here possible but the default one is the continuous-continuous for the reasons explained in chapter 3.

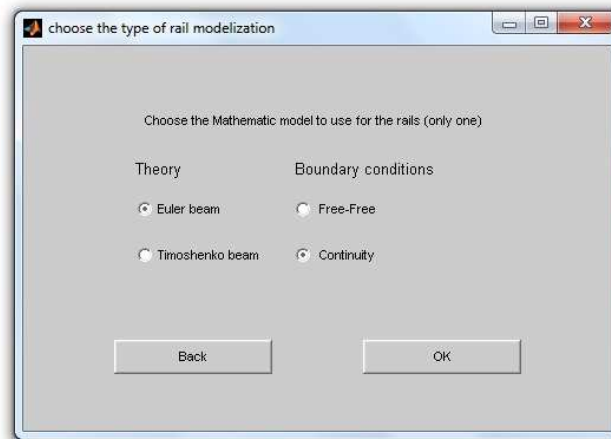


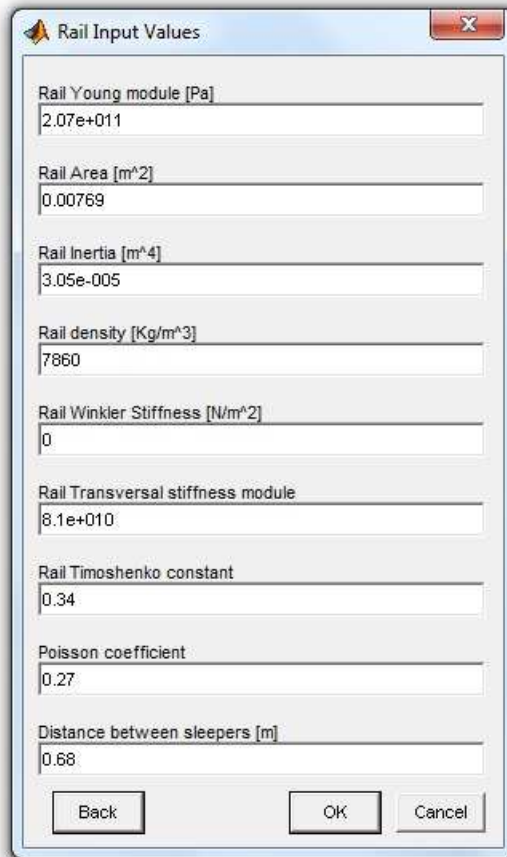
Figure 4.11. Rails mathematical model

It is important to notice that to appreciate differences between the Euler beam results and the Timoshenko one it is necessary to consider high frequencies modes, because at low frequencies the two theories almost approximate each other (see annex A figure A.2.3).

Notice that for rails it is not asked to enter the length value but the distance between two sleepers ( $LV$ ); this because the total length will be obviously calculated as

$$LR = LV * NT \quad (4.3)$$

where  $NT$  is the number of sleepers as aforementioned.



The image shows a software dialog box titled "Rail Input Values". It contains several input fields with the following labels and values:

| Property                                   | Value     |
|--|-----------|
| Rail Young module [Pa]                     | 2.07e+011 |
| Rail Area [m <sup>2</sup> ]                | 0.00769   |
| Rail Inertia [m <sup>4</sup> ]             | 3.05e-005 |
| Rail density [Kg/m <sup>3</sup> ]          | 7860      |
| Rail Winkler Stiffness [N/m <sup>2</sup> ] | 0         |
| Rail Transversal stiffness module          | 8.1e+010  |
| Rail Timoshenko constant                   | 0.34      |
| Poisson coefficient                        | 0.27      |
| Distance between sleepers [m]              | 0.68      |

At the bottom of the dialog box, there are three buttons: "Back", "OK", and "Cancel".

Figure 4.12. Rails properties

### 4.3.8 Ballast mathematical model and properties GUI windows

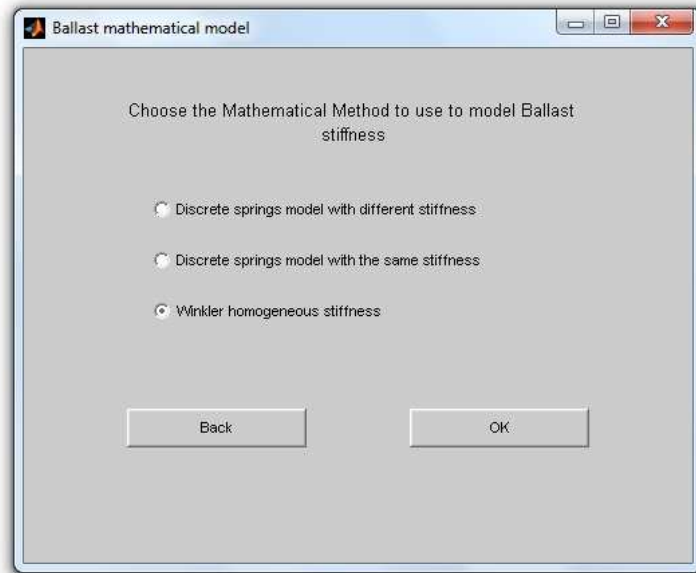


Figure 4.13. Ballast mathematical model

An important component of the track is the ballast. Its mechanical properties are difficult to appreciate and its mathematical model difficult to define.

This is the main non-linear component of the system and so the user has the possibility to decide which model to use time after time and, as it will be shown later in this chapter, it is also possible to insert user-defined non linear components of ballast connections forces.

As illustrated in figure 4.13 three options have been implemented to model the ballast:

1. a series of discrete springs (and dampers) with different stiffness  $kB$  (and damping coefficients  $cB$ ).
2. a series of discrete springs (and dampers) all with the same stiffness  $kB$  (and damping coefficients  $cB$ ).
3. a Winkler approach to model the stiffness  $KWT$  (see annex B) and a series of dampers with a constant damping coefficient ( $cB$ ).

Choosing option 2 or option 3 the next GUI will ask for constant  $cB$  and  $kB$  or  $KWT$ , respectively<sup>4</sup>. Obviously in both cases no irregularities are possible in the ballast model.

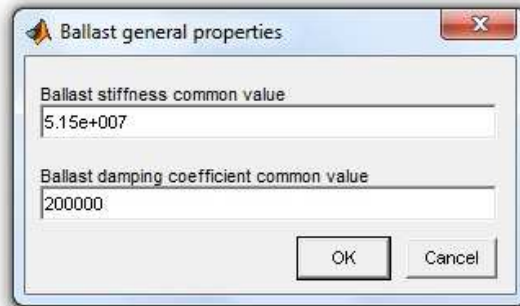
In setting  $cB$  and  $kB$  values take in mind the number of points used for sleepers discretization, because here both values refer to each single element ( dimension :  $N/m$  and  $N/(m/s)$  ).

Notice that, in the case of vehicle-structure-interaction program, Winkler foundation theory doesn't make any sense and this for the obvious reason of finite stiffness of the structure that lay, in this case, under the Winkler foundation. Thus in the bridge-interaction program the ballast models are only two and all the considerations here done hold good.

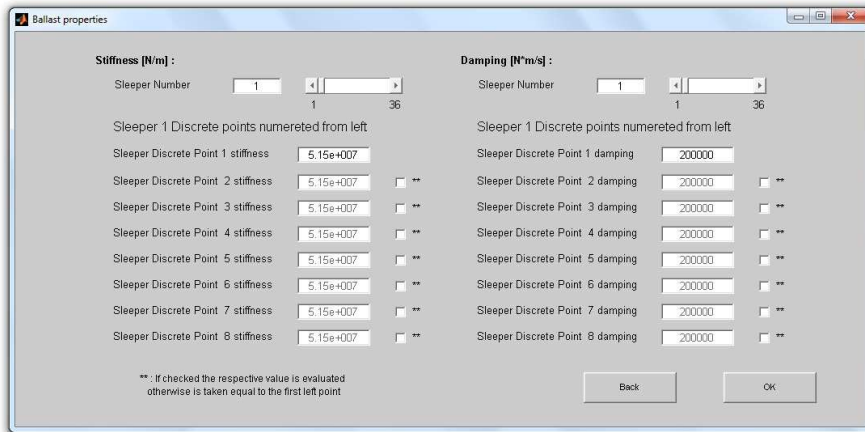
The following show the GUIs arising from the choice of the first ballast model (figure 4.3.8).

---

<sup>4</sup>If a Winkler method is chosen, in the simple Vehicle-track program, automatically  $kB$  is set equal to zero and vice-versa if a set of springs is used.



(a) General properties



(b) Singular points properties

Figure 4.14. Ballast GUIs

In GUI 4.3.8 it is so possible to set irregularities in the track way ballast, having the possibility of changing all the connection elements of an entire sleeper or also one by one each sleeper discretization point.

### 4.3.9 Simulated temporal space

As aforementioned the train starts from five sleepers from the beginning of the track way to avoid problems at the extremes. Similarly the simulation should stop when the first wheelset (the nearest to the end of the way) reaches the last but four sleeper.

The time at which this happens depends obviously from the start time and from train velocity.

The way followed in the program definition to stop the simulation at the right time is illustrated in figure 4.15.

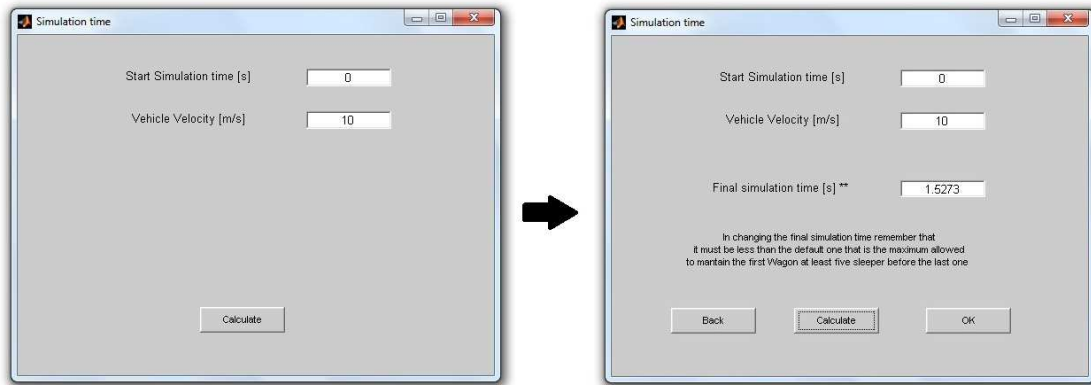


Figure 4.15. Simulated time

The user must enter the values of start time ( $T_{ic}$ ) and of train velocity ( $V$ ), being the last a constant value and then to press “calculate”.

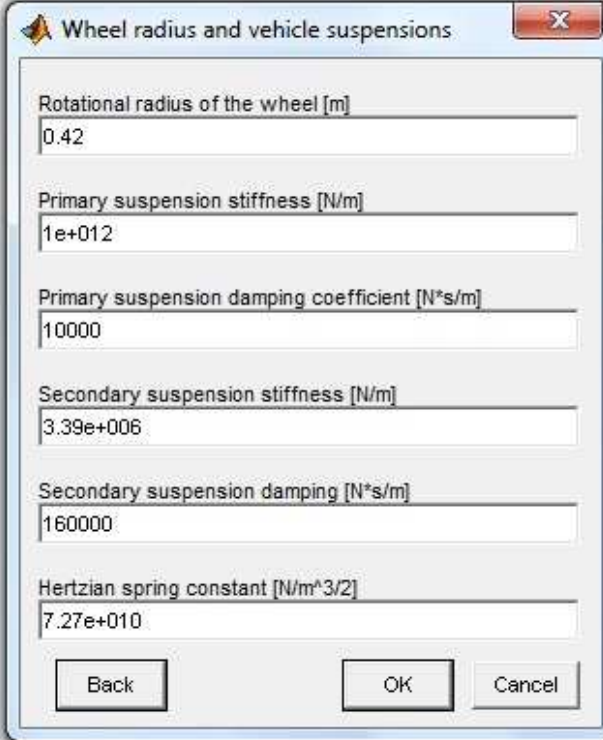
From these values and considering the rail length and sleepers distance, the program calculates the maximum final time of the simulation as:

$$T_{fc_{max}} = T_{ic} + \frac{(LR/2 - EJE_{pos_1} - LV * 5)}{V} \quad (4.4)$$

where  $EJE_{pos_1}$  is exactly the x-position of the first wheelset.

The user can finally change this default final simulation time paying attention not to increase it (as written in the GUI footnote).

### 4.3.10 Other input values



The screenshot shows a dialog box with the title "Wheel radius and vehicle suspensions". It contains seven input fields, each with a label and a value:

- Rotational radius of the wheel [m]: 0.42
- Primary suspension stiffness [N/m]: 1e+012
- Primary suspension damping coefficient [N\*s/m]: 10000
- Secondary suspension stiffness [N/m]: 3.39e+006
- Secondary suspension damping [N\*s/m]: 160000
- Hertzian spring constant [N/m<sup>3/2</sup>]: 7.27e+010

At the bottom of the dialog box, there are three buttons: "Back", "OK", and "Cancel".

Figure 4.16. Some other input values

These are other values of interest for the simulation.

- Rotational radius of the wheel [ $m$ ]  $R_w$  : is the radius of the wheels (in meters) used to calculate optional wheels irregularities (see equation (3.15) chapter 3).
- Primary and secondary suspension stiffness (respectively  $ks1$  and  $ks2$ ) : are the values of primary and secondary suspensions stiffness coefficients (misured in  $N/m$ ) that will be used in next GUIs to identify the stiffness matrix of the vehicle.
- Primary and secondary suspension damping coefficient (respectively  $cs1$  and  $cs2$ ) : are the values of primary and secondary suspensions damping coefficients

(measured in  $N/(m/2)$ ) that will be used in next GUIs to identify the damping matrix of the vehicle.

- Hertzian spring constant  $[N/(m^{3/2})]$  : is the value of the hertzian contact spring taken into account to calculate the wheel contact force (see equation (3.13) chapter 3).

#### 4.3.11 Vehicle matrices: DOF matrix ( $MAT\_DOF$ )

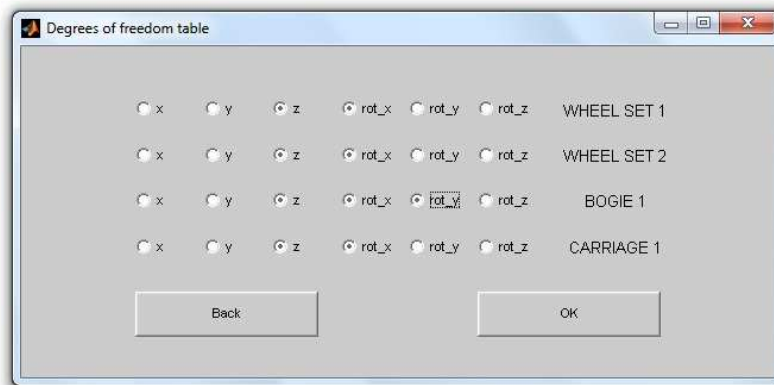


Figure 4.17. DOF matrix

In figure 4.17 it is shown the DOF matrix of the vehicle.

This is an important step in the input part because from the reading of this matrix the program will opportunely assembly the stiffness and damping matrices of the vehicle.

For each component of the vehicle there are six degrees of freedom check boxes.

The user should opportunely check, time after time, the right boxes considering the number of elements chosen in the first GUI 4.3.3.

Figure 4.17 shows the DOF matrix for the case considered till now (2 wheelsets - 1 bogie - half carriage) and the chosen DOF are right those of vertical displacement ( $z$ ), rigid rotation around x-axis ( $rot\_x$ ) and only for the bogie the third one, that is the rigid rotation around y-axis ( $rot\_y$ ).

The program will then calculate the numerated matrix as follows:  $MAT\_DOF$  matrix is a  $a \times 6$  matrix where  $a$  is the number of vehicle elements and 6, the number of columns, corresponds to the 6 degrees of freedom. To each cell where the degree of freedom is selected a 1 is inserted in the matrix, while all the others are 0. The matrix is then numerated ( $MAT\_DOF\_N$ ) from 1 to  $GDLV$  where  $GDLV$  is the total number of DOF of the vehicle.



For instance, the corresponding DOF matrix of figure 4.17 is :

$$\begin{vmatrix} 0 & 0 & 1 & 1 & 0 & 0 \\ 0 & 0 & 1 & 1 & 0 & 0 \\ 0 & 0 & 1 & 1 & 1 & 0 \\ 0 & 0 & 1 & 1 & 0 & 0 \end{vmatrix}$$

and the respective numerated one is:

$$\begin{vmatrix} 0 & 0 & 1 & 2 & 0 & 0 \\ 0 & 0 & 3 & 4 & 0 & 0 \\ 0 & 0 & 5 & 6 & 7 & 0 \\ 0 & 0 & 8 & 9 & 0 & 0 \end{vmatrix}$$

In the actual version of the program wheelsets can have at most 2 DOF while Boggies and carriages 3, but the program takes already into consideration the possibility of future developments.

In doing so it is programmed for assembly all the vehicle matrices considering this complete DOF numerated matrix.

The vehicles components can all have six space DOF and so their matrices. The limitation in the program developed is given by rails and sleepers that, instead, take into account only vertical vibration.

The following GUI window (figure 4.18) is only explicative but it is important to pay attention to it because it gives the numeration used for vehicle components.

This bodies numeration will be usefull in the understanding of the next GUIs.

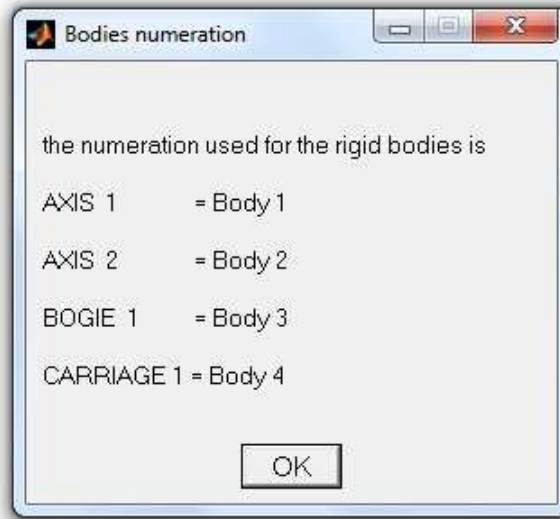


Figure 4.18. Vehicle components numeration

### 4.3.12 Vehicle matrices: Inertia rigid body properties Matrix (*IRBP*)

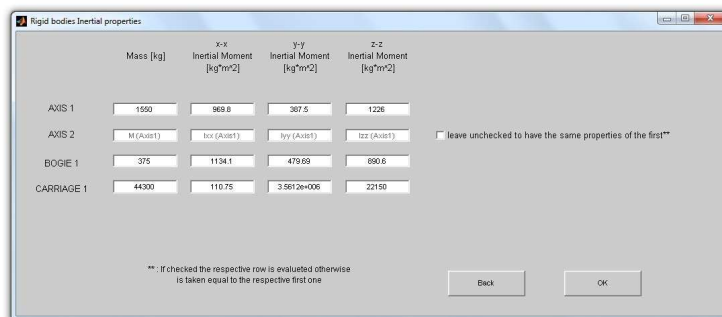


Figure 4.19. Inertia rigid body properties Matrix *IRPB*

Figure 4.19 shows the input data necessary to assembly the vehicle inertia matrix. Here also each row corresponds to a vehicle body (wheelset, bogie, carriage) and each column to an inertia property:

1. Mass [*kg*];
2. x-x moment of inertia (*Ixx*);

3. y-y moment of inertia ( $I_{yy}$ );
4. z-z moment of inertia ( $I_{zz}$ ).

Obviously the z-z moment of inertia is not a quantity of interest for this work (rotation around z is never considered as DOF) but as for the other cases future developments could require it.

Finally the small check box at the right side of the GUI should be checked only when the user wants to insert different values for vehicle similar components.

In this example the only part of the vehicle repeated is the wheelset so this small check box is available only for it. As written in the footnote when the check box is unchecked all the repeated bodies properties are taken equal to the first respective body (the only active in the GUI).

If the user wants to change one or more properties of all the repeated bodies all at once it is sufficient to leave unchecked the boxes and to change the property of the first similar one.

Whereas, if the user wants to diversify similar components, he should insert the values of the respective entire row , remembering to check also the relative check box to make the program evaluating it.

### 4.3.13 Vehicle matrices: Vehicle external forces( $Ext\_F$ )

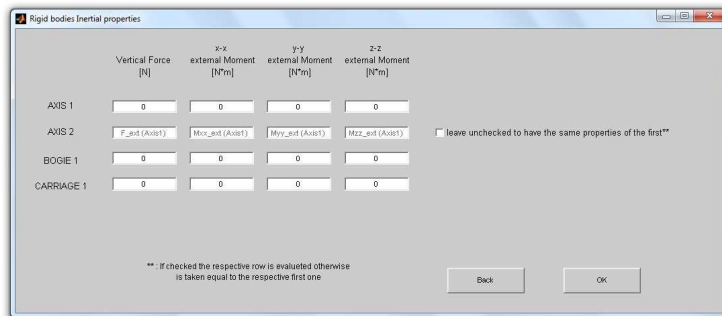
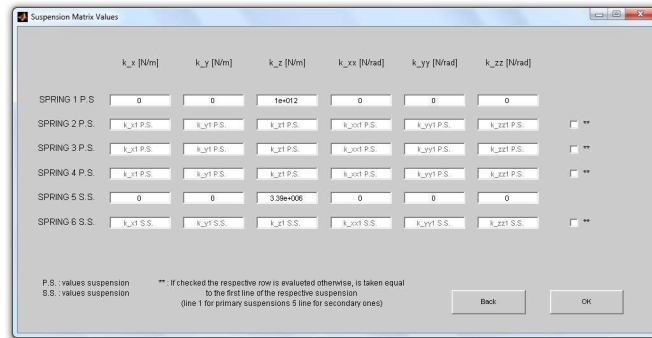


Figure 4.20. External constant forces acting on vehicle DOF

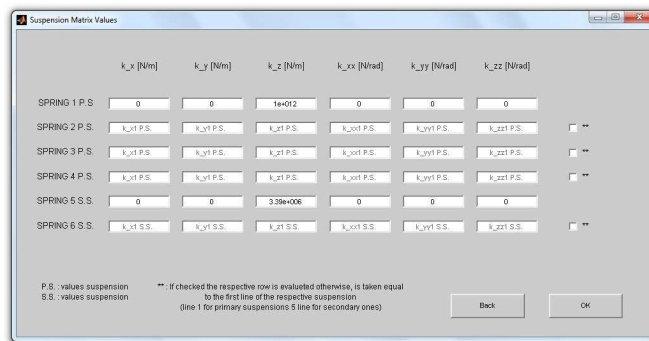
GUI window shown in figure 4.20 permits to insert in the model external constant forces acting on vehicle DOF (the weight is already taken into account in the force vector assembly using the inertial mass previously defined in GUI 4.19).

Concerning the small check boxes same considerations aforementioned hold true.

### 4.3.14 Vehicle matrices: Suspensions matrices (*MAT\_LS\_K* & *MAT\_LS\_C*)



(a) Vehicle suspensions stiffness coefficients



(b) Vehicle suspensions damping coefficients

Figure 4.21. Vehicle suspensions matrix

In figures 4.21(a) and 4.21(b) the GUIs relative to vehicle suspensions are shown.

The first one shows the matrix pertaining to springs stiffness.

All the necessary information are already in the figure so just notice that, also in this case, using the check boxes it is possible to make overall changes to the springs of the system all at once.

It is important to notice that suspensions are divided between primary suspensions and secondary ones, *P.S.* and *S.S.* respectively, and the check boxes work also here only with similar elements. To change all primary suspensions stiffness (or damping coefficients) it is sufficient to change the first P.S. row, and similarly to

change all secondary suspensions dampers it is the first secondary suspension line that should be modified.

Changing all the values of a single row and left clicking the relative right check box will instead modify the relative suspension values.

Take in mind that it is possible to change and check only some rows and leave the others unchecked and equal to the first similar one, but it is not possible to change only some values for a single row, because when computed a row needs only numerical values.

### 4.3.15 Vehicle matrices: Suspensions connection matrices (*Conn\_MAT\_K* & *Conn\_MAT\_C*)

|               | body at side 1 | x1 [m] | y1 [m] | z1 [m] | body at size 2 | x2 [m]  | y2 [m] | z2 [m] |
|---------------|----------------|--------|--------|--------|----------------|---------|--------|--------|
| SPRING 1 P.S. | 1              | 0      | 1      | 0      | 3              | 0.8635  | 1      | 0      |
| SPRING 2 P.S. | 1              | 0      | -1     | 0      | 3              | 0.8635  | -1     | 0      |
| SPRING 3 P.S. | 2              | 0      | 1      | 0      | 3              | -0.8635 | 1      | 0      |
| SPRING 4 P.S. | 2              | 0      | -1     | 0      | 3              | -0.8635 | -1     | 0      |
| SPRING 5 S.S. | 3              | 0      | 0.75   | 0      | 4              | 7.4675  | 0.75   | 0      |
| SPRING 6 S.S. | 3              | 0      | -0.75  | 0      | 4              | 7.4675  | -0.75  | 0      |

P.S.: Primary suspension  
S.S.: Secondary suspension

\*\* : if checked the respective row is evaluated otherwise, is taken equal to the first line for the primaries or to the line 5 for the secondary ones

(a) Vehicle springs positions

|               | body at side 1 | x1 [m] | y1 [m] | z1 [m] | body at size 2 | x2 [m]  | y2 [m] | z2 [m] |
|---------------|----------------|--------|--------|--------|----------------|---------|--------|--------|
| DAMPER 1 P.S. | 1              | 0      | 1      | 0      | 3              | 0.8635  | 1      | 0      |
| DAMPER 2 P.S. | 1              | 0      | -1     | 0      | 3              | 0.8635  | -1     | 0      |
| DAMPER 3 P.S. | 2              | 0      | 1      | 0      | 3              | -0.8635 | 1      | 0      |
| DAMPER 4 P.S. | 2              | 0      | -1     | 0      | 3              | -0.8635 | -1     | 0      |
| DAMPER 5 S.S. | 3              | 0      | 0.75   | 0      | 4              | 7.4675  | 0.75   | 0      |
| DAMPER 6 S.S. | 3              | 0      | -0.75  | 0      | 4              | 7.4675  | -0.75  | 0      |

P.S.: Primary suspension  
S.S.: Secondary suspension

\*\* : if checked the respective row is evaluated otherwise, is taken equal to the first line for the primaries or to the line 5 for the secondary ones

(b) Vehicle dampers positions

Figure 4.22. Vehicle suspensions position

In figure 4.3.15 are illustrated the GUIs pertaining to connection vectors between suspension elements.

For each element it is indicated which are the bodies connected<sup>5</sup>

Notice that both figures 4.22(a) and 4.22(b) have the same values for connection matrices of springs and dampers. This only means that they are located in the same position using a lumped element approach, but the model would still work also if these two elements were split up and located in different positions.

---

<sup>5</sup>this is the reason why GUI 4.18 gives the numeration used for vehicle parts.

### 4.3.16 Wheels irregularities selection



Figure 4.23. Irregularites selection question dialog box

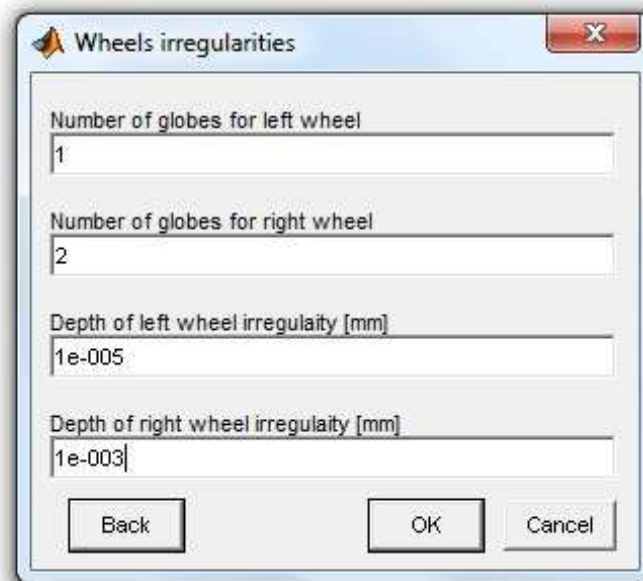


Figure 4.24. Irregularites parameters definition

Thanks to GUI window 4.23 it is possible to decide, on a case by case basis, if to study an irregular wheels problem or not.

Parameters required in the case of a positive answer to the question dialog box 4.23 are shown in the next GUI window 4.24 and refer to the irregularity function described before in chapter 3 , equation (3.15) .

Each Wheel can have a different number of wheel globes ( $N_i$ ,  $i = 1,2$ ) and a different irregularity amplitude ( $H_{irr,i}$ ,  $i = 1,2$ ), thus making the problem asymmetric.

### 4.3.17 Numerical integration method

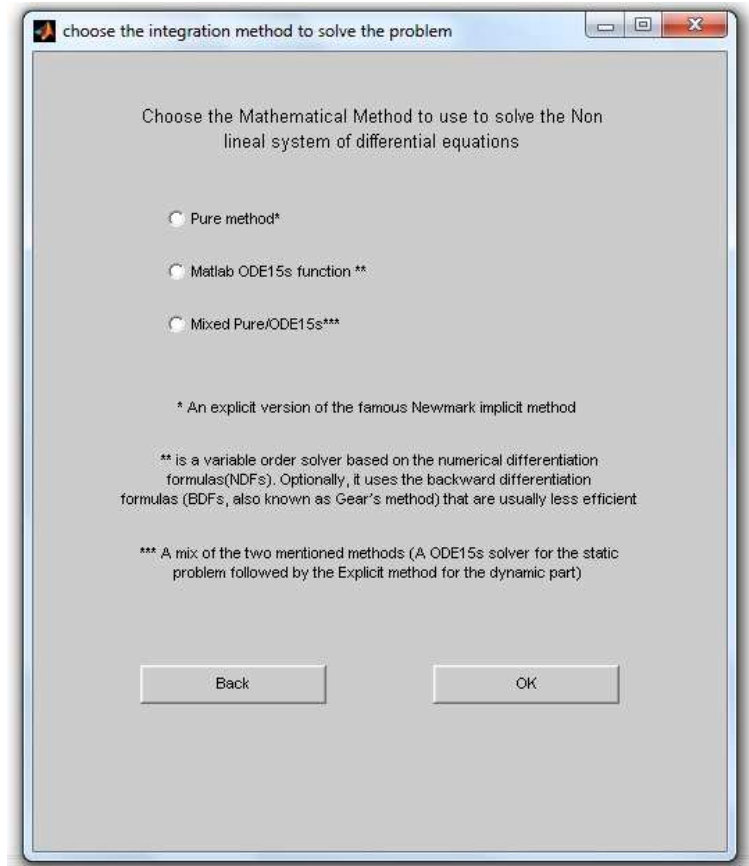


Figure 4.25. Types of integrators implemented in the program

An important matter in defining the program was the choice of the numerical integrator.

As well known, initial value problems for ordinary differential equations (ODEs) can be numerically integrated using different types of solver. *Matlab* has some first order solvers implemented, as for instance Runge-kutta 2-3 or 4-5 order, ODE23 and ODE45 respectively, and some others that on a case by case basis should be properly chosen (for example considering the degree of stiffness of the system).



Considering that the total system is described by a second order differential equations system, the use of these built-in solvers needs a little rearrangement of the system (3.28) as aforementioned in section 3.6.1 of chapter 3.

The program, as visible in figure 4.25, offers three ways to solve the system:

- Pure method : is the explicit second order method described in annex C;
- Matlab ode15s function : it is a variable order system as written in the second footnote of the GUI (\*\*);
- Mixed Pure/Ode15s : the built-in ODE15s solver is used to solve the static problem<sup>6</sup> while the explicit second order method is used to solve the dynamic one.

Obviously it would be interesting to study the efficiency of each solving method for different kind of problems (different size, linear and non linear problems ect. ect.).

Mainly, for simple problems, crudely comparing obtained results , the “Mix” solver seems to be the most efficient but, specially for particular non linear cases, the accuracy of its results should be thoroughly proved to establish the supremacy of this method.

---

<sup>6</sup>as described later, in order to calculate the initial values of the problem, first the static problem is solved, and its solution is then used has the initial one for the dynamic problem (train in motion).

### 4.3.18 Beams number of modes

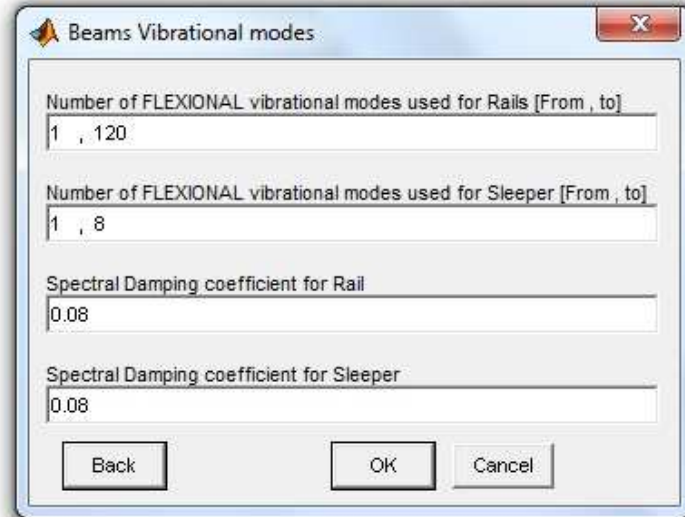


Figure 4.26. Number of vibrational modes and spectral damping coefficients used for each beam

In this small GUI it is possible to establish the number of vibrational modes used for each beam model (Rails and sleepers here, rails, sleepers and underlying structure in the bridge interaction program).

Moreover in the same GUI it is asked to enter the values of spectral damping coefficients for each beam modelled track component. These spectral damping values are constant for all the modes of the same beam, but considering all the simplifications done till now, this should not influence to much the accuracy of the model.

Getting the right value for spectral damping coefficients is not a simple matter and so the way followed in this work has been to use small values taken from reference [2].

Finally, it is important to notice that the number of modes used for rails is always much larger than the number of sleepers modes. This is obviously due to their natural frequencies, that, in the case of short sleepers, are higher and more spaced in respect to those of the same modes of rails.

### 4.3.19 Saving GUI

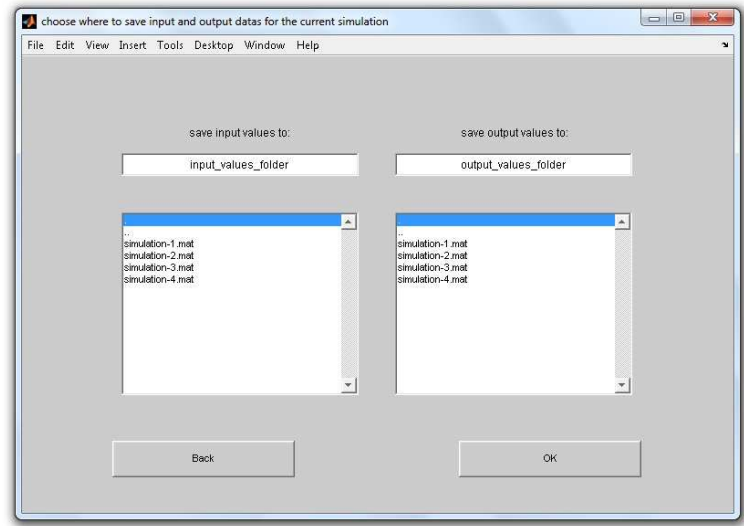


Figure 4.27. Saving GUI

This is the last input GUI and the user should only enter the name of the files where to save input and output data of the running simulation. Before running the simulation all the variables set till now are saved in the specified file located in the input folder.

## 4.4 Solving part

During the solving part of the program, before starting the solution of the differential equation system, with whatever solver, two more message boxes (figures 4.28) inform the user about the possibility of insert a non linear component in the definition of railpads and of ballast connection forces (equations (3.18) and (3.20) of chapter 3)

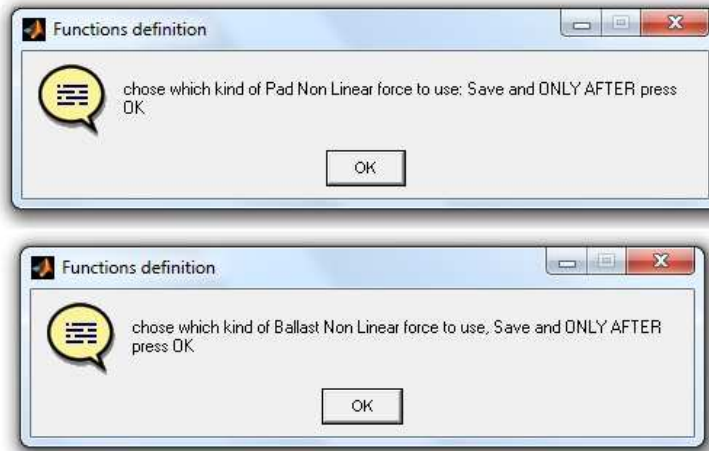


Figure 4.28. Non linear forces

Simultaneously with the messages the program will open, one by one, two *Matlab* \*.m files, which are precisely the non-linear function definition for pad and ballast.

In order to not consider these non linear components the user should only press the *OK* button without changing any thing in the opened .m files.

When a non linear component is required for one or both connection elements the user should instead insert the force expression, following the legend in the upper part of the .m files to understand the meaning of the variables.

#### 4.4.1 simulation time

A very important task during the development of the program has been to reduce the simulation time.

In fact *Matlab* proved to be a low efficiency programming language at least to heandle this kind of problems.

Moreover the use of GUIs makes the program even slower, and if in the input part this slowdown is neither perceptible, during the calculation it is almost not recommended (for example the using of waitbars or feature to display the simulation time).

Each of the solvers implemented proved to be, on a case by case basis, more efficient than the other.

It should be made an accurate analysis with a large use of tests do understand when to use one instead of the other and the reason why, but this was not the aim of this work that wanted only to set up the total system and show its behavior in studying this kind of problems.

## 4.4.2 Output data

The output values obtained from each simulation are the total  $x$  vector and its velocity  $v$  (see equation (3.26) chapter 3). This two vectors are saved in the file specified for the output data in GUI 4.27.

From this two values it is obviously possible to go back to all the quantities of interest as the interaction forces and substructures dynamic behaviour.

At the end of the simulation a last GUI (figure 4.29) permits to see the results with the plot of the main quantities of interest.

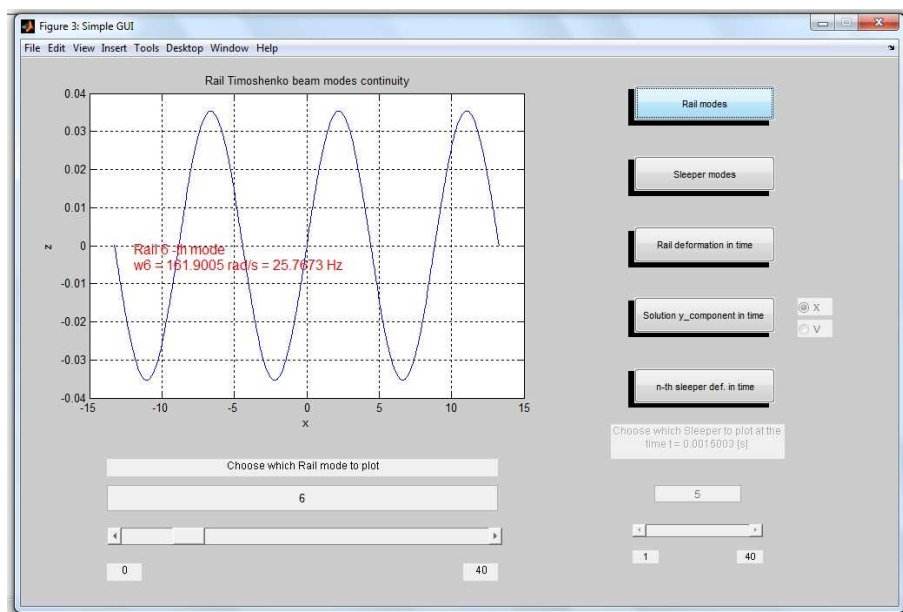


Figure 4.29. Main quantities of interest plot

## 4.5 Bridge interaction program

As aforementioned, the “Bridge version of the program” and the one discussed till now are more or less alike. The only difference in GUIs used is the specification of the bridge mechanical properties and modal ones.

These bridge GUIs are not here discussed because they follow the notation used till now and are simple to understand.

## 4.6 Frequency response function FRF program

For both cases of single track-vehicle problem and the Bridge interaction one, a small software capable of calculating the respective *FRF* has been done.

Also in this case the differences in the GUIs used are a few.

Here it is only explained the last GUI of these FRF programs that is shown in figure 4.29

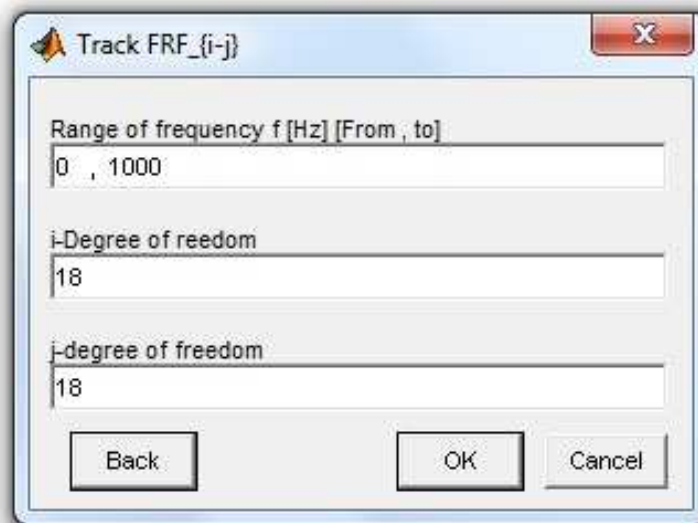


Figure 4.30. FRF parameters selection

Memory limits prevent the program from calculating the all  $H(i\omega)$  FRF, but only the  $H_{i,j}$  components that the user wants to.

For this reason the user is asked to enter the range of frequencies in which to calculate the FRF and also the  $i$  and  $j$  components of the FRF to calculate;

It is very important to notice that both  $i$  and  $j$  can assume a single scalar value or be a vector of values, case in which the FRF is then calculated for all the possible combinations of  $i$  and  $j$  vectors components ( $H_{i(1),j(1)}$  ,  $H_{i(1),j(2)}$  ,  $H_{i(2),j(1)}$  ect.).

# Chapter 5

## Simulations results

### 5.1 Program Validation

Mainly, the program developed follows the procedure described in Ref. [1].

In order to verify the proposed model in the time domain, lots benchmark tests of moving vehicle on the track should be performed to compare results to those obtained by already validated methods.

Comparing results obtained from experimentation or at least from similar benchmarks tests , it could be possible to establish the accuracy of this simplified model and evaluate the error trend in function of the most important parameters as the number of modal modes or the theory used. FEM Analysis of more complicated models could also be used to evaluate the computational efficiency of this simpler model.

Being not possible to have these tests results the following way has been used.

Results discussed in [1] have been considered holding good also in this work so that the simple case of Timoshenko free-free Rail and Euler free-free sleeper on a Winkler foundation is the used one to validate the others. Thus, once demonstrated the accordance of new model results with the above-mentioned ones the program has been considered well-functioning.

However to validate the accuracy of the implemented program it should be necessary to run several test simulations with different combinations of mathematical models and non linear components for both cases of track over a bridge and not.

Obviously this was not possible during this short thesis work, but, in this chapter, some achieved tests results are shown and discussed.

From last GUI , figure 4.29, it is possible at least to see and analyze , the correct trend of simulation results rather than their accuracy and basically they seem to be correct.

The following quantities were obtained and analyzed for each simulation, and in

this chapter some of these results are shown and discussed:

- Rails , Sleepers and Bridge deformations in time;
- DOF  $\mathbf{x}$  vector progress in time;
- FRF for different models with or without wheelsets.

## 5.2 Tests results

As aforementioned for both cases of simple vehicle-track system and vehicle-track-structure one it has been analyzed the temporal response of the non-linear system and the frequency response function.

In the first case the main output data of interest are the deformations of the various elements composing the system that are :

- $z_a(x,t)$  with  $a = 1, \dots, N_{ax}$ ;
- $v_r(x,t)$  with  $r = 1, \dots, N_r$ ;
- $u_s(y,t)$  with  $s = 1, \dots, N_{as}$ ;
- $w(x,t)$  .

In fact from these variables values it is possible to go back to all the other quantities of interest in engineering problems as loads, mechanical stresses and interaction forces.

In the second case of FRF analysis, obviously, the only output is given by the FRF itself. Thus it was studied the effect of the vehicle as well as others simulation parameters on system FRF calculated on a rail point<sup>1</sup>.

Notice that the temporal response model is more accurate than the FRF for the studied system , this because it takes into account problem non-linearities , introducing so less error components in the mathematical model, that is already greatly simplified.

---

<sup>1</sup>It could be interesting to evaluate the FRF also in other track points, as it is possible to do in the program, but these results are not discussed here.



## 5.3 Temporal response

### 5.3.1 Vehicle-Track system

The parameters used in next simulations were selected from Ref. [1] and are shown in table 5.3.1 that summarises the mechanical properties of track and vehicle.

The rail is considered mainly as a Rayleigh-Timoshenko beam and the sleepers are modelled as Euler-Bernoulli beams on a Winkler foundation, but some comparisons between different models are also discussed.

Concerning boundary conditions the rail has been studied, mainly, with a continuous-continuous beam while the sleepers are modelled with a free-free beam (also in this case some comparisons with other boundary conditions are later analyzed).

The ballast stiffness is so modelled here as a Winkler foundation while its damping effect is taken into account through the use of 8 discrete dampers.

A total of 50 Sleepers have been used.

Concerning modal properties, used values are visible in table 5.3.1.

The train Velocity has been set equal to  $V = 30 \text{ m/s}$  and the total time of simulation is  $T = 0.8173 \text{ s}$  according to equation (4.4).

Considering that in the case of sleepers the difference between the Timoshenko theory and the Euler-Bernoulli one is small because of the small number of modal modes considered, the following test simulations were run:

1. A simple problem with the only non-linear component due to wheels-rail contact force ; Sleepers and rail modelled with Euler-Bernoulli beam theory with free-free and continuous-continuous boundary conditions , respectively.
2. The same simple problem studied always with Euler-Bernoulli theory in sleepers case and with Timoshenko one for rails with the same boundary conditions as above.
3. Two irregular cases (once deriving from irregular wheels and once fro a ballast discontinuity), studied with Timoshenko continuous-continuous beam for rails and Euler free-free beam for sleepers.

The resulting range of frequencies for rails and sleepers is respectively:  
Euler modelled Sleepers :

$$\omega_n = [0 , 675] \text{ Hz}$$

Rails :

---

<sup>2</sup>because a Winkler ballast model has been chosen

| Denotation | Parameter                                    | Value                             |
|------------|--|-----------------------------------|
| Track      |  |                                   |
| $E_r$      | Young's modulus of rail                      | 207 GPa                           |
| $I_r$      | Rail moment of inertia                       | $3.05 \times 10^{-5} \text{ m}^4$ |
| $A_r$      | Rail cross-sectional area                    | $7.7 \times 10^{-3} \text{ m}^2$  |
| $k_r$      | Timoshenko shear coefficient                 | 0.34                              |
| $\rho_r$   | Rail density                                 | 7860 kg/m <sup>3</sup>            |
| $L_r$      | Rail length                                  | 33.32 m                           |
| $N_s$      | Number of sleeper                            | 50                                |
| $E_s$      | Young's modulus of sleeper                   | 20 GPa                            |
| $I_s$      | Sleeper moment of inertia                    | $1.18 \times 10^{-5} \text{ m}^4$ |
| $A_s$      | Sleeper cross-sectional area                 | 0.0157 m <sup>2</sup>             |
| $\rho_s$   | Sleeper density                              | 2500 kg/m <sup>3</sup>            |
| $L_s$      | Sleeper length                               | 2.36 m                            |
| $D_s$      | Distance between sleepers                    | 0.68 m                            |
| $k_p$      | Railpad stiffness                            | 200 MN/m                          |
| $c_p$      | Railpad damping                              | 50 kN/m/s                         |
| $k_b$      | Ballast stiffness per rail seat <sup>2</sup> | 0 kN/m <sup>2</sup>               |
| $c_b$      | Ballast damping per rail seat                | 105 kN/m <sup>2</sup> /s          |
| Vehicle    |  |                                   |
| $N_{ax}$   | Number of wheelsets                          | 2                                 |
| $M_c$      | Carriage mass                                | $22 \times 10^3 \text{ kg}$       |
| $M_b$      | Bogie frame mass                             | 4000 kg                           |
| $I_b$      | Bogie frame pitch moment of inertia          | 479.6 kg · m <sup>2</sup>         |
| $M_w$      | Wheelset mass                                | 1500 kg                           |
| $L_w$      | Distance between wheels in a single bogie    | 3 m                               |
| $k_H$      | Constant of Hertzian contact model           | 72.7 GN/m <sup>3/2</sup>          |
| $k_{s1}$   | Primary suspension stiffness                 | 1 MN/m                            |
| $c_{s1}$   | Primary suspension damping                   | 10 KN/m/s                         |
| $k_{s2}$   | Secondary suspension stiffness               | 3.39 MN/m                         |
| $c_{s2}$   | Primary suspension damping                   | 160 KN/m/s                        |

| Denotation | Parameter                     | Value |
|------------|-------------------------------|-------|
| Track      |                               |       |
| $N_{mr}$   | Total number of Rails modes   | 101   |
| $N_{ms}$   | Total number of sleeper modes | 7     |
| $\zeta$    | Rail modal damping coeff.     | 0.08  |
| $\xi$      | Sleeper modal damping coeff.  | 0.08  |

- Euler modelled :  $\lambda_n = [0 , 4573] Hz$
- Timoshenko modelled :  $\lambda_n = [0 , 2360] Hz$

The range used for sleepers is much smaller than the rails one, but it was proved that mainly the first 3 or 4 sleeper flexural modes are sufficient to study its deformation because these are the mostly excited modes.

Concerning rails , figure 5.1 illustrates the plot of Timoshenko natural frequencies versus Euler-Bernoulli ones. As expected, considering a big range of frequencies the difference between the two models becomes significant.

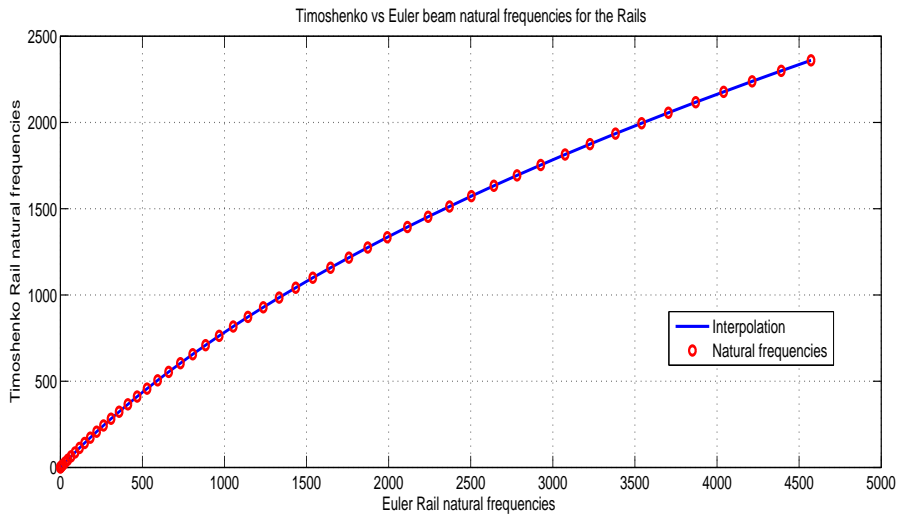


Figure 5.1. Timoshenko vs Euler-Bernoulli rails natural frequencies

This huge difference is visible also in the deformation of the variuos elements as

in the interconnection forces. In figure 5.2 are shown wheels-rail contact forces for both cases of rails mathematical modeling.

Notice that the system is here symmetric and without any asymmetric disturbance also system response is so. Deformation and forces of the right part of track are so equal to left ones (rail 1 = rail 2, wheel left = wheelset right , ect.).

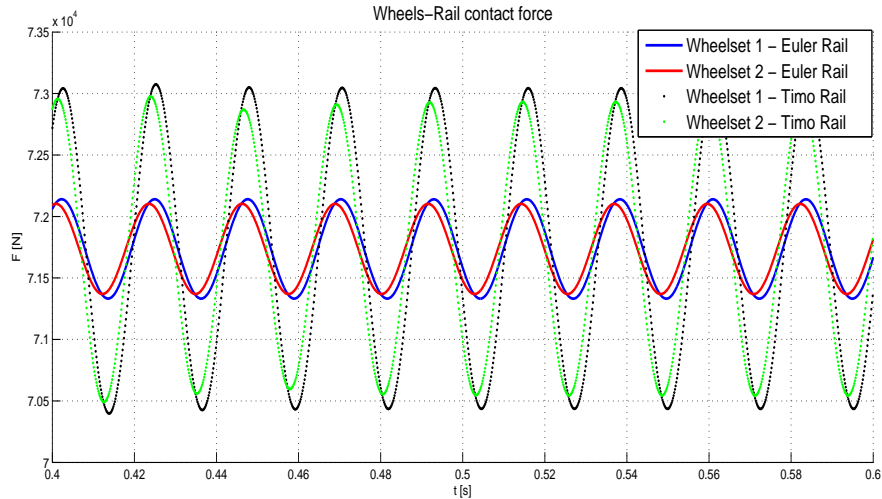


Figure 5.2. Timoshenko vs Euler-Bernoulli rails natural frequencies

Euler Rail is so more rigid than Timoshenko one and this results in different vibration modes for the total structure, that, as aforementioned, in the second case is less rigid. Contact forces are so bigger in Timoshenko modelled rail, because, under the action of an equal external force (vehicle weight), a less rigid system will deform more, as results from figure 5.2.

This was also discussed in Ref. [2] with free-free Timoshenko rail.

Timoshenko beam permits to analyze the influence of some vibration modes that are not “caught” from Euler theory and so the first model is the considered one from now on.

In figure 5.3 it is possible to see rail deformation at the time  $t = 0.4355$  s. The maximum deformation value is of the order of  $10^{-4}$  m -  $10^{-3}$  m and actually this is the order of magnitude expected here and obtained also from Ref. [1].

For the same time instant, in figure 5.4, it is illustrated the deformation of some sleepers and also in this case the range of deformation amplitude is the expected one; notice that, as aforementioned , the system response is absolutely symmetric.

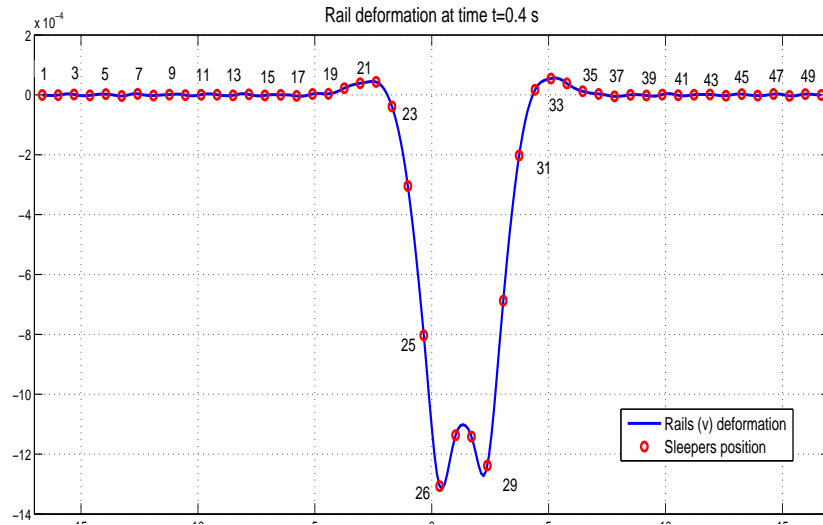


Figure 5.3. Rail deformation at  $t = 0.4355$  s

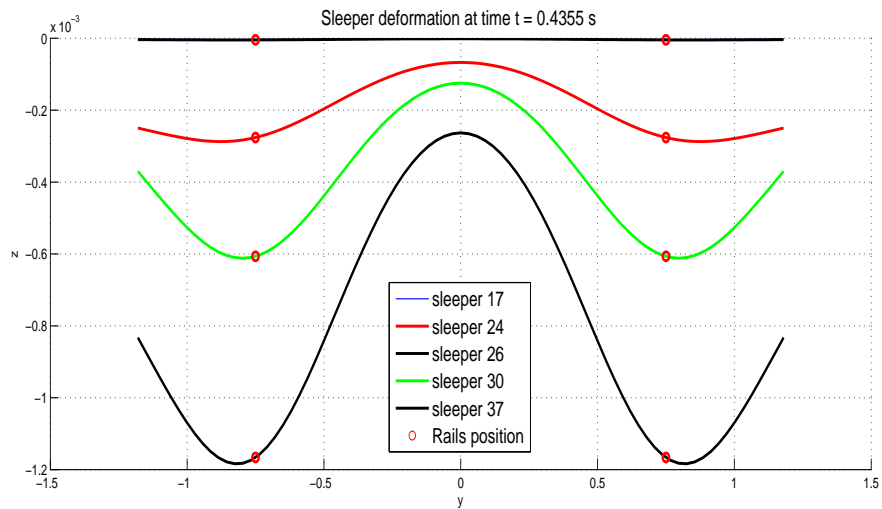


Figure 5.4. Sleepers 17 , 24 , 26 , 30 , 37 , deformation at  $t = 0.4355$  s

Using thus Timoshenko theory to model both rails , two more simulations have been run to analyze the effect of some sorts of irregularities on the Vehicle-track system.

An irregularity 1 mm , 1 globe wheel function has been used for both wheels of all wheelsets while in the last simulation ballast properties have been changed for sleeper 25<sup>3</sup> ( $kb_{25} = 60$  MN/m ,  $cb_{25} = 28000$  N/(m/s)).

<sup>3</sup>As aforementioned in section 4.3.8 to permit an irregular ballast it is not permitted to use

Figure 5.5 shows so contact forces deriving from both irregularities while figure 5.6 illustrates a zoom of rail deformation in the contact zone.

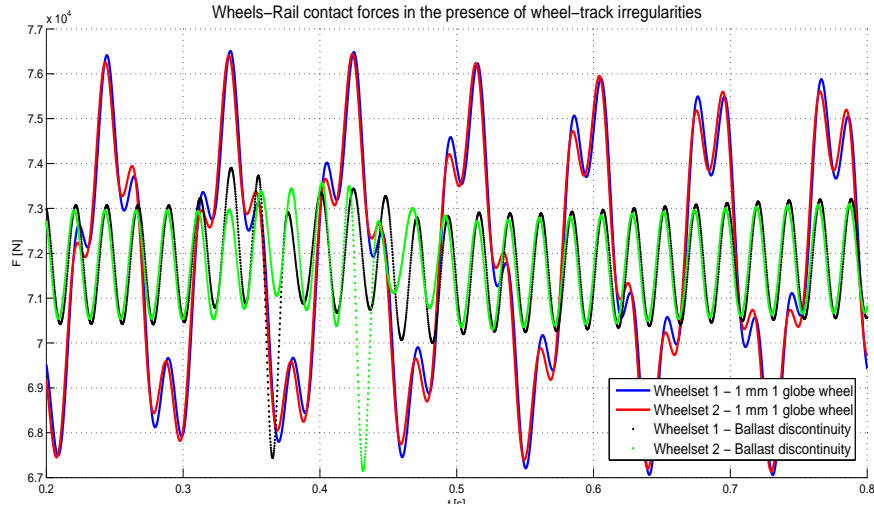


Figure 5.5. Wheels-rail contact forces for some irregular systems

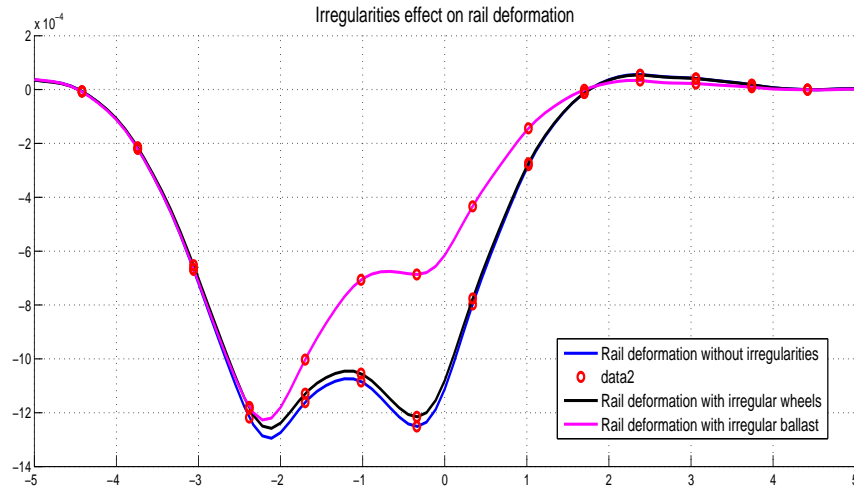


Figure 5.6. Rails deformation for two irregular cases

Finally, considering  $\mathbf{x}$ -vector components and remembering its definition, given in equation 3.26, it is possible to plot its components in time and watch their progress.

a Winkler model , and the general values used here for discrete elements of all  $N_s$  sleepers are ( $kb_i = 10 \text{ MN/m}$  ,  $cb_i = 31000 \text{ N/(m/s)}$ )

For instance, in figure 5.7 , it is possible to observe carriage  $z$ -displacement ( eighth x-component for the system considered ) in time for above discussed simple and irregular problems, and to verify its correct trend.

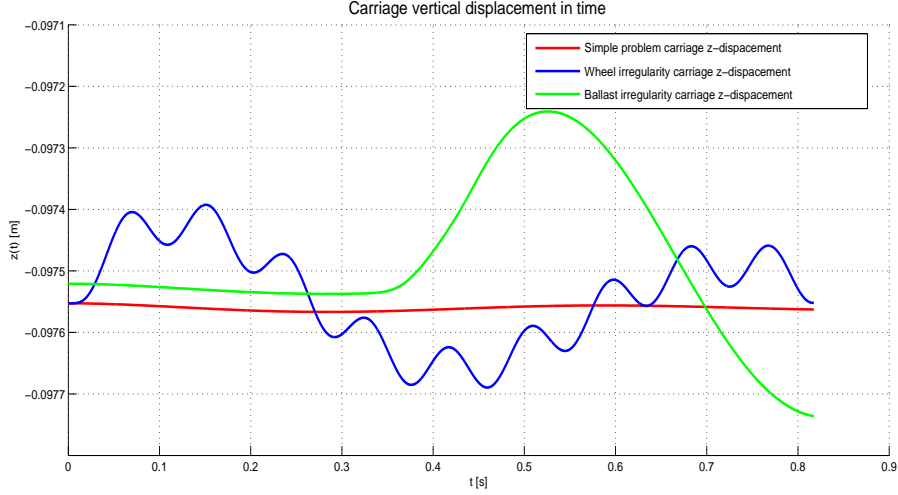


Figure 5.7. Carriage vertical displacement in time for the cases of simple problem (red line), wheels irregularity (blue line) and ballast discontinuity (green line)

### 5.3.2 Vehicle-Track-Structure system

The same results discussed till now have been obtained for the structure interaction version of the program and in this subsection temporal response results are discussed.

Vehicle-track simulation parameters are also here those visible in table 5.3.1 while concerning bridge properties they refers to table 5.3.2.

It is very important to notice that, in this case of track-bridge interaction , the ballast can no longer be modelled with a Winkler elastic foundation, and this because of Winkler theory hypothesis (see annex B).

If a Winkler foundation model were used , elastic component of the interaction forces acting on the bridge would be annuled and so only damping forces would reach the structure, thus making bridge response senseless.

For this reason the elastic component of ballast interaction force is here modelled with a discrete series of eight springs with a stiffness coefficient of  $k = 10 \text{ MN/m}$ , located in the same positions of relative dampers.

The range of bridge frequencies , using a modal truncation approach , is thus:

$$\tau = [6.02 \quad , \quad 385.28] \quad Hz$$

<sup>3</sup>because a Winkler ballast model has been chosen

| Denotation          | Parameter                     | Value                  |
|---------------------|-------------------------------|------------------------|
| Physical properties |                               |                        |
| $E_{Br}$            | Young's modulus of the bridge | 50GPa                  |
| $I_{Br}$            | Bridge moment of inertia      | 8.26 m <sup>4</sup>    |
| $A_{Br}$            | Bridge cross-sectional area   | 9.125 m <sup>2</sup>   |
| $\rho_{Br}$         | Bridge density                | 7860 kg/m <sup>3</sup> |
| $L_{Br}$            | Bridge length                 | 33.32 m                |
| Modal properties    |                               |                        |
| $N_{mBr}$           | Number of Bridge modes        | 8                      |
| $\mu$               | Bridge modal damping coeff.   | 0.04                   |

Also in this case, as for sleepers, the number of modal modes that take part in system total response , is much smaller than rails one and also in this case it was proved that increasing this number of modes doesn't change perceptibly bridge or system temporal response.

Obviously , contact forces depend on which beam theory is adopted to model rails and the results obtained for both theories are almost the same of those deriving from the simple vehicle-track model, as shown in figure 5.8.

Using, for the same reasons as before , Timoshenko beam theory to model both rails, similar test simulations were run to verify the good trend of results for the vehicle-track-structure program and below some deriving results are shown .

Figure 5.9 shows both rail and bridge deformations ate time  $t = 0.4355$  s while figure 5.10 shows some sleepers deformation at the same temporal instant.

Also in this case two irregular problems were tested and figure 5.11 shows deriving contact forces.

Finally, figure 5.12 shows differences in rail deformation for the cases of :

- Simple regular problem ;
- Irregular wheel problem ( 1 mm depth , 1 globe wheels );
- Irregular ballast problem ( $kb_{25} = 80$  MN/m ,  $cb_{25} = 26000$  N/(m/s)).

Obviously the order of magnitude of the total system deformation is here a little bigger being the system less rigid because of the bridge presence.



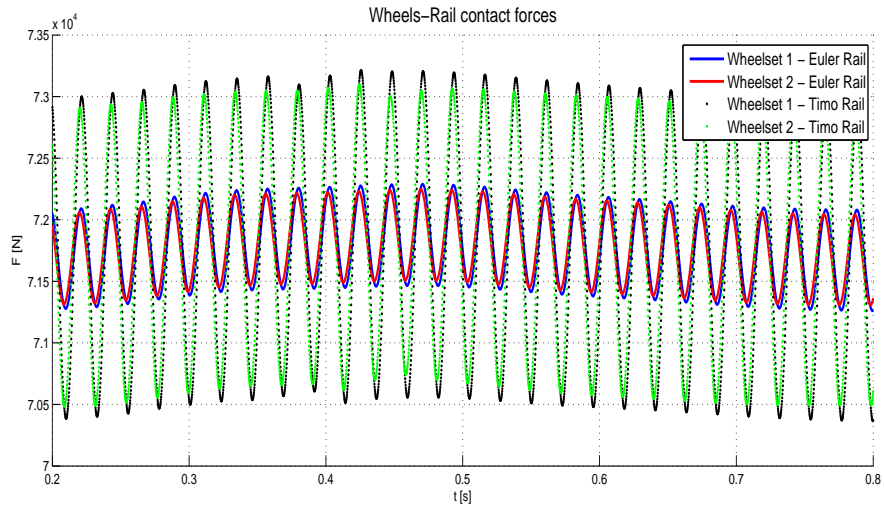


Figure 5.8. Timoshenko vs Euler-Bernoulli rails natural frequencies

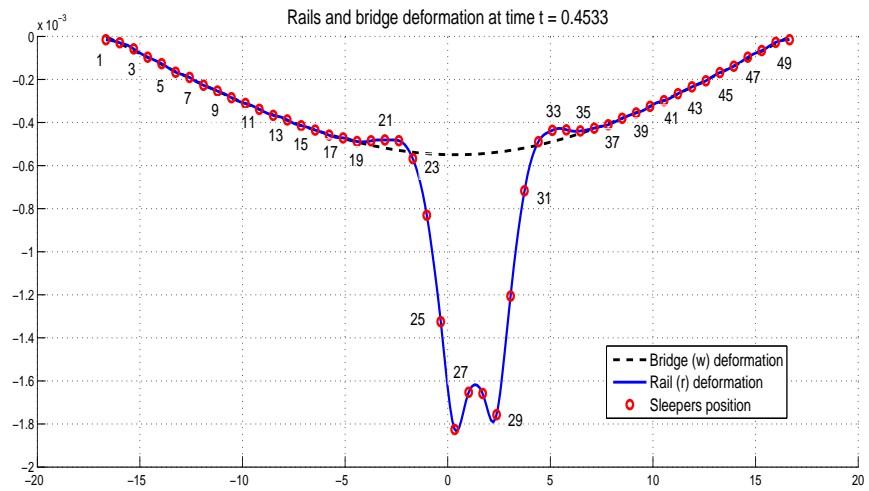


Figure 5.9. Rail and bridge deformation at  $t = 0.4355$  s

Take in mind that the deformation amplitude is not the only value of interest but stresses and loads depends on its derivates that near the wheel-rail contact zone have a very high slope.

For instance, in the case of Euler-Bernoulli beam theory ,  $M(x)$  bending moment ,  $Q(x)$  shear force and  $\sigma_x$  cross section axial stress can be related to  $u$  deflection with the use of equations (5.1), (5.2) and (5.3).

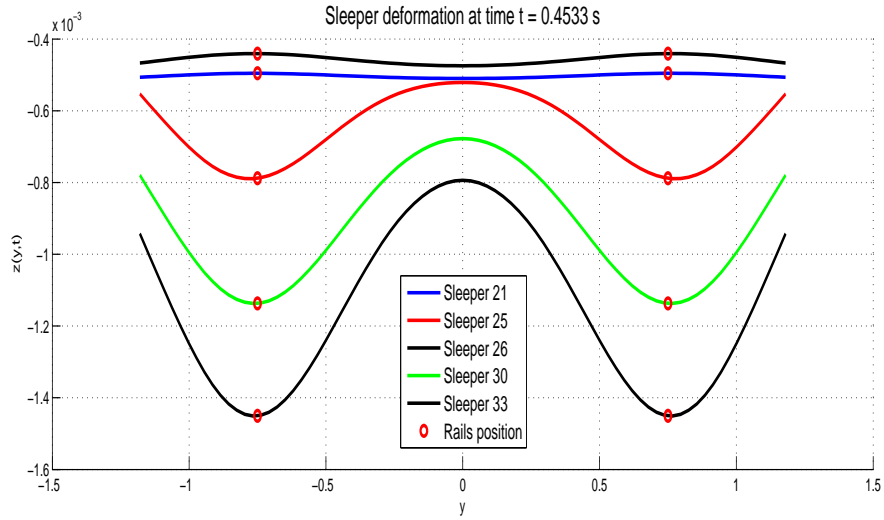


Figure 5.10. Sleepers 23 , 27 , 29 , 31 , 33 , deformation at  $t = 0.4355$  s

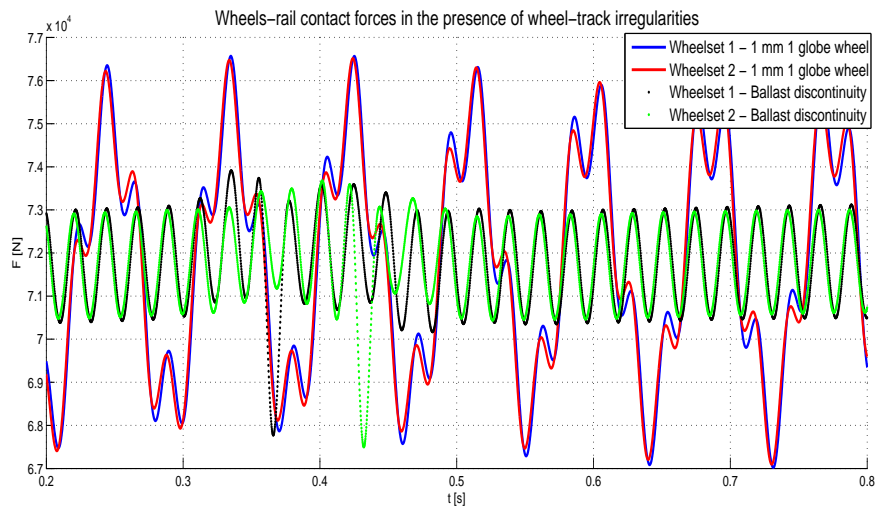


Figure 5.11. Wheels-rail contact forces for some irregular systems

$$\sigma_{x_{max}} = -\frac{Eh}{2} \frac{d^2 u}{dx^2} \quad (5.1)$$

$$M = -EI \frac{d^2 u}{dx^2} \quad (5.2)$$

$$Q = -EI \frac{d^3 u}{dx^3} \quad (5.3)$$

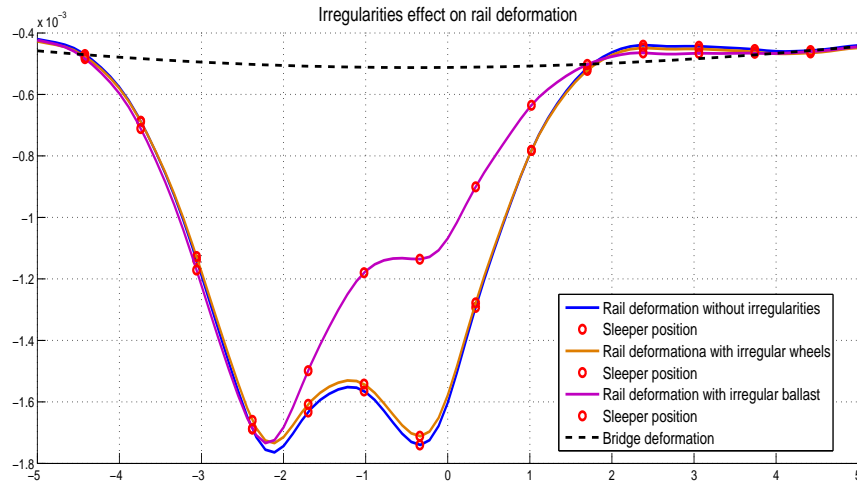


Figure 5.12. Rail and bridge deformation for some irregular cases

## 5.4 FRF: System Frequency response function

Obtaining an accurate FRF of the system is always a very important goal to achieve in systems dynamic analysis.

In this work the FRF was obtained for both cases of track over a structure or not and for each case it was implemented the track alone model and the vehicle-track one, where in the last case, a simplified model for the vehicle is used.

To insert the vehicle in the FRF model it is then necessary to consider its modal properties.

To maintain a certain level of simplicity and to be coherent with the temporal solution problem, the vehicle is modelled with its wheelsets only (1,2 or 4) and for each wheelset only two vehicle modes are taken into consideration and they are the two rigid body ones.

Obviously this is a great simplification and it would be interesting to evaluate the discrepancy in the results comparing this model with a more complicated one as a FEM one could be.

Notice also that in this kind of studies often the FRF used is the one relative to the track-alone and this is the one used in Ref. [2] to validate the model used as a starting point for this work.

### 5.4.1 Vehicle-Track system

The track properties are the same as those used in the temporal response program aforementioned in table 5.3.1. However the number of sleepers used is 25 and considering that the range of frequencies of interest reaches 4000 Hz, the number of beam modes is 84 for rails and 14 for sleepers; doing so the maximum frequency, taken into consideration for both elements, exceed sufficiently the right limit of 4000 Hz.

In order to evaluate the influence of all modal modes, damping is not considered and the track-receptance is calculated on the first sleeper after the center of the rail, avoiding so neglecting lots of rail modes as would happen considering the mid rail point where all odd modes have a zero deflection and so do not take part in FRF composition.

As aforementioned the starting model of this work was that based on the free-free Timoshenko beam used for both rails and sleepers.

In figure 5.13 it is shown the FRF obtained for the track-alone system for both cases of free-free Timoshenko beam and continuous-continuous one and in figure 5.14 it is illustrated a zoom of [100 1000] Hz frequency interval.

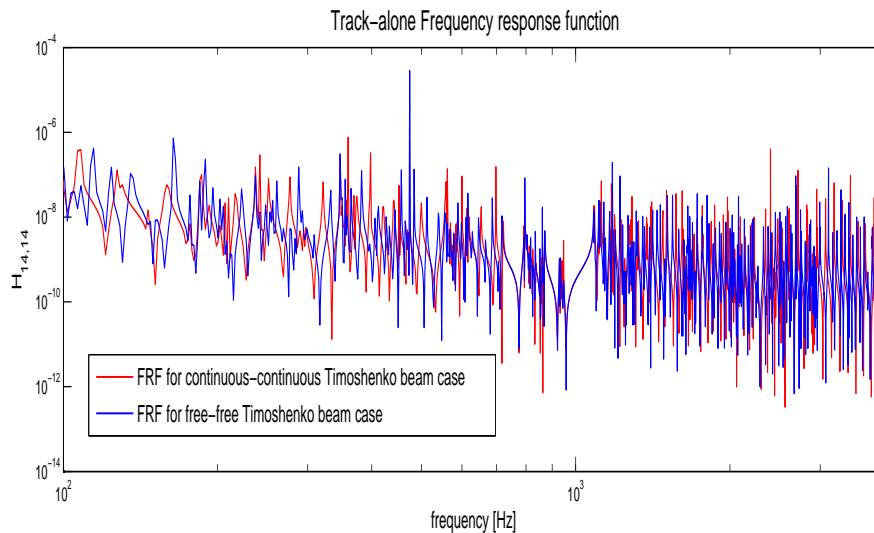


Figure 5.13. FRF for a non-damped model with 25 sleeper bays . Comparison between a Timoshenko continuous-continuous rail beam and a Timoshenko free-free one

In order to evaluate vehicle influence on system FRF a more simplified track-model is used. The number of system DOF must be reduced to decrease the number of resonances.

To make this comparison a 6 sleepers bays track, with one or two wheelsets located at  $x = -0 \text{ m}$  and  $x = -1.5 \text{ m}$  from rail center, is used and the FRF is studied on a rail point located at the fourth sleeper. Rails are modelled with a

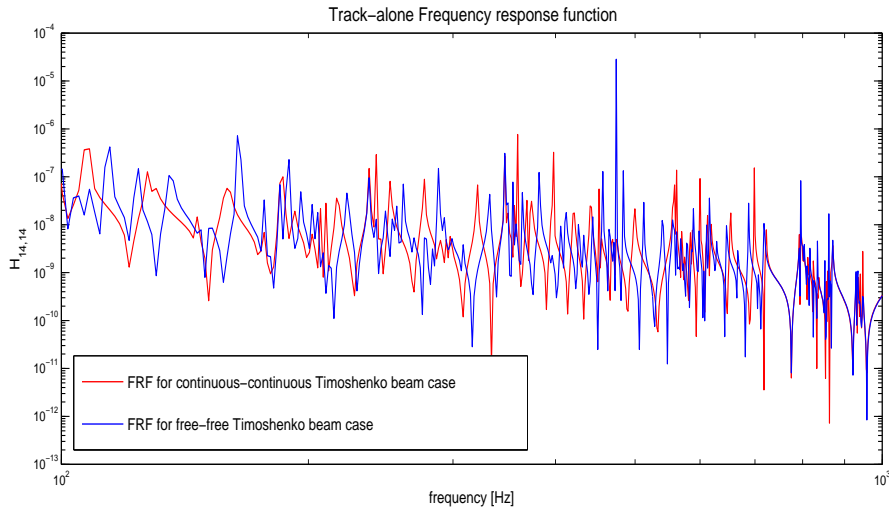


Figure 5.14. FRF for a non-damped model with 25 sleeper bays . Comparison between a Timoshenko continuous-continuous rail beam and a Timoshenko free-free one

14 modes continuous-continuous Timoshenko beam while sleepers are studied with a free-free Euler beam considering 14 modes as well. Figure 5.15 shows obtained results for this reduced problem.

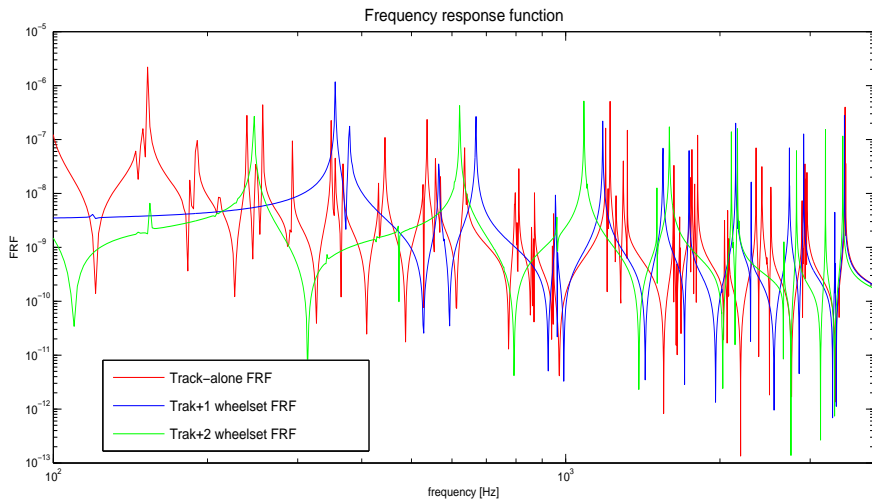


Figure 5.15. Vehicle influence on the FRF. Comparison between track-alone system, 1 wheelset-track and 2 wheelsets-track system.

Moreover, the same FRF was calculated for 1 wheelset in different positions of the track and the results are shown in figure 5.16

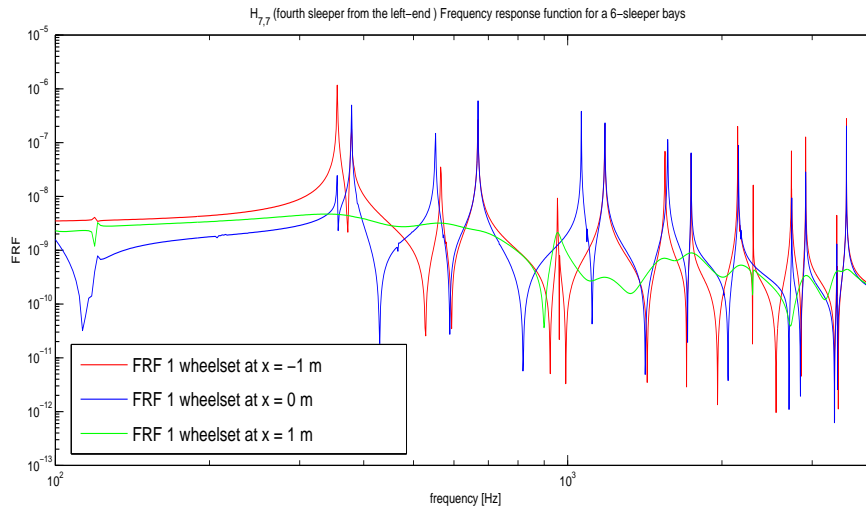


Figure 5.16. Vehicle influence on the FRF. Comparison between FRF calculated for different wheelset positions on the track.

Unfortunately there are not still FEM result for a similar simulation and so the only conclusions from a coarse analysis of obtained FRF is that the order of magnitude is the expected one and that the vehicle influence on the total system is not neglectable in its dynamic properties definition.

## 5.4.2 Vehicle-Track-Structure system

As for the simple vehicle-track system, hereafter some FRF results obtained for the structure interaction case are shown and some comparisons with different simulation parameters and mathematical models are discussed.

First the FRF for a undamped 25 sleepers bay track is calculated using different rails models (Timoshenko free-free beam and Timoshenko continuous-continuous beam) and figures 5.17 and 5.18 (being the second a zoom in the range of frequency 100:1000 Hz) show achieved results.

Bridge is obviously treated as a pinned-pinned beam because it is the only model implemented.

The number of modes used is 84 for rails and 14 for sleepers while only 12 modes were used for the bridge that has, in fact, very big natural frequencies due to its physical properties that are the same above mentioned in table 5.3.2.

Afterward the vehicle was insert in the model through the same simplifications used for the vehicle-track model and the FRF resulting from different run simulations are shown in figures 5.19 and 5.20 were, in both cases, a very small undamped system was used to clearly distinguish system different natural frequencies.

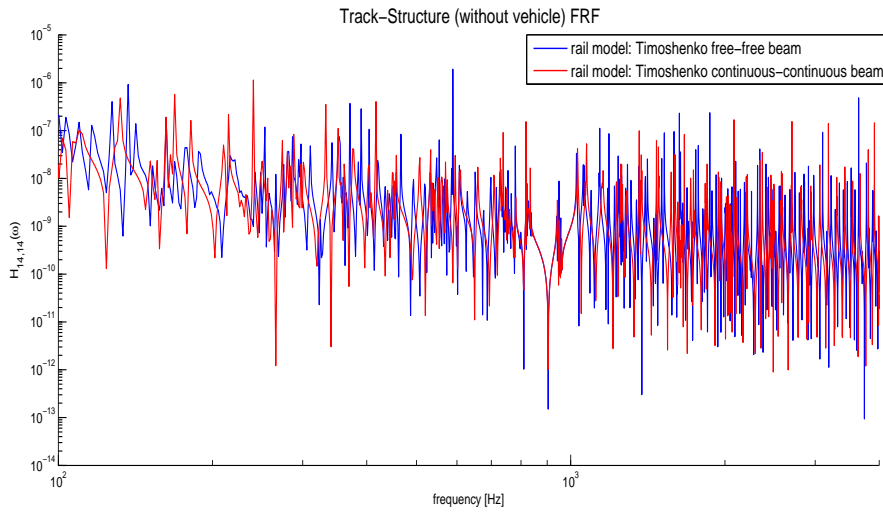


Figure 5.17. FRF for a non-damped model with 25 sleeper bays . Comparison between a Timoshenko continuous-continuous rail beam and a Timoshenko free-free one

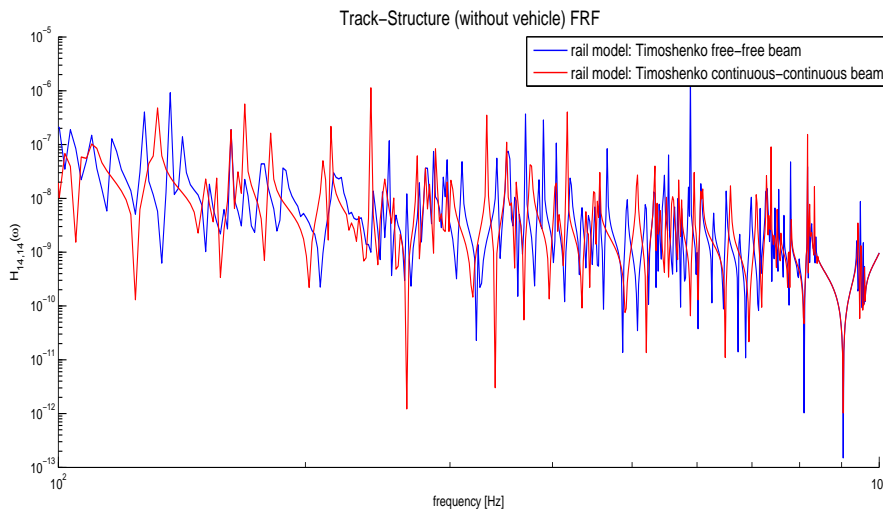


Figure 5.18. FRF for a non-damped model with 25 sleeper bays . Comparison between a Timoshenko continuous-continuous rail beam and a Timoshenko free-free one

The system is here also, as in the vehicle-track case, composed by 6 sleepers bay, and the FRF is obtained for a point in the first rail ( positive y-position ) located on the fourth sleeper from track left-end. The number of modes used is chosen, also here, considering that the range of interest reaches 4000 Hz, and is 14 for both sleepers and rails while bridge modes number is only 3.

Wheelset number effect is thus visible in figure 5.19 while wheelset position effect can be derived from the analysis of figure 5.20

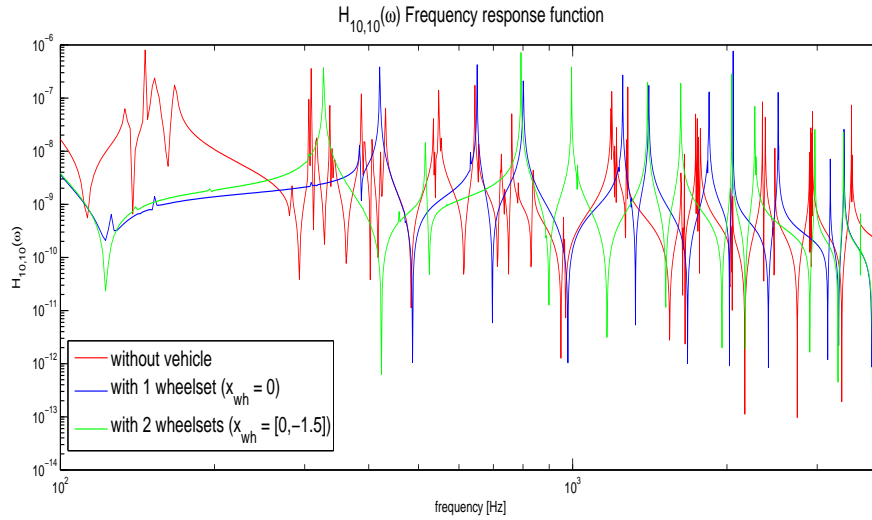


Figure 5.19. Vehicle influence on the FRF. Comparison between track-alone system, 1 wheelset-track and 2 wheelsets-track system.

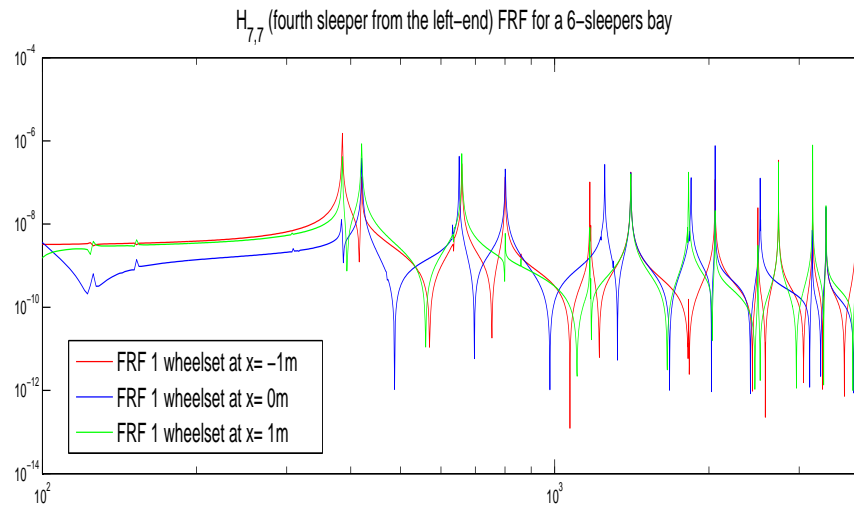


Figure 5.20. Vehicle influence on the FRF. Comparison between FRF calculated for different single-wheelset positions on the track.



## 5.5 Rail models: Euler-Bernoulli and Timoshenko

A goal of this thesis was to show differences between rail models implemented.

As aforementioned, concerning sleepers both models give rise to the same set of frequencies because of the small number of modes considered.

In this short section it is proved that concerning rail models, instead, from the two beam theories result two different dynamic characteristics of the system also using a continuous-continuous beam ( Ref. [1] shows this system behavior for a free-free beam ).

Moreover it is possible to establish that, at least for simple problems, there are not big differences in the results obtained with the same model using different boundary conditions.

It is interesting to prove that discrepancies between Euler-Bernoulli theory and Timoshenko one become significant only at high frequency values as it is expected to be.

To verify this model behavior it is sufficient to compare two FRF of the same system ( the presence of an underlying structure is here neglected being its influence not important for this last goal ).

Figures 5.21(a) and 5.21(b) show results obtained for the same system once a bit damped  $cb \neq 0$  and  $cp \neq 0$  and once totally undamped.

Finally, for the four cases of rail model, in figure 5.22 it is shown the contact force of one wheel for a system without structure, and here also the response doesn't depend on the boundary conditions used, but only on the model .

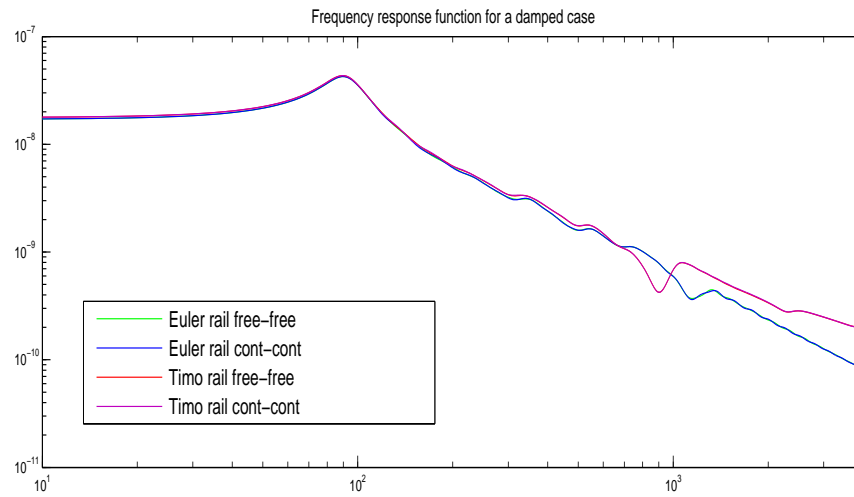
Differences in systems results for different boundary constrained rails, using the same beam theory, are thus not neglectable only when considering the FRF of a totally undamped system, because, as a little damping factor is insert in the model this discrepancy is lost.

## 5.6 conclusions

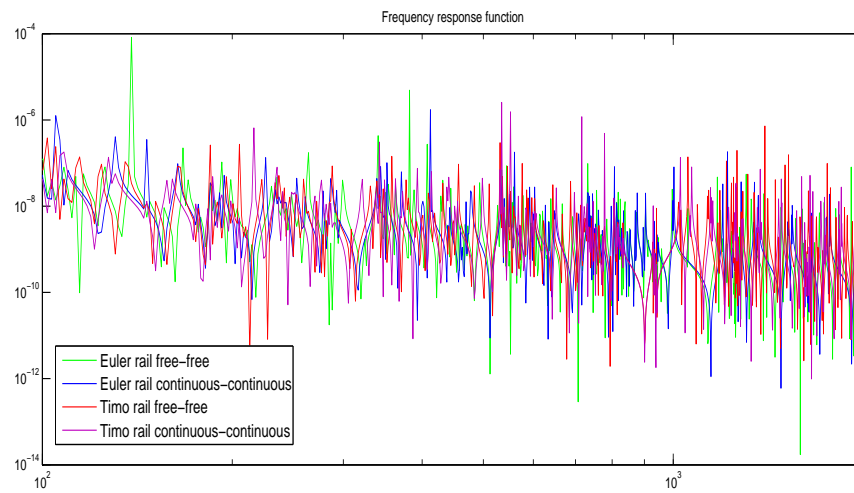
From the analysis of all run simulations and also from figures 5.21(a) , 5.21(b) and 5.22 it is possible to establish that concerning temporal solution rail boundary conditions don't influence the solution appreciably.

Considering instead the model used, same conclusions as in Ref. [1] can be drawn, that is, both the temporal response and FRF of the system change considerably when considering different beam theories for rails.

Obviously, remember that a good validation of the developed model would need some experimental results or at least , as aforementioned, some already validated models comparisons, but notice also that obtained results fit well expected ones.



(a)



(b)

Figure 5.21. (a) Comparison between FRF calculated for different Rail models for the damped system.;(b) Comparison between FRF calculated for different Rail models for the same system but undamped

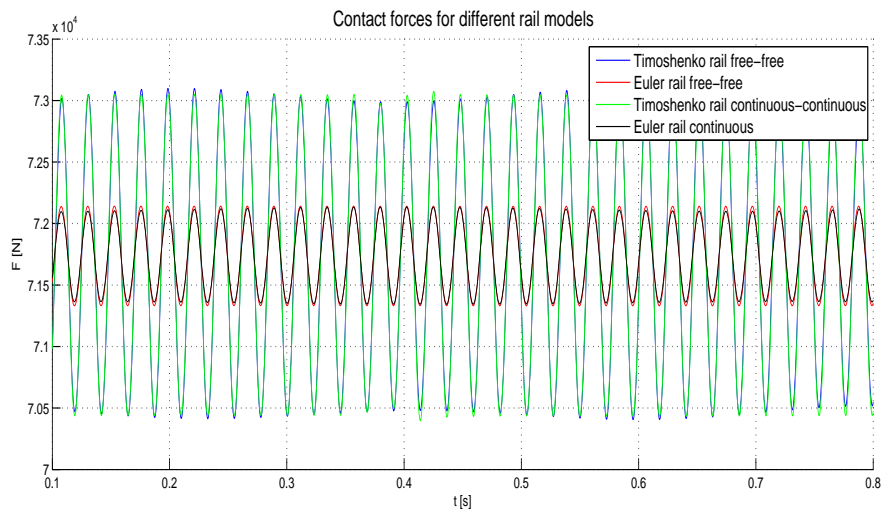


Figure 5.22. Comparison between contact forces calculated for all the possible rail models combinations .

# Chapter 6

## Conclusions

### 6.1 Summary

This work presents a program for simulations of vehicle-track and vehicle-track-structure dynamic interaction . The method used is computationally efficient in the sense that a reduced number of coordinates is sufficient and doesn't require high efficiency computers.

The method proposes a modal substructuring approach of the system by modelling rails , sleepers and underlying structure with modal coordinates, the vehicle with physical lumped elements coordinates and by introducing interconnection elements between these structures (wheel-rail contact, railpads and ballast) by means of their interaction forces.

The Frequency response function (FRF) is also calculated for both cases of track over a structure (a bridge, a viaduct ...) and for the simple vehicle-track program; for each case the vehicle effect on the FRF is then analyzed through the comparison of the FRFs obtained introducing or not a simplified vehicle on the system.

Concerning the simple vehicle-track program the used method derives from the work discussed in Ref. [2] that was validated through the comparison with the method developed by CHARMEC group in Ref. [3].

Making use of small changes in the mathematical models of the system elements and implementing new ones, a wider range of problems is made possible to study and the direct visualization of the results, at the end of each simulation, permits a better understanding of the problem and to control at least the good trend of the values obtained more than their accuracy.

Considering instead the bridge interaction program, although the vehicle and the track are modelled using the same method as for the simple program , to verify the correctness, or at least the good behaviour of the program in studying this kind of problems, it would be necessary to validate it with an already validated program or

through the use of some experimental results.

Using a “user friendly” approach, obtained through the use of *Matlab* GUIs ( graphical user interfaces ), the program is made available to every kind of user also with few informatics skills while concerning future developments, a wide range of possibilities was taken into account using a “modular” approach in developing the program.

Certainly the use of FEM analysis would be useful to validate achieved results but for such big systems a FEM model could be very computational expensive and also concerning experimentation it is surely difficult to have the necessary results.

## 6.2 Future developments

Vehicles matrices are already implemented considering the possibility of increasing the number of DOF used , that would permit, with some program changes, to study also transversal or longitudinal vibration that are obviously very important in this kind of problems.

As aforementioned, the FRF of the total system (Vehicle-track-structure) needs a linearization of the model in each subpart and moreover, to insert the vehicle in the FRF model, it is necessary to making use of further simplifications.

For these reasons the obtained FRFs will be certainly affected by error and in order to reduce this effect it should be necessary to refine upon the vehicle model.

As described in subsection 3.8.2 of chapter 3.1 the vehicle was implemented in the FRF model with the use of its wheelsets modal coordinates considering only the two rigid body modes.

It would be so interesting to reduce the level of this simplification considering a more complex vehicle model. A possible solution to increase the model accuracy could be given by the use of FEM analysis in modelling the vehicle.

Obtaining thus vehicle modal properties from a FEM program, it could be possible to insert them in the track-structure FRF developed program without increasing too much total system size and so guaranteeing a low computational model and an high efficient program.

Concerning temporal response an accurate study of ballast properties it is certainly recommended in order to achieve more accurate results.

As aforementioned the temporal response program already offers the possibility of considering non-linear interaction forces for this system subpart, but its effect on system response was not studied in this thesis, specially because of the lack of information about which non-linear function to use.

### 6.3 Achievements

In this thesis work only test simulations were run to verify the correct behaviour of the program more than its accuracy, needing the last a further specific study aimed at the comparison with already validated results.

In order to test the program, the run simulations considered only simple problems, symmetrical and almost regular ( only few vehicle-track irregularities were introduced ) because this is the normal procedure to follow.

Obtained results are very satisfactory and also concerning program usability the use of GUIs permitted to achieve the desired results.

It is important to notice that program parameters definition took a large part of this work and also for this reason the author would like to point out that in such a short period it would have been difficult to obtain more results than those achieved.

The goal of making possible the study of a very wide range of problems was well achieved through the implementation of lots of program variables that following an “user’s choice” approach permit exactly to keep the program as general as possible.

All in all the achievements obtained are in author’s opinion more than satisfactory, hoping that the reader could share this opinion.

# Appendix A

## Euler-Bernoulli and Timoshenko Beam theories

Two mathematical models, namely the shear-deformable (Timoshenko) model and the shearindefeormable (Euler-Bernoulli) model, are presented in this Annex.

In Euler-Bernoulli beam theory, shear deformations are neglected, and plane sections remain plane and normal to the longitudinal axis. In the Timoshenko beam theory, plane sections still remain plane but are no longer normal to the longitudinal axis. The difference between the normal to the longitudinal axis and the plane section rotation is the shear deformation.

Since the Timoshenko beam theory is higher order than the Euler-Bernoulli theory, it is known to be superior in predicting the transient response of the beam and the it is important to notice that superiority of the Timoshenko model is more pronounced for beams with a low aspect ratio<sup>1</sup>.

### A.1 Euler-Bernoulli theory

Euler-Bernoulli beam theory is a simplification of the linear theory of elasticity which provides a means of calculating the load-carrying and deflection characteristics of beams. It covers the case for small deflections of a beam which is subjected to lateral loads only. It is thus a special case of Timoshenko beam theory which accounts for shear deformation and is applicable for thick beams.

The main assumption of this method is that shear stress and rotational inertia do not take part in beam section rotation and doing so it does not account for the

---

<sup>1</sup>The aspect ratio of a shape is the ratio of its longer dimension to its shorter dimension. It may be applied to two characteristic dimensions of a three-dimensional shape, such as the ratio of the longest and shortest axis, or for symmetrical objects that are described by just two measurements, such as the length and diameter of a rod

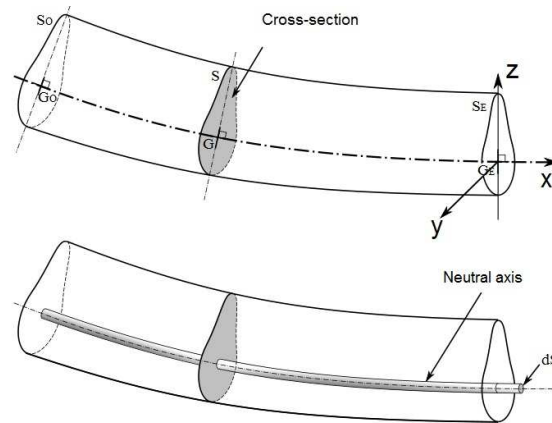


Figure A.1. Schematic of cross-section of a bent beam showing the neutral axis.

effects of transverse shear strain.

It was proved that the use of this theory is limited to those cases in which the range of frequencies of exciting forces is less than 500 Hz.

Below the governing equation of beam dynamic behaviour is derived and it is analyzed its solution for different cases.

### A.1.1 Equation of motion

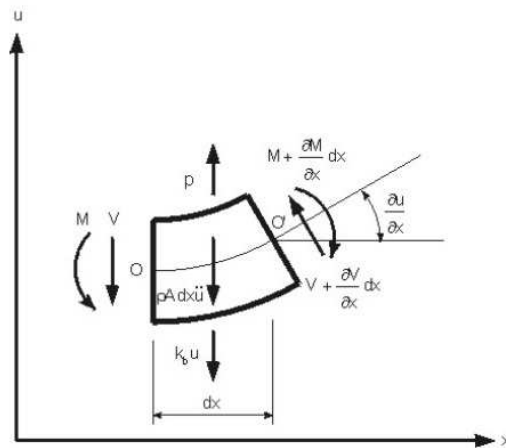


Figure A.2. Free body diagram of a differential element of a beam subject to bending

In figure A.2 it is shown the free body diagram for a differential beam element



subjected to bending on x-y plane. The element is located over an elastic support and a  $p(x,t)$  force per unit length is acting on it.

The support stiffness constant is  $k_b$  while  $M(x,t)$  and  $V(x,t)$  represent the bending moment and the shear force.

Let:

- $\rho$  : element material density;
- $\rho A(x)dx \frac{\partial^2 u(x,t)}{\partial t^2}$  : inertial force acting on differential element;
- $A(x)$  : cross section area.

The forces equilibrium equation along  $u$  direction and the moments one in the direction perpendicular to x-y plane about the point  $O$  are:

$$\frac{\partial V(x,t)}{\partial x} + p(x,t) - k_b u(x,t) = \rho A(x) \frac{\partial^2 u(x,t)}{\partial t^2} \quad (\text{A.1})$$

$$\frac{\partial M(x,t)}{\partial x} - V(x,t) = 0 \quad (\text{A.2})$$

Combining equations (A.1) and (A.2) a unique differential equation for beam motion is obtained:

$$\frac{\partial^2 M(x,t)}{\partial x^2} + p(x,t) - k_b u(x,t) = \rho A(x) \frac{\partial^2 u(x,t)}{\partial x^2} \quad (\text{A.3})$$

Using then the *Navier* hypothesis of linear distribution of stresses across the section it is possible to establish the relationship between the bending moment and the element deformation, also known as *Euler-Bernoulli theory*:

$$M(x,t) = -EI(x) \frac{\partial^2 u(x,t)}{\partial x^2} \quad (\text{A.4})$$

where  $E$  is the Young module of the material and  $I(x)$  is the straight cross section inertia.

From equations (A.3) and (A.4) it derives the motion equation for the lateral vibrations of an non-uniform beam.

$$\frac{\partial^2}{\partial x^2} \left[ E(x)I(x) \frac{\partial^2 u(x,t)}{\partial x^2} \right] + \rho A \frac{\partial^2 u(x,t)}{\partial t^2} + k_b u(x,t) = p(x,t) \quad (\text{A.5})$$

When the section is uniform, that is  $E$  and  $I$  are constant, the equation turns into:

$$EI \frac{\partial^4 u(x,t)}{\partial x^4} + \rho A \frac{\partial^2 u(x,t)}{\partial t^2} + k_b u(x,t) = p(x,t) \quad (\text{A.6})$$

that is the partial differential equation of motion of a constant section beam subjects to bending and over an elastic support.

The general solution to the linear differential equation is the sum of the general solution of the related homogeneous equation ( $p(x,t) = 0$ ) and the particular one.

### A.1.2 Free Vibration without damping

Let

$$a^2 = \frac{EI}{\rho A} \quad (\text{A.7})$$

$$b^2 = \frac{k_b}{\rho A} \quad (\text{A.8})$$

The free vibration equation derives from equation (A.6) where it is imposed that  $p(x,t) = 0$

$$a^2 \frac{\partial^4 u(x,t)}{\partial x^4} + \frac{\partial^2 u(x,t)}{\partial t^2} + b^2 u(x,t) = 0 \quad (\text{A.9})$$

To solve equation (A.9) it is used the separation of variables method; the motion of the beam is given by the product of two functions  $U(x)$  and  $q(t)$ , where each one depends only to one variable, respectively  $x$  and  $t$ .

This gives rise to:

$$u(x,t) = U(x)q(t) \quad (\text{A.10})$$

and combining (A.9) and (A.10)

$$\frac{a^2}{U(x)} \frac{d^4 U(x)}{dx^4} + b^2 = -\frac{1}{q(t)} \frac{d^2 q(t)}{dt^2} = \omega^2 \quad (\text{A.11})$$

where in equation (A.11)  $\omega^2$  is a positive constant.

Since  $U(x)$  is independent of  $t$ ,  $q(t)$  independent of  $x$  and both equal to  $\omega^2$  the only possibility is that:

$$\frac{d^4 U(x)}{dx^4} - \lambda^4 U(x) = 0 \quad (\text{A.12})$$

$$\frac{d^2 q(t)}{dt^2} - \omega^2 q(t) = 0 \quad (\text{A.13})$$

where

$$\lambda^4 = \frac{\omega^2 - b^2}{a^2} = \frac{\rho A \omega^2 - k_b}{EI} \quad (\text{A.14})$$

This definition for wave length  $\lambda$  is valid also if  $k_b = 0$ , that is, when there is not the elastic support.

The well-known general form of the solution of equation (A.13) is:

$$q(t) = q_1 \cos \omega t + q_2 \sin \omega t \quad (\text{A.15})$$

where constants  $q_1$  and  $q_2$  depends from the initial conditions, that usually consist of  $u_0(x)$  displacement and  $v_0(x)$  velocity along all the beam longitude at initial time  $t = 0$ .

Concerning equation (A.12) general solution it is assumed that it is defined as:

$$U(x) = C e^{kx} \quad \text{where } C \text{ and } k \text{ are constants} \quad (\text{A.16})$$

Substituting equation (A.16) in equation (A.12) leads to:

$$k^4 - \lambda^4 = 0 \quad (\text{A.17})$$

which complex roots are:

$$k_{1,2,3,4} = \begin{cases} \pm \lambda \\ \pm i \lambda \end{cases} \quad (\text{A.18})$$

It is so possible to express general solution of equation (A.12) as:

$$U(x) = C_1' e^{\lambda x} + C_2' e^{-\lambda x} + C_3' e^{i\lambda x} + C_4' e^{-i\lambda x} \quad (\text{A.19})$$

Alternatively, using transcendental functions, it can be written as

$$U(x) = C_1 \cos(\lambda x) + C_2 \sin(\lambda x) + C_3 \cosh(\lambda x) + C_4 \sinh(\lambda x) \quad (\text{A.20})$$

where  $C_1$ ,  $C_2$ ,  $C_3$  and  $C_4$  can be obtained from the boundary conditions of the beam.

In table A.1 the possible boundary conditions and their mathematical expressions are defined:

Finally it is important to remember that *continuous-continuous* boundary conditions require only the conditions at one extreme to be the same as the second.

| Boundary conditions | Mathematical expression   |
|---------------------|---|
| Fix extreme         | zero displacement $u(x,t) _{x_{extreme}} = 0$   |
|                     | zero rotation $\theta(x,t) _{x_{extreme}} = 0$ $\left. \frac{\partial u(x,t)}{\partial x} \right _{x_{extreme}} = 0$        |
| Free extreme        | zero moment $M(x,t) _{x_{extreme}} = 0$ $\left. \frac{\partial^2 u(x,t)}{\partial x^2} \right _{x_{extreme}} = 0$           |
|                     | zero shear force $\theta(x,t) _{x_{extreme}} = 0$ $\left. \frac{\partial^3 u(x,t)}{\partial x^3} \right _{x_{extreme}} = 0$ |

Table A.1. Common boundary conditions in beam elements

### A.1.3 characteristic equation and mode shapes of a free-beam and a continuous one

Considering a beam with a length  $L$  with free free boundary conditions or with continuous-continuous ones, the mathematical expressions of the boundary conditions, in according to table A.1 are

| Free-Free beam  | Continuous beam   |        |
|---|---|--------|
| $\left. \frac{\partial^2 u(x,t)}{\partial x^2} \right _{x=0} = 0$ | $u(x,t) _{x=0} = u(x,t) _{x=L}$   |        |
| $\left. \frac{\partial^2 u(x,t)}{\partial x^2} \right _{x=L} = 0$ | $\left. \frac{\partial u(x,t)}{\partial x} \right _{x=0} = \left. \frac{\partial u(x,t)}{\partial x} \right _{x=L}$         | (A.21) |
| $\left. \frac{\partial^3 u(x,t)}{\partial x^3} \right _{x=0} = 0$ | $\left. \frac{\partial^2 u(x,t)}{\partial x^2} \right _{x=0} = \left. \frac{\partial^2 u(x,t)}{\partial x^2} \right _{x=L}$ |        |
| $\left. \frac{\partial^3 u(x,t)}{\partial x^3} \right _{x=L} = 0$ | $\left. \frac{\partial^3 u(x,t)}{\partial x^3} \right _{x=0} = \left. \frac{\partial^3 u(x,t)}{\partial x^3} \right _{x=L}$ |        |

From the above conditions applied to equation (A.20) the following systems of equations result:

- free-free beam

$$\begin{bmatrix} -1 & 0 & 1 & 0 \\ -\cos(\lambda L) & -\sin(\lambda L) & \cosh(\lambda L) & \sinh(\lambda L) \\ 0 & -1 & 0 & 1 \\ \sin(\lambda L) & -\cos(\lambda L) & \sinh(\lambda L) & \cosh(\lambda L) \end{bmatrix} \begin{Bmatrix} C_1 \\ C_2 \\ C_3 \\ C_4 \end{Bmatrix} = \begin{Bmatrix} 0 \\ 0 \\ 0 \\ 0 \end{Bmatrix} \quad (\text{A.22})$$

- continuous-continuous beam

$$\begin{bmatrix} 0 & \sin(\lambda L) & 0 & \sinh(\lambda L) \\ \sin(\lambda L) & 0 & -\sinh(\lambda L) & 0 \\ 0 & \sin(\lambda L) & 0 & -\sinh(\lambda L) \\ \sin(\lambda L) & 0 & \sinh(\lambda L) & 0 \end{bmatrix} \begin{Bmatrix} C_1 \\ C_2 \\ C_3 \\ C_4 \end{Bmatrix} = \begin{Bmatrix} 0 \\ 0 \\ 0 \\ 0 \end{Bmatrix} \quad (\text{A.23})$$

Among all the solutions of equations (A.22) and (A.23) the significant one for dynamic problems is that in which the determinant of the respective matrix is equal to zero ( the other one is the trivial one  $C_1 = C_2 = C_3 = C_4$  that implies absence of motion). Using this condition it is possible to establish three relationships between  $C_1$  ,  $C_2$  ,  $C_3$  and  $C_4$  coefficients and one further equation called *characteristic equations*.

The *characteristic equations* of both cases of constrained beam are so :

- **free-free beam characteristic equation**

$$\cos(\lambda_n L) \cosh(\lambda_n L) = 1 \quad (\text{A.24})$$

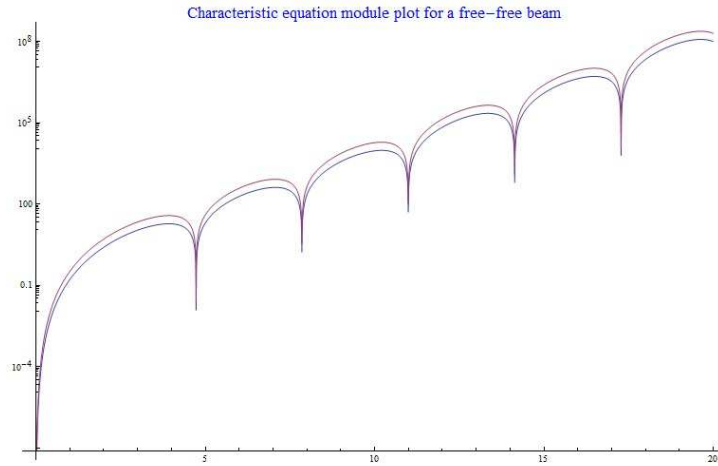
- **continuous beam characteristic equation**

$$\sin^2(\lambda_n L) \sinh^2(\lambda_n L) = 0 \quad (\text{A.25})$$

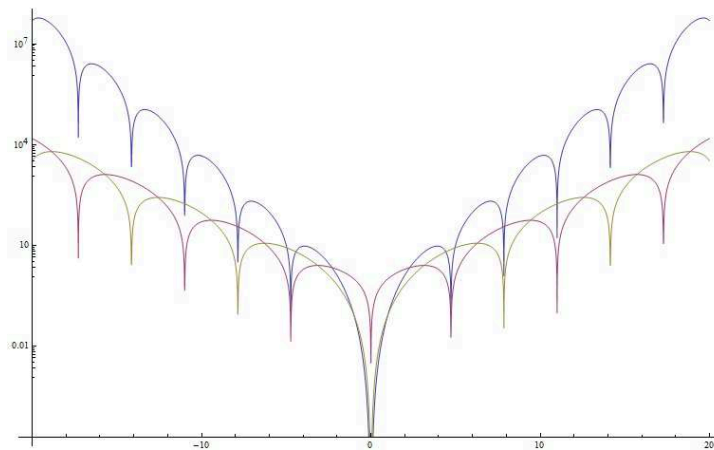
In figure A.1.3 it is shown the characteristic equation for a free-free constrained beam.

From figure A.3(b) it is possible to see how the total solution of the characteristic equation for the free-free constrained case is given by the union of solutions of two components, in fact the characteristic equation could be rewritten as:

$$-4 \cosh^2(\lambda L) \sin^2(\lambda L) + 4 \cos^2(\lambda L) \sinh^2(\lambda L) = 0 \quad (\text{A.26})$$



(a)



(b)

Figure A.3. Plot of the Absolute value of the characteristic equation for a free free beam

that after some simple mathematical steps becomes:

$$(\cosh(\lambda L) \sin(\lambda L) + \cos(\lambda L) \sinh(\lambda L)) * (\cosh(\lambda L) \sin(\lambda L) - \cos(\lambda L) \sinh(\lambda L)) = 0 \quad (\text{A.27})$$

Solving these equations permits to obtain the values of  $\lambda_n L$  that accomplishes the characteristic equation and put these values in equation (A.20), where  $C_1$ ,  $C_2$ ,  $C_3$  and  $C_4$  coefficients have been substituted by their relationships, leads to the

natural mode shapes expressions:

- **free-free beam natural mode shapes:**

$$U_n(x) = C_n [\cos(\lambda_n x) + \cosh(\lambda_n x) + C_{n1}^* (\sin(\lambda_n x) + \sinh(\lambda_n x))] \quad (\text{A.28})$$

$$\text{where } C_{n1}^* = \frac{\cosh(\lambda L) - \cos(\lambda L)}{\sin(\lambda L) - \sinh(\lambda L)}$$

- **continuous beam natural mode shapes:**

$$U_{n_{\text{even}}}(x) = C_n * (\cos \lambda_n(x + L/2) + C_{n2}^* \cosh \lambda_n(x + L/2)) \quad (\text{A.29})$$

$$U_{n_{\text{odd}}}(x) = C_n * (\sin \lambda_n(x + L/2) + C_{n2}^* \sinh \lambda_n(x + L/2)) \quad (\text{A.30})$$

$$\text{where } C_{n2}^* = \frac{\sin(\lambda L)}{\sinh(\lambda L)}$$

where  $C_{n2}^*$  is a scaling factor used to normalize the modes.

Notice that for each value of  $\lambda_n$  there are two vibration modes and this means that their natural frequencies coincide.

#### A.1.4 Normalization, main properties and natural frequencies

The normalization adopted is in respect of the mass per unit length and can be expressed as follows:

$$\int_0^L U_n^2(x) dx = C_n^2 L = \frac{1}{\rho A} \quad (\text{A.31})$$

Moreover it is simple to demonstrate that the mode shapes are perpendicular to each other, that is:

$$\int_0^L U_n(x) U_m(x) dx = 0 \quad \text{if } n \neq m \quad (\text{A.32})$$

Each mode shape has its own natural frequency of vibration  $\omega_n$  that derives from equation (A.14) and the values obtained for  $\lambda$  :

$$\omega_n = \sqrt{a^2 \lambda_n^4 + b^2} = \sqrt{\frac{EI}{\rho A} \lambda_n^4 + \frac{k_b}{\rho A}} \quad (\text{A.33})$$

If the beam is not collocated over an elastic support equation (A.33) becomes obviously:

$$\omega_n = \sqrt{a^2 \lambda_n^4} = \sqrt{\frac{EI}{\rho A} \lambda_n^4} \quad (\text{A.34})$$

Watching more carefully equations (A.24) , (A.25) and (A.34) it is possible to understand how wave lengths  $\lambda_n$  depend only on beam length and its boundary conditions while natural frequencies depend also on the main mechanical properties of the element.

### A.1.5 Rigid body modes

Depending on the boundary conditions, besides flexional vibration modes the beam has the possibility of *rigid body* displacements.

For a free-free constrained beam the rigid body modes consist of a rigid lateral translation and a rigid rotation around the beam center of gravity while for the continuous-continuous one there is only one mode that is the rigid translation one, this because of obviously considerations.

The rigid body modes mathematical expressions are:

$$U_{-1}(x) = C_{-1} \quad (\text{A.35})$$

$$U_0(x) = C_0 \left( x - \frac{L}{2} \right) \quad (\text{A.36})$$

where in equations (A.35) and (A.36) the numeration followed is that used for the free-free beam case (in a continuous beam mode  $-1$  does not exist and so the first and only rigid mode, mode 0, is that of rigid translation ).

It is simple to demonstrate that both modes respect perpendicularity condition, as well as the boundary conditions of the beam.

Regarding their natural frequencies, it is possible, going backwards, to calculate first the rigid body modes wave lengths  $\lambda_{-1}$  and  $\lambda_0$  and then, using these values, to calculate their natural frequencies.

$$\frac{d^4 U_{-1}(x)}{dx^4} - \lambda_{-1} U_{-1}(x) = 0 \Rightarrow \lambda_{-1} = 0 \quad (\text{A.37})$$



$$\frac{d^4 U_0(x)}{dx^4} - \lambda_0 U_0(x) = 0 \Rightarrow \lambda_{-1} = 0 \quad (\text{A.38})$$

And so, using equation (A.33), it is possible to calculate rigid body modes natural frequencies as:

$$\omega_n = \sqrt{b^2} = \sqrt{\frac{k_b}{\rho A}} \quad n = -1, 0 \quad (\text{A.39})$$

that means that for a beam that is not supported by an elastic support ( $k_b = 0$ ) the rigid body natural frequencies are null.

$\lambda = 0$  is a trivial solution of the characteristic equation and both rigid modes of the free-free constrained beam are associated to this value, that means that  $\lambda = 0$  is a double root to which two auto-functions are associated with.

The modes normalization to unit mass per length, like for all the others modes, can be expressed like this :

$$\int_0^L U_n^2(x) dx = \frac{1}{\rho A} \quad n = -1, 0 \quad (\text{A.40})$$

And so,  $C_{-1}$  and  $C_0$  values are:

$$\int_0^L U_n^2(x) dx = C_{-1}^2 L = \frac{1}{\rho A} \quad \Rightarrow C_{-1} = \frac{1}{\rho AL} \quad (\text{A.41})$$

$$\int_0^L U_n^2(x) dx = C_0^2 L^3 / 12 = \frac{1}{\rho A} \quad \Rightarrow C_0 = \sqrt{\frac{12}{\rho AL^3}} \quad (\text{A.42})$$

Finally, with the use of equations (A.41) and (A.42), the mathematical expressions for rigid body modes become:

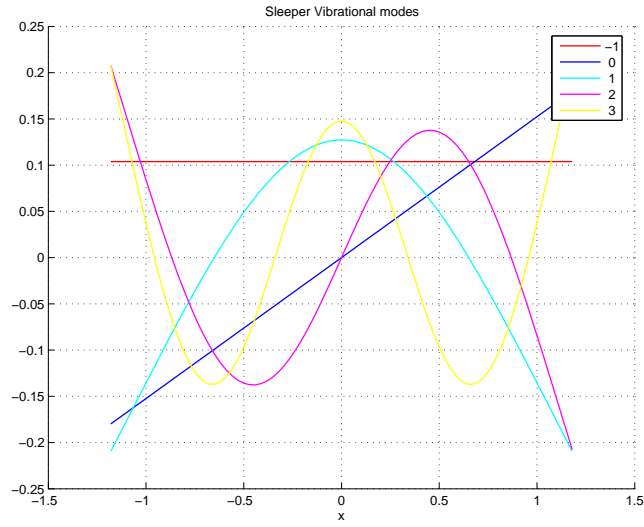
$$U_{-1}(x) = \frac{1}{\rho AL} \quad (\text{A.43})$$

$$U_0(x) = \sqrt{\frac{12}{\rho AL^3}} \left(x - \frac{L}{2}\right) \quad (\text{A.44})$$

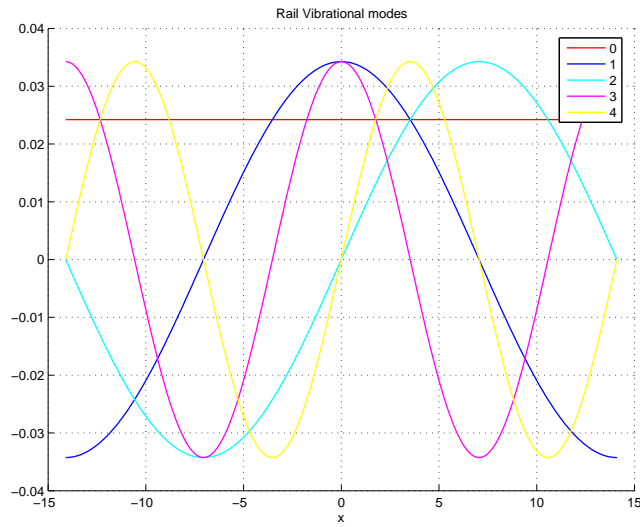
In figures A.4(a) and A.4(b) are shown the first five modes for both cases of Euler free-free constrained beam and continuous-continuous one applied, respectively, to a sleeper and to a rail of the thesis work<sup>2</sup>.

---

<sup>2</sup>As aforementioned Euler modes depend only on beam length and boundary conditions, thus, the problem is much simplified



(a)



(b)

Figure A.4. Plot of first 5 vibration modes for a free-free constrained beam (fig (A.4(a))) and for a continuous one (fig(A.4(b))) using the Euler-Bernoulli approach.

### A.1.6 Pinned-pinned constrained beam

Before discussing the case of forced vibrations, the same mathematical expressions derived for Euler free-free and continuous beams are obtained for the pinned-pinned beam case, used in the work to model the underlying structure (a bridge, a viaduct ect. ect.).

In this last case the boundary conditions are:

$$\begin{aligned}
 & \text{pinned-pinned beam} \\
 & u(x,t)|_{x=0} = 0 \\
 & u(x,t)|_{x=L} = 0 \\
 & \left. \frac{\partial^2 u(x,t)}{\partial x^2} \right|_{x=0} = 0 \\
 & \left. \frac{\partial^2 u(x,t)}{\partial x^2} \right|_{x=L} = 0
 \end{aligned} \tag{A.45}$$

Above boundary conditions expressions bring to the following system of equations written in matrix form

$$\begin{bmatrix} 1 & 0 & 1 & 0 \\ \cos(\lambda L) & \sin(\lambda L) & \cosh(\lambda L) & \sinh(\lambda L) \\ -1 & 0 & 1 & 0 \\ -\cos(\lambda L) & -\sin(\lambda L) & \cosh(\lambda L) & \sinh(\lambda L) \end{bmatrix} \begin{Bmatrix} C_1 \\ C_2 \\ C_3 \\ C_4 \end{Bmatrix} = \begin{Bmatrix} 0 \\ 0 \\ 0 \\ 0 \end{Bmatrix} \tag{A.46}$$

Like other Euler beam cases, the solution of interest for dynamic problems is the one given by the singularity of this matrix that gives rise to three C coefficients relationships and one more equation called *pinned-pinned characteristic equation*, shown below

$$\sin(\lambda_n L) * \sinh(\lambda_n L) = 0 \tag{A.47}$$

which solutions with C coefficients relationships , put in equation (A.20) , leads to natural mode shapes expressions for a pinned-pinned constrained beam

$$U_n(x) = C_n * \sqrt{2} \sin(\lambda_n x) \tag{A.48}$$

where  $C_n$  coefficient depends on which kind of normalization is used, that in this work, as aforementioned, is to unit mass per unit length and can be obtained making use of equation (A.31).

Natural frequencies are here also derivable from equation (A.33) and concerning rigid body modes, it is important to notice that in pinned-pinned constrained beam there are no ones, this due to the boundary conditions of this particular case.

In figure A.5 it is possible to see the first five modes for a pinned-pinned beam used in the program to model the underlying structure.

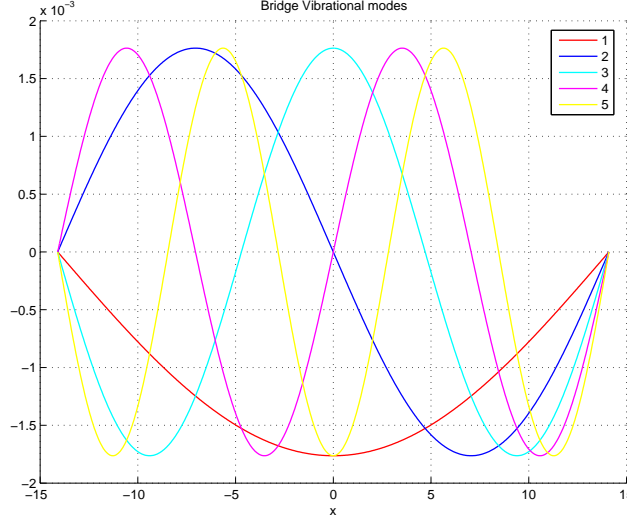


Figure A.5. First 5 modes plot for a pinned-pinned constrained beam

### A.1.7 Forced vibrations

The second part of the total solution of equation (A.6) is given by the particular one ( $p(x,t) \neq 0$ ) that is here obtained making use of a modal superposition approach.

Doing so, the solution is given by a linear combination of the basis terms of the mathematical infinite space used to describe the physic space of possible deformations.

$$u(x,t) = \sum_{n=-1}^{\infty} U_n(x)q_n(t)^3 \tag{A.49}$$

where  $U_n(x)$  is the  $n$ th vibration mode, that depends on beam boundary conditions, and  $q_n(t)$  its modal coordinate.

Thus, combining equations (A.49) with (A.6) it results:

---

<sup>3</sup>from here on a free-free constrained beam is considered and so the numeration of the modes starts from  $-1$ .

$$EI \sum_{n=-1}^{\infty} \frac{\partial^4 U(x)}{\partial x^4} q_n(t) + \rho A \sum_{n=-1}^{\infty} U_n(x) \frac{\partial^2 q(t)}{\partial t^2} + k_b \sum_{n=-1}^{\infty} U_n(x) q_n(t) = p(x,t) \quad (\text{A.50})$$

that after some mathematical manipulations becomes:

$$\frac{d^2 q_n(t)}{dt^2} + \omega_n^2 q_n(t) = P_n(t) \quad n = -1, 0, 1, \dots, \infty \quad (\text{A.51})$$

where  $P_n(t)$  is the  $n$ th modal force calculated as:

$$P_n(t) = \int_0^L p(x,t) U_n(x) dx \quad (\text{A.52})$$

In case of punctual forces acting on discrete points, as supposed in the work done, modal forces can be obtained as follows :

$$P_n(t) = \sum_{i=1}^{N_f} p_i(t) U_n(x_i) \quad (\text{A.53})$$

where in equation (A.53)  $N_f$  stands for the number of punctual forces  $p_i(t)$  acting on  $x_i$  positions of the beam.

To take into consideration damping properties of the beam it is then possible to add some sort of modal damping coefficient that for track studies is usually of few percentage points (0.04 : 0.1). Doing so equation (A.51) becomes

$$\frac{d^2 q_n(t)}{dt^2} + 2\zeta_n \omega_n \frac{dq_n(t)}{dt} + \omega_n^2 q_n(t) = P_n(t) \quad n = -1, 0, 1, \dots, \infty \quad (\text{A.54})$$

Once obtained modal coordinates  $q_n$  values it is possible to have the system response through equation (A.49)

Obviously in practical problems it is not possible to have all the infinite members of the mathematical space, as equations A.49, A.50 and A.51 would need, so it is necessary some kind of problem size reduction, that in the work done, as aforementioned in section 2.4, is the modal truncation.

Doing so the physic space of possible deformations is approximated by a mathematic subspace where the dimension of the subspace determinates the accuracy of the solution, that is, a finite number of modes is used to represent system response.

Let  $N_m$  be the number of mode shapes chosen.

Doing so the deformation of the beam can be expressed as follows:

$$u(x,t) = \sum_{n=-1}^{N_m} U_n(x) q_n(t) \quad (\text{A.55})$$

### A.1.8 Stresses

Besides deflection, the beam equation describes forces and moments and can thus be used to describe stresses.

Both the bending moment and the shear force cause stresses in the beam. The stress due to shear force is maximum along the neutral axis of the beam (when the width of the beam is constant along the cross section of the beam; otherwise an integral involving the first moment and the beam's width needs to be evaluated for the particular cross section), and the maximum tensile stress is at either the top or bottom surfaces.

Thus the maximum principal stress in the beam may be neither at the surface nor at the center but in some general area.

However, shear force stresses are often negligible in comparison to bending moment stresses and considering the fact that stress concentrations commonly occur at surfaces, the maximum stress in a beam is likely to be at the surface.

For a one-dimensional linear elastic material, the stress is related to the strain by  $\sigma = E\varepsilon$  where  $E$  is the Young's modulus. Hence the stress in an Euler-Bernoulli beam is given by

$$\sigma_x = -zE \frac{d^2u}{dx^2} \tag{A.56}$$

where  $z$  is the distance from the neutral axis.

## A.2 Timoshenko beam theory

The Timoshenko beam theory was developed by Ukrainian-born scientist Stephen Timoshenko in the beginning of the 20th century.

The model takes into account shear deformation and rotational inertia effects, making it suitable for describing the behaviour of short beams, sandwich composite beams or beams subject to high-frequency excitation when the wavelength approaches the thickness of the beam.

The resulting equation is of 4th order, but unlike ordinary beam theory (i.e. Bernoulli-Euler theory) there is also a second order spatial derivative.

Physically, taking into account the added mechanisms of deformation, effectively lowers the stiffness of the beam, while the result is a larger deflection under a static load and lower predicted eigenfrequencies for a given set of boundary conditions. The latter effect is more noticeable for higher frequencies as the wavelength becomes shorter, thus decreasing the distance between opposing shear forces.

If the shear modulus of the beam material approaches infinity, thus making the beam rigid in shear, and if rotational inertia effects are neglected, Timoshenko beam theory converges towards ordinary beam theory.

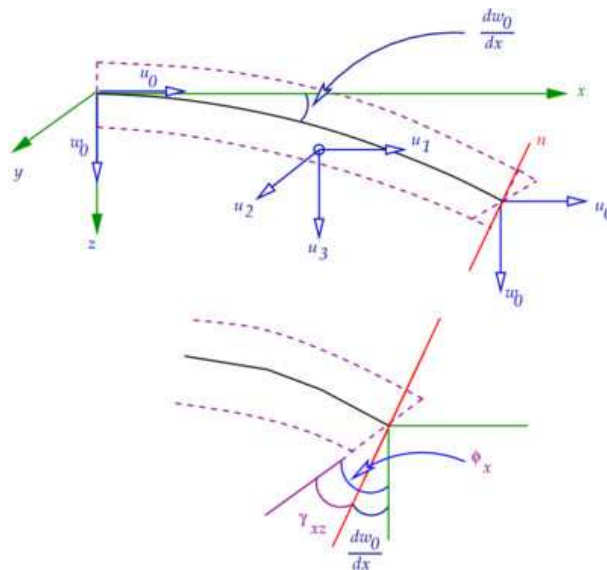


Figure A.6. Schematic of cross-section of a bent beam showing the neutral axis.

As aforementioned the main difference between this theory and the Euler-Bernoulli one is that cross sections do not remain straight and so there are two independent variables of interest (displacement and rotation) at each point.

Below the governing equation of beam dynamic behaviour is derived and it is analyzed its solution for different cases.

### A.2.1 Equation of motion

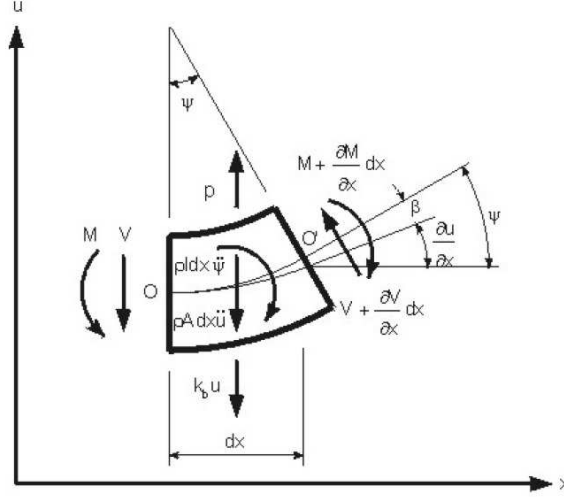


Figure A.7. Free body diagram of a differential element of a Timoshenko beam subject to bending

In figure A.7 it is shown the free body diagram for a Timoshenko differential element.

The element is subjected to bending on plane x-u, is collocated over an elastic support of  $k_b$  stiffness coefficient and is excited by an external force per unit length  $p(x,t)$ , where the bending moment is  $M(x,t)$  and the shear force  $V(x,t)$ .

The total deformation is here split in two components:

- a bending dependent one :  $u_M(x,t)$ ;
- a shear dependent one :  $u_S(x,t)$ .

Thus the total deformation can be expressed as:

$$u(x,t) = u_M(x,t) + u_S(x,t) \quad (\text{A.57})$$

The angle of rotation due to the bending moment is then  $\Psi(x,t)$  and the shear dependent one is  $\beta(x,t)$ .

The mathematical relations between rotations and deformations are so:

$$\Psi(x,t) = \frac{\partial u_M(x,t)}{\partial x} \quad (\text{A.58})$$

$$\beta(x,t) = \frac{\partial u_S(x,t)}{\partial x} \quad (\text{A.59})$$



Bending moment  $M(x,t)$  and shear force  $V(x,t)$  are related to lateral displacement and rotation of the element as follows:

$$M(x,t) = -EI \frac{\partial^2 u_M(x,t)}{\partial x^2} = -EI \frac{\partial \Psi(x,t)}{\partial x} \quad (\text{A.60})$$

$$V(x,t) = k'GA \frac{\partial u_S(x,t)}{\partial x} = k'GA \left( \frac{\partial u(x,t)}{\partial x} - \Psi(x,t) \right) \quad (\text{A.61})$$

where

- $G$  is the shear modulus;
- $E$  is the Young's modulus;
- $I$  is the area moment of inertia of the cross-section;
- $A$  is the area of the cross section
- $k'$  is the Timoshenko constant that depends on the shape of the undeformed section.

Considering the set of forces and moments acting on the differential element shown in figure A.7 it is possible to write the following equilibrium relations:

$$\rho A \frac{\partial^2 u(x,t)}{\partial t^2} - \frac{\partial V(x,t)}{\partial x} + k_b u(x,t) = p(x,t) \quad (\text{A.62})$$

$$-\frac{\partial M(x,t)}{\partial x} + V(x,t) - \rho I \frac{\partial^2 \Psi(x,t)}{\partial t^2} = 0 \quad (\text{A.63})$$

where

- $\rho$  is the density of the element material;
- $\rho A dx \frac{\partial^2 u(x,t)}{\partial t^2}$  is the translation inertia force acting on the element;
- $\rho I \frac{\partial^2 \Psi(x,t)}{\partial t^2}$  is the rotational inertia on x-u plane.

Simplifying equations (A.62) and (A.63) and making use of equations (A.60) and (A.61), the following system of partial differential equations:

$$\rho A \frac{\partial^2 u(x,t)}{\partial t^2} - k'GA \left( \frac{\partial^2 u(x,t)}{\partial x^2} - \frac{\partial \Psi(x,t)}{\partial x} \right) + k_b u(x,t) = p(x,t) \quad (\text{A.64})$$

$$EI \frac{\partial^2 \Psi(x,t)}{\partial x^2} + k'GA \left( \frac{\partial u(x,t)}{\partial x} - \Psi(x,t) \right) - \rho I \frac{\partial^2 \Psi(x,t)}{\partial t^2} = 0 \quad (\text{A.65})$$

where the unknown variables are  $u(x,t)$  and  $\Psi(x,t)$ .

As well as for the Euler-Bernoulli case the general solution of the system of equations (A.64) and (A.65) is the sum of the general solution of the related homogeneous equations ( $p(x,t) = 0$ ) and the particular one.

### A.2.2 Free vibration

The homogeneous solution of the system defined by equations (A.64) and (A.65) derives from the new system obtained, requiring the force term to be null  $p(x,t) = 0$ .

$$\rho A \frac{\partial^2 u(x,t)}{\partial t^2} - k'GA \left( \frac{\partial^2 u(x,t)}{\partial x^2} - \frac{\partial \Psi(x,t)}{\partial x} \right) + k_b u(x,t) = 0 \quad (\text{A.66})$$

$$EI \frac{\partial^2 \Psi(x,t)}{\partial x^2} + k'GA \left( \frac{\partial u(x,t)}{\partial x} - \Psi(x,t) \right) - \rho I \frac{\partial^2 \Psi(x,t)}{\partial t^2} = 0 \quad (\text{A.67})$$

Also in this case a *separation of variables* approach is used, thus:

$$u(x,t) = U(x)q(t) = U(x) (q_1 \cos(\omega t) + q_2 \sin(\omega t)) \quad (\text{A.68})$$

Let

$$r^2 = \frac{I}{A} \quad \gamma = \frac{EI}{k'GAL} \quad \lambda^4 = \frac{\rho A \omega^2}{EI} \quad \kappa = \frac{k_b}{EI} \quad (\text{A.69})$$

Combining equations (A.66) , (A.67) and (A.68) and making use of the defined coefficients (A.69) gives rise to the following simplified equation:

$$\left\{ \frac{d^4 U(x)}{dx^4} + [\lambda^4 (r^2 + \gamma) - \gamma \kappa] \frac{d^2 U(x)}{dx^2} - (\lambda^4 - \kappa) (1 - \lambda^4 \gamma r^2) U(x) \right\} q(t) = 0 \quad (\text{A.70})$$

Considering that  $q(t)$  can take whatever value, the required solution to equation (A.70) is:

$$\frac{d^4 U(x)}{dx^4} + [\lambda^4 (r^2 + \gamma) - \gamma \kappa] \frac{d^2 U(x)}{dx^2} - (\lambda^4 - \kappa) (1 - \lambda^4 \gamma r^2) U(x) = 0 \quad (\text{A.71})$$

Defining then  $\alpha_0$  and  $\alpha_1$  as

$$\alpha_1 = \frac{\lambda^4}{L^2} \left( \frac{r^2}{L^2} + \gamma \right) - \frac{\gamma\kappa L}{L^2} \quad \alpha_0 = \left( \frac{\lambda^4}{L^4} - \frac{\kappa L}{L^4} \right) \left( 1 - \frac{\lambda^4 \gamma r^2}{L^2} \right) \quad (\text{A.72})$$

it is possible to rewrite equation (A.70) as:

$$\frac{d^4 U(x)}{dx^4} + \alpha_1 \frac{d^2 U(x)}{dx^2} - \alpha_0 U(x) = 0 \quad (\text{A.73})$$

whose solution is :

$$U(x) = C_1 \cos \left( \frac{ax}{L} \right) + C_2 \sin \left( \frac{bx}{L} \right) + C_3 \cosh \left( \frac{cx}{L} \right) + C_4 \sinh \left( \frac{dx}{L} \right) \quad (\text{A.74})$$

where  $C_1, C_2, C_3, C_4$  constants depend on the boundary conditions of the beam and  $a, b, c, d$  are adimensional wave lengths.

Considering  $\alpha_0$  and  $\alpha_1$  definitions (equation (A.72)), substituting solution equation (A.74) in (A.73) and considering that vibration modes, as well as wave lengths, must be real, it results that:

$$U(x) = C_1 \cos \left( \frac{ax}{L} \right) + C_2 \sin \left( \frac{ax}{L} \right) + C_3 \cosh \left( \frac{dx}{L} \right) + C_4 \sinh \left( \frac{dx}{L} \right) \quad (\text{A.75})$$

where adimensional wave lengths  $a$  and  $d$  are given by the following relations:

$$a = L \left[ \frac{\lambda^4 (r^2 + \gamma) - \gamma\kappa}{2} + \left[ \left[ \frac{\lambda^4 (r^2 + \gamma) - \gamma\kappa}{2} \right]^2 + (\lambda^4 - \kappa) (1 - \lambda^4 \gamma r^2) \right]^{0.5} \right]^{0.5} \quad (\text{A.76})$$

$$d = -L \left[ \frac{\lambda^4 (r^2 + \gamma) - \gamma\kappa}{2} + \left[ \left[ \frac{\lambda^4 (r^2 + \gamma) - \gamma\kappa}{2} \right]^2 + (\lambda^4 - \kappa) (1 - \lambda^4 \gamma r^2) \right]^{0.5} \right]^{0.5} \quad (\text{A.77})$$

Free-free and continuous beam cases

Also in Timoshenko's method the modal properties of the beam depend on the boundary conditions, but, differently from Euler case, in Timoshenko's method also the others beam mechanical characteristics have an influence on them.

Possible boundary conditions are the same list in table A.1 but with different mathematic expressions.

The rotation of the section do not still correspond to the tangent of deflection curve and as aforementioned, bending moment and shear force are related to displacement and rotation with equations (A.60) and (A.61).

| Boundary conditions | Mathematical expression                           |
|---------------------|---|
| Fix extreme         | zero displacement $u(x,t) _{x_{extreme}} = 0$     |
|                     | zero rotation $\Psi(x,t) _{x_{extreme}} = 0$      |
| Free extreme        | zero moment $M(x,t) _{x_{extreme}} = 0$           |
|                     | zero shear force $\theta(x,t) _{x_{extreme}} = 0$ |

---

Table A.2. Beam common boundary conditions

Using the *separation of variables* method, as for the displacement  $u(x,t)$  (equation (A.68)), it is possible to write the following relations:

$$V(x,t) = V(x)q(t) \tag{A.78}$$

$$M(x,t) = M(x)q(t) \tag{A.79}$$

$$\Psi(x,t) = \Psi(x)q(t) \tag{A.80}$$

Combining opportunely equations (A.66) and (A.67) with equations (A.61) and (A.68) it is possible to obtain the following expression for the Shear force:

$$V(x) = -EI \frac{\lambda^4 - \kappa L^4}{a^2 d^2} \left[ \frac{d^3 U(x)}{dx^3} + \frac{a^2 - d^2}{L^2} \frac{dU(x)}{dx} \right] \tag{A.81}$$

where the following relations were considered

$$a^2 d^2 = L^4 (\lambda^4 - \kappa) (1 - \lambda^4 \gamma r^2) \tag{A.82}$$

$$a^2 d^2 = L^2 [\lambda^4 (r^2 + \gamma) - \gamma \kappa] \tag{A.83}$$

Combining then equations (A.75) and (A.81) the following shear force equation results:

$$V(x) = -EI \frac{\lambda^4 - \kappa L}{a^2 d^2} \left( ad^2 C_1 \sin \left( \frac{ax}{L} \right) - ad^2 C_2 \cos \left( \frac{ax}{L} \right) + \dots \right. \\ \left. \dots + a^2 d C_3 \sinh \left( \frac{dx}{L} \right) + a^2 d C_4 \cosh \left( \frac{dx}{L} \right) \right) \quad (\text{A.84})$$

The rotation due to bending moment  $\Psi(x)$  can be obtained substituting equation (A.84) in equation (A.61) :

$$\Psi(x) = C_1 \frac{a'}{L} \sin \left( \frac{ax}{L} \right) + C_2 \frac{a'}{L} \cos \left( \frac{ax}{L} \right) + C_3 \frac{d'}{L} \sinh \left( \frac{dx}{L} \right) + C_4 \frac{d'}{L} \cosh \left( \frac{dx}{L} \right) \quad (\text{A.85})$$

where

$$a' = a - \frac{\gamma(\lambda^4 - \kappa) * L^2}{a} \quad d' = d - \frac{\gamma(\lambda^4 - \kappa) * L^2}{d} \quad (\text{A.86})$$

Finally considering (A.60) and (A.85) it is possible to give the definition of the bending moment equation:

$$M(x) = \frac{EI}{L^2} \left( C_1 a a' \cos \left( \frac{ax}{L} \right) + C_2 a a' \sin \left( \frac{ax}{L} \right) + C_3 d d' \cosh \left( \frac{dx}{L} \right) + C_4 d d' \sinh \left( \frac{dx}{L} \right) \right) \quad (\text{A.87})$$

Equations (A.75), (A.84), (A.85) and (A.87) permit to calculate the  $C$  coefficients values that accomplish the boundary conditions.

The characteristic equations for both cases of free-free beam and continuous one are given below :

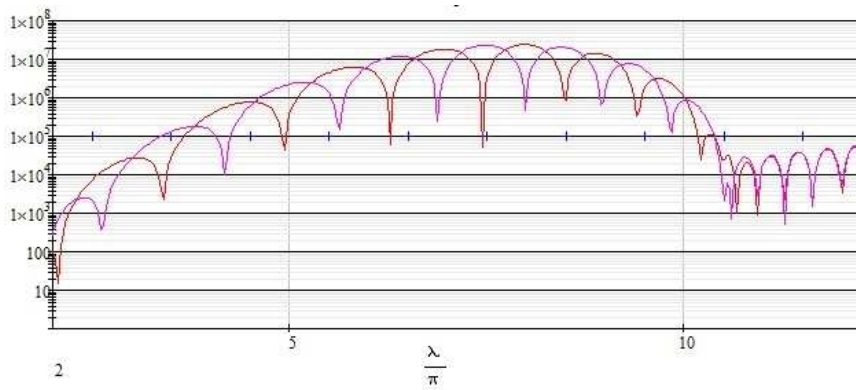
- **free free constrained beam characteristic equation**

$$2a(\lambda)^2 a(\lambda)' d(\lambda)^2 d(\lambda)' (1 - \cosh d \cos a(\lambda)) + \\ + (a(\lambda)^4 a(\lambda)'^2 - d(\lambda)^4 d(\lambda)'^2) \sinh d(\lambda) \sin a(\lambda) = 0 \quad (\text{A.88})$$

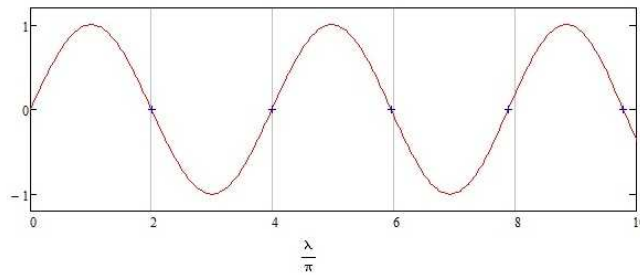
• continuous-continuous constrained beam characteristic equation

$$\sin\left(\frac{a(\lambda)}{2}\right) \cosh\left(\frac{d(\lambda)}{2}\right) = 0 \quad (\text{A.89})$$

In figure A.2.2 the characteristic equations for a free-free Timoshenko beam and for a continuous one are plotted .



(a)



(b)

Figure A.8. Plot of the characteristic equation for a free-free constrained beam (fig (A.8(a))) and for a continuous-continuous one (fig (A.8(b))) using the Timoshenko approach

Once obtained  $n \lambda_n$  solutions of equations (A.88) or (A.89) it is possible to obtain the mode shapes of the beam simply applying them to equation (A.75) that is:

$$U_n(x) = C_{1n} \cos\left(\frac{a_n x}{L}\right) + C_{2n} \sin\left(\frac{a_n x}{L}\right) + C_{3n} \cosh\left(\frac{d_n x}{L}\right) + C_{4n} \sinh\left(\frac{d_n x}{L}\right) \quad (\text{A.90})$$

and the same for  $\Psi_n(x)$ ,  $M_n(x)$  and  $V_n(x)$  through equations (A.84), (A.85) and (A.87).

In figures A.9(a) and A.9(b) are shown the first five modes for both cases of Timoshenko free-free constrained beam and continuous-continuous one applied respectively to a sleeper and to a rail of the thesis work<sup>4</sup>.

### A.2.3 Modes normalization and natural frequencies

Also in the Timoshenko method, modes can be scaled, in fact they still represent a basis of eigenfunctions for the mathematic space or subspace and so do not have a fix module (If  $x$  is an eigenvector of the matrix  $A$  with eigenvalue  $\alpha$ , then any multiple  $\alpha x$  is the same eigenvector of  $A$  with the same eigenvalue).

The normalization adopted is the same of the Euler case (to unit of mass per length) but the mathematic relation is different:

$$\int_0^L (\rho A U_n^2(x) + \rho I \Psi_n^2(x)) dx = \rho A C_{1n}^2 2 \int_0^L (U_n^{*2}(x) + r^2 \Psi_n^{*2}(x)) dx = \rho A L C_{1n}^2 I_{c_n} \quad (\text{A.91})$$

where:

- $U_n(x)$  and  $\Psi_n(x)$  are the  $n$ th modes of transversal deformation and of cross area rotation, respectively defined in equations (A.75) and (A.87);
- $r$  is the rotation radius of the cross section of the beam defined in (A.69);
- $U_n^{*2} = U_n^2/C_{1n}$  and  $\Psi_n^{*2} = \Psi_n^2/C_{1n}$

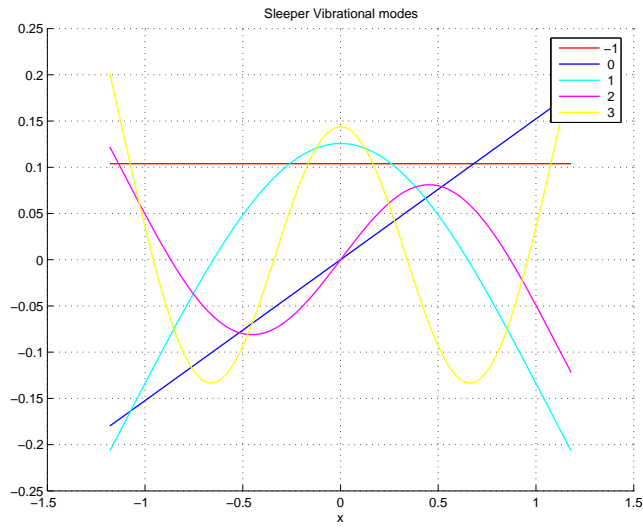
Thus the value of  $C_{1n}$  is given by equation (A.92):

$$C_{1n} = \frac{1}{\sqrt{\rho A L I_{c_n}}} \quad (\text{A.92})$$

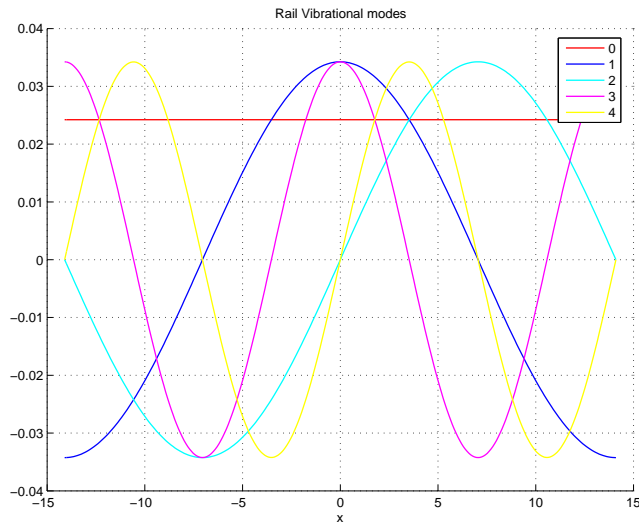
Figure A.2.3 shows the trend of the first 82 modos for a free-free constrained beam (beam mechanical properties influenced obviously the values of  $I_{c_n}$  integral).

---

<sup>4</sup>As aforementioned Timoshenko modes depend on beam length and on boundary conditions, but, unlike Euler method, they depend also on the main mechanical properties of the material



(a)



(b)

Figure A.9. Plot of first 5 vibration modes for a free-free constrained beam (fig (A.4(a))) and for a continuous-continuous one (fig(A.4(b))) using the Timoshenko approach



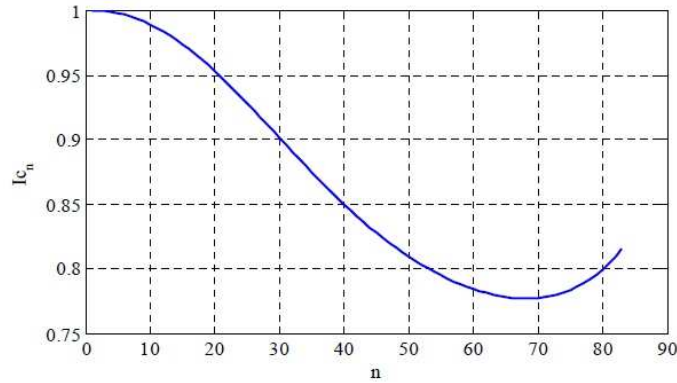


Figure A.10. Integral  $I_{c_n}$  trend for the first 82 vibration modes for a free-free constrained beam

Finally the expression for the calculation of natural frequencies is:

$$\omega_n = \sqrt{\frac{EI}{\rho AL^4} \lambda_n^4} \quad (\text{A.93})$$

The natural frequencies obtained with Timoshenko theory are obviously a bit smaller than the Euler ones and this because The Euler beam is more rigid.

In Euler theory in fact the cross section is supposed to be always perpendicular to the neutral axis and this makes the beam more rigid and its natural frequencies higher.

To appreciate this difference it is necessary to consider high frequencies modes because, because this discrepancy becomes greater with the increasing of the modes number ,as figure A.2.3 shows.

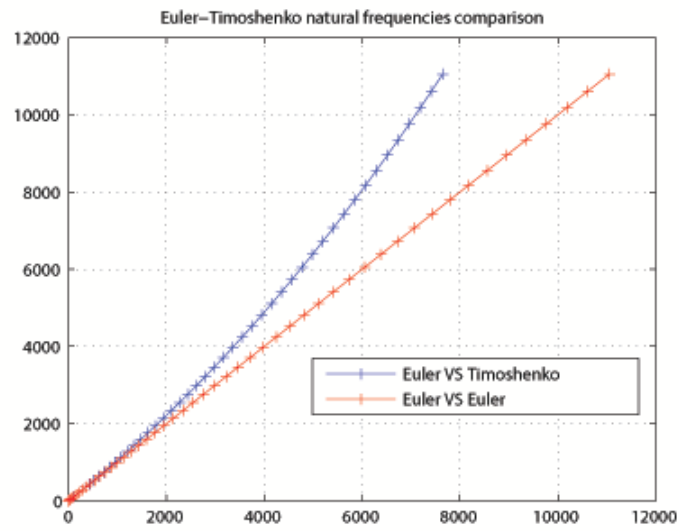


Figure A.11. Comparison between Euler-Bernoulli frequencies and Timoshenko ones for the same beam

# Appendix B

## Winkler Foundation

In this short Annex a short introduction to Winkler foundation theory is given.

### B.1 Concept of Elastic Foundations

In figure B.1 it is shown a simple case of beam over an elastic foundation and its simplified model.

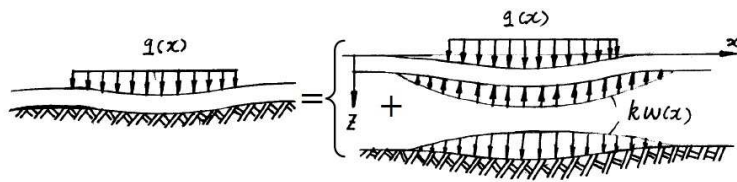


Figure B.1. Distributed load  $q(x)$  acting on an infinite beam over an elastic foundation of  $k$  stiffness

In Winkler method a linear relationship between the force on the foundation ( $f_f$ ) and the deflection  $w$  is assumed, thus, considering a foundation of  $k_0$  stiffness coefficient  $[N/m]$ , it is possible to write the following relation:

$$f_f = k_0 w \quad (B.1)$$

Equation (B.1), in the case of a  $b$  width beam, become obviously:

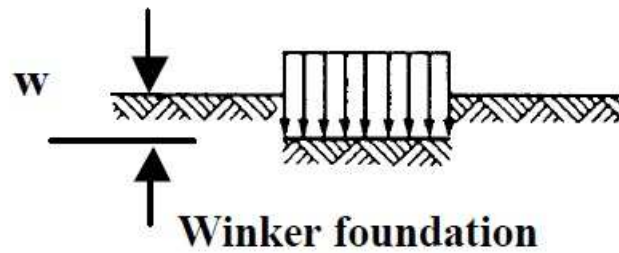
$$p = k_0 b w \quad (B.2)$$

where in (B.2)  $k_0$  is a stiffness per unit of width  $[N/m^2]$ .

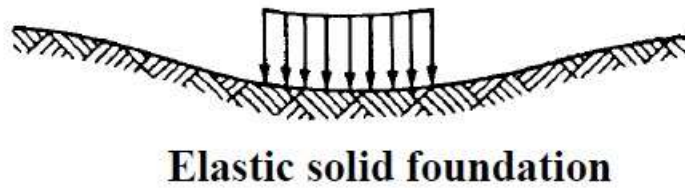
It is important to notice yet an important restriction of the model: the contact is never broken between beam and foundation and this is a matter of particular

importance that can be solved only with the use of more complicated models as those of Elastic solid Foundation.

In figure it is possible to better understand this first restriction of Winkler foundation model compared to more complex ones.



(a)



**Elastic solid foundation**

(b)

Figure B.2. Deflections of foundation models under uniform pressure. No beam is present.

## B.2 Governing Equations For Uniform Straight Beams on Elastic Foundations

In this section the governing equation for a simple case of beam over an elastic Winkler foundation is presented.

To obtain the governing equation an Euler-Bernoulli approach will be used.

Considering the differential element of an uniform beam over an elastic support and the forces acting on it (fig: B.3), it is possible to write the following equilibrium equations:

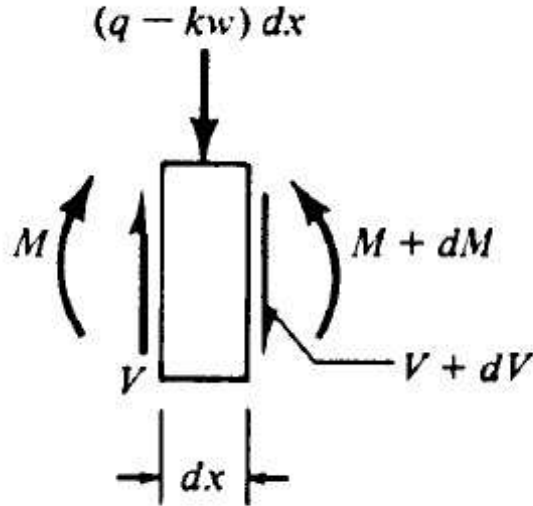


Figure B.3. Beam cross section differential element and forces acting on it.

- forces equilibrium

$$\frac{dV}{dx} = -q + kw \quad (\text{B.3})$$

- moments equilibrium

$$\frac{dM}{dx} = V \quad (\text{B.4})$$

Equations (B.3) and (B.4) opportunely combined, yield to the *Euler-Bernoulli beam governing equation of movement* (section A.1 of annex A).

$$EI \frac{d^4 w}{dx^4} + kw = q(x,t) \quad (\text{B.5})$$

To solve this equation lots of methods have been developed, as aforementioned in this thesis work.

Finally it is important to notice that Winkler effect on beam natural frequencies is that of increasing the stiffness of the system, that is, increasing its natural frequencies of vibration .

# Appendix C

## Two step numerical integration method used

In this Annex the explicit two-step method algorithm used to solve the differential equations system is developed.

The proposed numerical integration, avoids solving simultaneous linear algebraic equations in each time step and it is valid for arbitrary damping matrix and diagonal mass matrix frequently encountered in practical engineering dynamic systems.

Accordingly, computational speeds of this method applied to large system analysis can be far higher than those of other popular methods.

Accuracy, stability and numerical dissipation have been already investigated in Ref. [4] and in order to verify its accuracy and correctness linear and non linear examples were runned and the results carefully analyzed.

The proposed method can be used as fast as economical calculation tools for solving large-scale nonlinear dynamic problems in engineering.

### C.1 introduction

Step-by-step integration algorithms are widely used to solve equations of multi-degree of freedom systems in structural dynamics, especially in non-linear structural dynamics.

Discussions on these algorithms can be founded in lots of different technical journals and books.

However, for large-scale problems, as is frequently the case in modern dynamic analysis in practical engineering problems, the calculation speed become very low and the computational cost high. Therefore, it is necessary to develop more efficient integrations algorithms for large-scale complex system analysis.

Basically there are two general classes of algorithms for dynamic problems:

- implicit methods;
- explicit methods.

Implicit methods are for instance the *Newmark - $\beta$  method* or the *Wilson - $\theta$  method*. These implicit methods are normally more accurate and permit large time steps but the price to pay for these benefits is an high computational cost when applying this kind of algorithms to large-scale problems.

On the contrary, explicit schemes tend to be inexpensive.

It was pointed out that if lumped mass and damping matrices are used, an explicit scheme probably consists of pure vector operations. This is very convenient for computers with vector processors and the disadvantage of conditional stability can be partially alleviated through a vectorized implementation.

Thus these explicit algorithms become more competitive on large-scale problems compared to more stable implicit ones.

Moreover non-linear problems tend to be difficult to analyze for both kinds of algorithms and specially the time-step needs to be very small in both cases.

In this kind of dynamic problems, an important algorithm is that of the central differences method that when applied to non-linear structural dynamics is still supposed to solve a set of linear algebraic equations, in each time step, at least as long as the problem is an ideal one that is:

- the mass matrix is diagonal ;
- the damping matrix can be neglected or is proportional to the mass matrix and to the stiffness one.

However the second condition is difficult to satisfy for practical engineering problems, while the first one can be usually observed.

The explicit method used is supposed to be a simple one with at least the same stability limit as the central difference one, but needs only simple vectors operations in each step no matter which kind of damping matrix is used.

Its stability and dissipation in non linear cases were proved and its efficiency in solving the equation system of this thesis work is also good.

## C.2 New Explicit integration method algorithm

The matrix equation of linear structural dynamics is :

$$\mathbf{M}\ddot{\mathbf{X}} + \mathbf{C}\dot{\mathbf{X}} + \mathbf{K}\mathbf{X} = \mathbf{F} \tag{C.1}$$

that can be also written as follows:

$$\mathbf{M}\mathbf{A} + \mathbf{C}\mathbf{V} + \mathbf{K}\mathbf{X} = \mathbf{F} \quad (\text{C.2})$$

where in equations (C.1) and (C.2)  $\mathbf{M}$ ,  $\mathbf{C}$  and  $\mathbf{K}$  are respectively the mass matrix, the damping matrix and the stiffness one,  $\mathbf{F}$  is the vector of applied loads (generally a function of time  $\mathbf{F} = \mathbf{F}(t)$ ) and  $\mathbf{X}$ ,  $\mathbf{V}$ ,  $\mathbf{A}$  ( $\mathbf{X}, \dot{\mathbf{X}}, \ddot{\mathbf{X}}$ ) are the vectors of displacements, velocities and accelerations, respectively.

The initial value problem consists of finding a function  $\mathbf{X} = \mathbf{X}(t)$  which satisfies equations (C.1) and (C.2) as well as the initial conditions

$$\mathbf{X}(0) = \mathbf{X}_0 \quad (\text{C.3})$$

$$\mathbf{V}(0) = \mathbf{V}_0 \quad (\text{C.4})$$

where  $\mathbf{X}_0$  and  $\mathbf{V}_0$  are given vectors of initial displacements and velocities, respectively.

### C.3 Integration scheme

The new explicit scheme for approximate solutions of equations (C.1) and (C.4) is proposed below:

$$\mathbf{X}_{n+1} = \mathbf{X}_n + \mathbf{V}_n \Delta t + \left(\frac{1}{2} + \Psi\right) \mathbf{A}_n \Delta t^2 - \Psi \mathbf{A}_{n-1} \Delta t^2 \quad (\text{C.5})$$

$$\mathbf{V}_{n+1} = \mathbf{V}_n + (1 + \varphi) \mathbf{A}_n \Delta t - \varphi \mathbf{A}_{n-1} \Delta t \quad (\text{C.6})$$

where  $\mathbf{X}_n, \mathbf{V}_n$  and  $\mathbf{A}_n$  are the approximations to  $\mathbf{X}(t = n\Delta t), \mathbf{V}(t = n\Delta t)$  and  $\mathbf{A}(t = n\Delta t)$ , respectively,  $\Delta t$  is the time step and  $\Psi$  and  $\varphi$  are free parameters that control the stability and numerical dissipation of the algorithm.

Obviously, the above scheme is similar in form to the well-known *Newmark method*, in fact the construction of this new scheme is enlightened by the latter.

Substituting equation (C.4) into equation (C.1) at time step  $t = (n + 1)\Delta t$

$$\mathbf{M}\mathbf{A}_{n+1} + \mathbf{C}\mathbf{V}_{n+1} + \mathbf{K}\mathbf{X}_{n+1} = \mathbf{F}_{n+1} \quad (\text{C.7})$$

and rearranging the terms yield to:

$$\mathbf{A}_{n+1} = \mathbf{M}^{-1} \tilde{\mathbf{F}}_{n+1} \quad (\text{C.8})$$

where



$$\begin{aligned} \tilde{\mathbf{F}}_{n+1} = & \mathbf{F}_{n+1} - \mathbf{K}\mathbf{X}_n - (\mathbf{C} + \mathbf{K}\Delta t) \mathbf{V}_n + \dots \\ & \dots - \left[ (1 + \varphi) \mathbf{C} + \left( \frac{1}{2} + \Psi \right) \mathbf{K}\Delta t \right] \mathbf{A}_n \Delta t + (\varphi \mathbf{C} + \Psi \mathbf{K}\Delta t) \mathbf{A}_{n-1} \Delta t \end{aligned} \quad (\text{C.9})$$

in which  $\mathbf{F}_{n+1} = \mathbf{F}[t = (n + 1)\Delta t]$

To start the integration procedure, one can easily let  $\varphi = \Psi = 0$  at the first time step and use the initial conditions (C.4) as well as

$$\mathbf{A}_0 = \mathbf{M}^{-1} (\mathbf{F}_0 - \mathbf{C}\mathbf{V}_0 - \mathbf{K}\mathbf{X}_0) \quad (\text{C.10})$$

Therefore the scheme is self-starting. If the mass matrix is diagonal, as it is frequently the case in structural dynamics and as it is assumed here to be, the new integration algorithm is explicit and needs not to solve any equation.

## C.4 Stability

To investigate the stability of the new explicit method a linear homogeneous form of equation (C.7) without damping and for a single-degree of freedom was considered; the results obtained from *Wan-Ming Zhai* Ref.[4] are here reported:

$$a_{n+1} + \omega^2 x_{n+1} = 0 \quad (\text{C.11})$$

where  $k = \sqrt{k/m}$ .

the difference form of equation (C.11) is:

$$x_{n+2} + \left[ \left( \frac{1}{2} + \Psi \right) \Omega^2 - 2 \right] x_{n+1} + \left[ \left( \frac{1}{2} + \varphi - 2\Psi \right) \Omega^2 + 1 \right] x_n + (\Psi - \varphi) \Omega^2 x_{n-1} = 0 \quad (\text{C.12})$$

where  $\Omega = \omega\Delta t$

The eigenvalue equation of equation (C.12) takes the following form:

$$\lambda^3 + \left[ \left( \frac{1}{2} + \Psi \right) \Omega^2 - 2 \right] \lambda^2 + \left[ \left( \frac{1}{2} + \varphi - 2\Psi \right) \Omega^2 + 1 \right] \lambda + (\Psi - \varphi) \Omega^2 = 0 \quad (\text{C.13})$$

The requirement for stability is  $|\lambda| \leq 1$ . By use of the transformation

$$\lambda = \frac{1 + Z}{1 - Z} \quad (\text{C.14})$$

equation (C.13) becomes

$$[4 + 2(\varphi - 2\Psi)\Omega^2] Z^3 + [4 + (4\Psi - 4\varphi - 1)\Omega^2] Z^2 + 2\varphi\Omega^2 Z + \Omega^2 = 0 \quad (\text{C.15})$$

and then the requirement for stability is simply  $R_e(Z) \leq 0$ .

Thus stable steps can be derived and they are shown in table C.1.

---

| $\varphi$                   | $\Psi$                                   | $\Delta t$  |
|-----------------------------|--|---|
| $\varphi > \frac{1}{2}$     | $\Psi < \varphi$                         | $\Delta t \leq \frac{1}{\omega} \sqrt{\frac{2\varphi - 1}{(\varphi - \Psi)(2\varphi + 1)}}$   |
| $\varphi > \frac{1}{2}$     | $\Psi \geq \varphi$                      | $\Delta t \leq \frac{1}{\omega} \sqrt{\frac{2}{2\Psi - \varphi}}$   |
| $\varphi = \frac{1}{2}$     | $\Psi \geq \frac{1}{2}$                  | $\Delta t \leq \frac{2}{\omega} \sqrt{\frac{1}{4\Psi - 1}}$   |
| $0 < \varphi < \frac{1}{2}$ | $\varphi < \Psi < \varphi + \frac{1}{4}$ | $\frac{1}{\omega} \sqrt{\frac{1 - 2\varphi}{(\Psi - \varphi)(2\varphi + 1)}} \leq \Delta t \leq$<br><br>$Min \left\{ \frac{1}{\omega} \sqrt{\frac{2}{2\Psi - \varphi}}, \frac{2}{\omega} \sqrt{\frac{1}{4(\varphi - \Psi) + 1}} \right\}$ |
| $0 < \varphi < \frac{1}{2}$ | $\Psi \geq \varphi + \frac{1}{4}$        | $\frac{1}{\omega} \sqrt{\frac{1 - 2\varphi}{(\Psi - \varphi)(2\varphi + 1)}} \leq \Delta t \leq \frac{1}{\omega} \sqrt{\frac{2}{2\Psi - \varphi}}$  |

Table C.1. Conditions of stability of the new explicit method

It can be seen from table C.1 that the range of stable steps is very wide.

When  $\Psi = \varphi = \frac{1}{2}$ , the stability limit is  $\Delta t \leq 2\omega$ , which is the same as that of the central difference method and these are the coefficients values used in the track-program.

It is important to notice that when a non-linear case is treated this minimum time-step seems to be different from the theoretical one. Before implementing the integrator some tests have been done and the result was that the best coefficients to use, considering solution stability and accuracy were  $\Psi = \varphi = \frac{1}{2}$ .

## C.5 Accuracy

Applying Taylor formula to  $A_{n-1}$  it results:

$$\mathbf{A}_{n-1} = \mathbf{A}_n - \dot{\mathbf{A}}_n \Delta t + \frac{1}{2} \ddot{\mathbf{A}}_n \Delta t^2 - \dots \quad (\text{C.16})$$

where a superposed dot denotes a time derivate as commonly used. Substituting equation (C.16) into equation (C.6) yields to:

$$\mathbf{X}_{n+1} = \mathbf{X}_n + \mathbf{V}_n \Delta t + \frac{1}{2} \mathbf{A}_n \Delta t^2 + \Psi \dot{\mathbf{A}}_n \Delta t^3 - \frac{1}{2} \Psi \ddot{\mathbf{A}}_n \Delta t^4 + \mathbf{O}(\Delta t^5) \quad (\text{C.17})$$

$$\mathbf{V}_{n+1} = \mathbf{V}_n + \mathbf{A}_n \Delta t + \varphi \dot{\mathbf{A}}_n \Delta t^2 + \mathbf{O}(\Delta t^3) \quad (\text{C.18})$$

Local truncation errors can be written as

$$\mathbf{E}(X) = \left(\frac{1}{6} - \Psi\right) \dot{\mathbf{A}}_n \Delta t^3 + \left(\frac{1}{24} + \frac{1}{2} \Psi\right) \ddot{\mathbf{A}}_n \Delta t^4 + \mathbf{O}(\Delta t^5) \quad (\text{C.19})$$

$$\mathbf{E}(V) = \left(\frac{1}{2} - \varphi\right) \dot{\mathbf{A}}_n \Delta t^2 + \left(\frac{1}{6} + \frac{1}{2} \varphi\right) \ddot{\mathbf{A}}_n \Delta t^3 + \mathbf{O}(\Delta t^4) \quad (\text{C.20})$$

If  $\Psi = \frac{1}{6}$  the order of accuracy of  $\mathbf{E}(X)$  is  $\mathbf{O}(\Delta t^4)$  and if  $\varphi = \frac{1}{2}$  the order of accuracy of  $\mathbf{E}(V)$  is  $\mathbf{O}(\Delta t^3)$ .

Otherwise the orders of accuracy decrease to  $\mathbf{O}(\Delta t^3)$  and  $\mathbf{O}(\Delta t^2)$ , respectively. Obviously the new explicit integration method has the same order of accuracy as that of Newmark's implicit method.

### C.5.1 Numerical dissipation

Concerning the numerical dissipation and amplitude decay, here are reported only the results of the article used [4].

When both  $\varphi$  and  $\Psi$  are larger than  $\frac{1}{2}$  or one of them is larger than  $\frac{1}{2}$  and the other equals to  $\frac{1}{2}$ , there will be algorithmic damping to decrease amplitudes, and when  $\varphi = \Psi = \frac{1}{2}$  there is no numerical dissipation.

### C.5.2 Stability and Accuracy : examples

It is very important to remember that the minimum time step to reach the stability of the method can bring to completely wrong results anyway, because it assures that the solution is stable but it doesn't consider its accuracy.

Considering the following problem it is possible to better understand the difference between stability and accuracy of the solution.

$$\begin{aligned} \ddot{x} + kx &= f(t) \\ \dot{x}(0) &= 10 \\ x(0) &= 0 \end{aligned} \tag{C.21}$$

where  $t \in [0,20]$ .

Two different simulations were so run:

1.  $k = 50$
2.  $k(x) = \begin{cases} 50, & \text{if } 1.2 \leq x \leq 1.2 \\ 20, & \text{if } x \leq -1.2 \vee x \geq 1.2 \end{cases}$

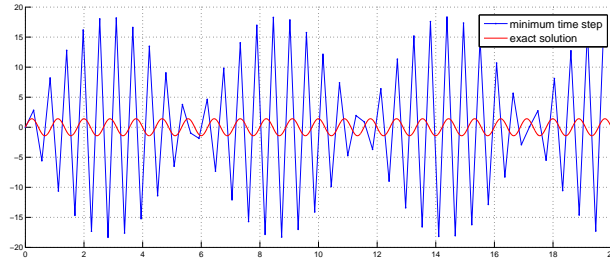
In the first linear case the minimum theoretical time step is  $dt = \frac{2}{\omega} = \sqrt{50} \approx 0.28$

Figures C.1(a) and C.1(b) show how this stability condition is here respected but at the same time the accuracy of the solution is very low, almost making the solution completely wrong.

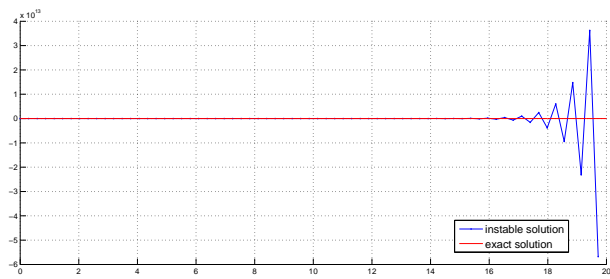
Concerning the non-linear problem instead the condition seems to be stable also for  $dt$  values major then the minimum one, and this is illustrated in figure C.2 where the used  $dt$  is major then  $\frac{2}{\omega}$ .

Finally figure C.3 shows that to reach a good level in the accuracy of the solution it is necessary to consider very small time steps and furthermore this accuracy decreases with the length of the time interval simulated.

Obviously more accurated analysis would be necessary to define the minimum time step to achieve a certain grade of accuracy but this is not a goal of the work done.



(a)



(b)

Figure C.1. Minimum time step stability condition for the linear example

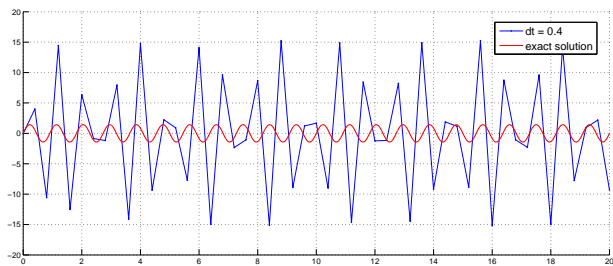


Figure C.2. Minimum time step stability condition for the non-linear example

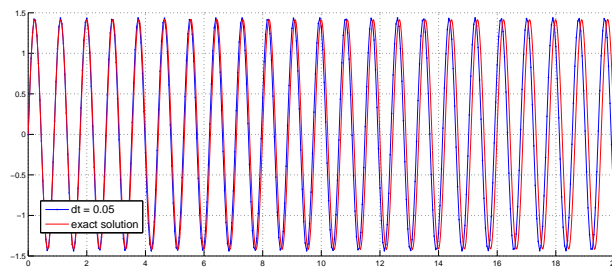


Figure C.3. Accuracy of the solution

# Bibliography

- [1] L. Baeza A. Rodaa J.C.O. Nielsen. Railway vehicle/track interaction analysis using a modal substructuring approach. *Journal of Sound and Vibration* 293, 2006.
- [2] A. Roda. *Modelo dinámico de la interacción vía-vehículo basado en subestructuración*. PhD thesis, Departamento de Ingeniería Mecánica y de Materiales, Universidad Politécnica de Valencia, 2006.
- [3] T.J.S. Abrahamsson J.C.O. Nielsen. Coupling of physical and modal components for analysis of moving non-linear dynamic systems on general beam structures. *International Journal for Numerical Methods in Engineering*, 1992.
- [4] Wan-Ming Zhai. Two simple fast integration methods for large-scale dynamic problems in engineering. *International journal for numerical methods in engineering vol 39*, 1996.
- [5] D. Harrison K.L. Johnson S.L. Grassie, R.W. Gregory. The dynamic response of railway track to high frequency vertical excitation. *Proceedings of the Institution of Mechanical Engineers, Part C: Journal of Mechanical Engineering Science* 24, 1982.
- [6] S.L. Grassie K.L. Knothe. Modelling of railway track and vehicle/track interaction at high frequencies. *Vehicle System Dynamics* 22, 1993.
- [7] U.Meneghetti E. Funaioli, A. Maggiore. *Lezioni di meccanica applicata alle macchine, prima parte:Fondamenti di meccanica delle macchine*. Patron editore, 1st, edition, 2005.